Western University
Scholarship@Western

Digitized Theses | Digitized Special Collections

1986

Structural Analysis Of Cardiovascular Tissue Using Quantitative Polarised Light Microscopy

Peter Whittaker

Follow this and additional works at: https://ir.lib.uwo.ca/digitizedtheses

Recommended Citation
Whittaker, Peter, "Structural Analysis Of Cardiovascular Tissue Using Quantitative Polarised Light Microscopy" (1986). *Digitized Theses*. 1565.
https://ir.lib.uwo.ca/digitizedtheses/1565

This Dissertation is brought to you for free and open access by the Digitized Special Collections at Scholarship@Western. It has been accepted for inclusion in Digitized Theses by an authorized administrator of Scholarship@Western. For more information, please contact tadam@uwo.ca, wlswadmin@uwo.ca.

National Library of Canada
Bibliothèque nationale du Canada

Canadian Theses Service
Services des thèses canadiennes

Ottawa Canada
K1A 0N4

CANADIAN THESES

THÈSES CANADIENNES

NOTICE

The quality of this microfiche is heavily dependent upon the quality of the original thesis submitted for microfilming. Every effort has been made to ensure the highest quality of reproduction possible.

If pages are missing, contact the university which granted the degree.

Some pages may have indistinct print especially if the original pages were typed with a poor typewriter ribbon or if the university sent us an inferior photocopy.

Previously copyrighted materials (journal articles, published tests, etc.) are not filmed.

Reproduction in full or in part of this film is governed by the Canadian Copyright Act, R.S.C. 1970, c. C-30.

AVIS

La qualité de cette microfiche dépend grandement de la qualité de la thèse soumise au microfilmage. Nous avons tout fait pour assurer une qualité supérieure de reproduction.

S'il manque des pages, veuillez communiquer avec l'université qui a conféré le grade.

La qualité d'impression de certaines pages peut laisser à désirer, surtout si les pages originales ont été dactylographiées à l'aide d'un ruban usé ou si l'université nous a fait parvenir une photocopie de qualité inférieure.

Les documents qui font déjà l'objet d'un droit d'auteur (articles de revue, examens publiés, etc.) ne sont pas microfilmés.

La reproduction, même partielle, de ce microfilm est soumise à la Loi canadienne sur le droit d'auteur, SRC 1970, c. C-30.

THIS DISSERTATION
HAS BEEN MICROFILMED
EXACTLY AS RECEIVED

LA THÈSE A ÉTÉ
MICROFILMÉE TELLE QUE
NOUS L'AVONS REÇUE

NL-339 (r. 86/06)

Canada

STRUCTURAL ANALYSIS OF CARDIOVASCULAR TISSUE USING QUANTITATIVE POLARISED LIGHT MICROSCOPY

by

Peter Whittaker

Department of Biophysics

Submitted in partial fulfilment

of the requirements for the degree of

Doctor of Philosophy

Faculty of Graduate Studies

The University of Western Ontario

London, Ontario

August, 1986

© Peter Whittaker 1986

Permission has been granted to the National Library of Canada to microfilm this thesis and to lend or sell copies of the film.

The author (copyright owner) has reserved other publication rights, and neither the thesis nor extensive extracts from it may be printed or otherwise reproduced without his/her written permission.

L'autorisation a été accordée à la Bibliothèque nationale du Canada de microfilmer cette thèse et de prêter ou de vendre des exemplaires du film.

L'auteur (titulaire du droit d'auteur) se réserve les autres droits de publication; ni la thèse ni de longs extraits de celle-ci ne doivent être imprimés ou autrement reproduits sans son autorisation écrite.

ISBN 0-315-33040-6

ABSTRACT

Prior to the advent of electron microscopy, polarised light was commonly used in structural research. New microscopical and mathematical methods have made the techniques worthy of reappraisal. I used quantitative polarised light microscopy to examine tissue structure at both the fibre and molecular level. Birefringent materials, those with an anisotropic molecular organisation (such as collagen, muscle and elastin), can be studied using polarised light. The optical properties of birefringent materials were used to determine fibre orientation. Two-dimensional orientation was measured on the planar rotating microscope stage and three-dimensional orientation on a Universal stage. Molecular organisation, which affects optical anisotropy, was assessed by measuring the path-difference or retardation when linearly polarised light passes through birefringent materials. Five projects, focussing on collagen and muscle in cardiovascular tissues, were undertaken to demonstrate the usefulness of polarised light microscopy in structural studies.

I measured the two-dimensional orientation of cardiac muscle fibres in *hypertrophic cardiomyopathy* and developed a quantitative method to complement the current qualitative method of diagnosis. I used the Universal stage to measure the *orientation of collagen fibres in brain arteries* and found that the fibres were predominantly circumferentially aligned at normal systolic pressures, but, at higher pressures a population of fibres had large longitudinal components of orientation. I measured the *retardation in scar collagen* produced following myocardial infarction and found that changes in the optical properties of collagen could be detected for at least six weeks after its production. A measured difference in *retardation in tendons from floppy mitral valves*, indicated that degraded collagen can also be detected using polarised light. Both fibre orientation and molecular organisation were assessed in *cerebral saccular aneurysms*. The aneurysm wall was layered and the collagen fibres were

organised in a complex three-dimensional weave, suggesting a strong structure; however, the retardation in the aneurysm was lower than normal, indicating less molecular organisation and a possible reason why aneurysms enlarge and rupture.

The general conclusion is that quantitative polarised light microscopy remains an effective method in structural analysis.

Acknowledgements

I would like to thank the following people for their help:

- my advisors Dr. P.B. Canham and Dr. D.R. Boughner both for their advice and for the financial support they provided from their research grants from the Ontario Heart and Stroke Foundation and the Medical Research Council of Canada.

- to the third member of my advisory committee Dr. J. Starkey for providing equipment and assisting with computer programming.

- Dr. R.A. Kloner, Wayne State University, Dr. Maria T. Vivaldi, Harvard University, Dr J.C. Kaufmann, U.W.O., Dr. Mary Bell, Wake Forest University, and Dr. M.D. Silver, University of Toronto for providing the tissue.

- to the Summer students I worked with: John Lloyd, Terrie Romano and Monika Schwab. The latter two also helped with the translation of articles as did Karin Przyklenk.

- Jan Hicks, Sharon Barwick and Rashida Khalfan for their histological assistance.

- Dr. R.C. Buck for providing electron microscopy sections.

Table of Contents

Certificate of examination ii
Abstract iii
Acknowledgements v
Table of Contents vi
List of Photographic Plates ix
List of Tables x
List of Figures xi

CHAPTER ONE INTRODUCTION 1

CHAPTER TWO
METHODS

2.1. Polarised Light 7
2.1.1. Mathematical representation 7
2.2. Two-Dimensional Orientation 12
2.2.1. Statistical analysis 14
2.3. Three-Dimensional Orientation 16
2.3.1. Statistical analysis 18
2.4. Retardation Measurements 20
2.4.1. Imbibition analysis 24
2.4.2. Measurement of retardation on stained tissue 29
2.5. Tissue Staining 33
2.5.1. Picrosirius red 33
2.5.2. Other stains 35
2.6. Orientation Measured by Retardation 35
2.7. Tissue Preparation 37

CHAPTER THREE

TWO-DIMENSIONAL ORIENTATION METHOD
3.1. Introduction 39
3.2. Methods 41
3.2.1. Statistical analysis 42
3.3. Results 43
3.3.1. Descriptive results 43
3.3.2. Quantitative results 43
3.4. Discussion 47

CHAPTER FOUR

THREE-DIMENSIONAL ORIENTATION METHOD

4.1. Introduction 53
4.2. Methods 55
4.2.1. Tissue selection 55
4.2.2. Orientation of medial collagen 55
4.2.3. Orientation of adventitial collagen 56
4.3. Results 56

4.3.1. Medial collagen orientation 56
4.3.2. Adventitial collagen orientation 60
4.4. Discussion 60

CHAPTER FIVE

MOLECULAR ORGANISATION METHODS
5.1. Introduction 67
5.2. Methods 68
5.3. Results 70
5.4. Discussion 74

CHAPTER SIX

STRUCTURE OF CEREBRAL ARTERY BIFURCATIONS
6.1. Introduction 77
6.2. Methods 79
6.3. Results 81
6.4. Discussion 84

CHAPTER SEVEN

MOLECULAR ORGANISATION OF COLLAGEN IN SACCULAR ANEURYSMS
7.1. Introduction 88
7.2. Methods 89
7.2.1. Tissue preparation 89
7.2.2. Stained tissue 89
7.2.3. Unstained tissue 89
7.3. Results 90
7.3.1. Stained tissue 90
7.3.2. Unstained tissue 90
7.4. Discussion 90

CHAPTER EIGHT

COLLAGEN FIBRE ORGANISATION IN SACCULAR ANEURYSMS
8.1. Introduction 98
8.2. Methods 100
8.2.1. Tissue preparation 100
8.2.2. Two-dimensional orientation 100
8.2.3. Three-dimensional orientation 100
8.3. Results 101
8.3.1. Two-dimensional orientation 101
8.3.2. Three-dimensional orientation 101
8.4. Discussion 106

CHAPTER NINE

MOLECULAR ORGANISATION OF COLLAGEN IN FLOPPY VALVE DISEASE
9.1. Introduction 108
9.2. Methods 111
9.3. Results 112
9.4. Discussion 116

CHAPTER TEN

DISCUSSION
10.1. Polarised Light Microscopy As A Tool In Structural Studies 121
10.2. Fibre Orientation 122
10.3. Molecular Organisation 126
10.4. Relationship between optical properties and mechanical properties 129
10.5. Summary 129

References 131
Vitae 139

List of photographic plates

plate	Description	Page
1	Polarised light micrograph showing the change in extinction pattern when an HCM specimen is rotated	44
2	Cross section of cerebral artery stained with picrosirius red	57
3	Orientation of collagen fibrils in the medial gap and in the adventitia distant from the gap	83
4	Section of aneurysm wall showing its laminated appearance	102

List of tables

Table	Description	Page
1	Materials whose ultrastructure was discovered using polarised light	5
2	Imbibition media and their refractive indices	25
3	Statistical analysis of medial collagen orientation	59
4	(a) Statistical analysis of adventitial collagen orientation (b) analysis of the three orientation groups observed at high pressures	62
5	Regional variation in retardation for stained aneurysm collagen	94
6	Correlation of histological findings on mitral valve tendons with autopsy and surgical reports	115

List of Figures

Figure	Description	Page
1	Sectional patterns of polarised light beams	3
2	The polarising microscope	9
3	Orientation of birefringent fibres at extinction	11
4	Components of a unit vector	15
5	The universal stage	17
6	Construction and use of Lambert equal area projections	19
7	Analysis of scatter diagrams using Fisher statistics	21
8	Example form birefringence curve	23
9	Retardation measured as a function of imbibing time in a 20% glycerol solution	26
10	Form birefringence curve for reconstituted collagen	28
11	Schematic representation of the effect of dye binding on birefringence	30
12	Molecular configurations of eosin and sirius red F3B	32
13	Relationship between retardation and sample thickness for eosin stained collagen	34
14	Relationship between retardation and orientation	36
15	Summary of the methods	38
16	Cross section of the heart and schematic representation of the ventricular septum	40
17	Muscle orientation distributions for normal and hypertrophic cardiomyopathy cases	45
18	Mean angular deviations for the muscle orientation distributions	46
19	Muscle orientation distributions for normal and HCM cases in the blinded study	48
20	Examples of cumulative frequency curves for normal cases and apparently normal regions of HCM tissue	49
21	Graph of cumulative frequency curve slope versus angular deviation	50

22	Scatter diagram showing medial collagen orientation	58
23	Scatter diagram showing adventitial collagen orientation	61
24	Illustration of helical and spiral components of orientation	63
25	Form birefringence curves for scar collagen and visceral pericardium	71
26	Intrinsic birefringence of scar collagen and visceral pericardium	72
27	Graph of retardation vs. time post-occlusion for stained scar collagen	73
28	Graph of intrinsic birefringence vs age fornormal chordae	75
29	Schematic representation of a cerebral artery bifurcation cut in cross-section	80
30	Scatter diagram showing collagen orientation in the medial gap and in the rest of the adventitia	82
31	Histograms showing collagen fibril diameters in the medial gap and at locations distant from the gap	85
32	Histograms showing the comparison of retardation measurements taken in aneurysm collagen from the adventitia in stained sections	91
33	Form birefringence curves for aneurysm and adventitial collagen	92
34	Form birefringence curves showing regional variation in theoptical properties of aneurysm collagen	93
35	Diagram of a saccular aneurysm showing the forcesacting on it	99
36	Two dimensional orientation of collagen in the aneurysm wall	103
37	Graph of angle difference between layers vs aneurysm thickness	104
38	Scatter diagrams of collagen orientation in aneurysms	105
39	The mitral valve	109
40	Combined form birefringence curves for "normal" and "abnormal" chordae tendineae	113
41	Intrinsic birefringence of "normal" and "abnormal" chordae tendineae	114

The author of this thesis has granted The University of Western Ontario a non-exclusive license to reproduce and distribute copies of this thesis to users of Western Libraries. Copyright remains with the author.

Electronic theses and dissertations available in The University of Western Ontario's institutional repository (Scholarship@Western) are solely for the purpose of private study and research. They may not be copied or reproduced, except as permitted by copyright laws, without written authority of the copyright owner. Any commercial use or publication is strictly prohibited.

The original copyright license attesting to these terms and signed by the author of this thesis may be found in the original print version of the thesis, held by Western Libraries.

The thesis approval page signed by the examining committee may also be found in the original print version of the thesis held in Western Libraries.

Please contact Western Libraries for further information:
E-mail: libadmin@uwo.ca
Telephone: (519) 661-2111 Ext. 84796
Web site: http://www.lib.uwo.ca/

"If light is man's most useful tool, polarised light is the quintessence of utility". Shurcliff (1962)

CHAPTER 1 INTRODUCTION

Since it was supplanted by electron microscopy in the early 1940s, polarised light microscopy has been underutilised as a method of analysis in medical research. My belief was that it holds considerable potential for providing a new and informative approach to several modern problems of tissue structure analysis and was worthy of reappraisal. I therefore used quantitative polarised light microscopy to examine tissue structure at both the molecular and fibre level in a variety of cardiovascular tissues: cerebral arteries, cardiac muscle and mitral valve chordae tendineae. Structural organisation is important in tissues that have a mechanical function. In such tissues there is an intimate relationship between function, mechanical properties and structure. An appreciation of structural organisation provides a greater understanding of the basis of function and mechanical properties in both normal and pathological tissue.

In general, tissue structure may be studied at three different levels:

(1) The type of material in the tissue. This is the simplest element of structure and is usually determined histologically.

(2) The amount of the different types of material in the tissue. This can be determined using biochemistry or stereological and morphometric methods.

(3) The organisation of the different materials in the tissue. This can be divided into fibre and molecular organisation.

(3a) Fibre organisation is perhaps the most difficult aspect of structure to measure. Microdissection techniques, examination of histological sections and electron microscopy have all been used; however, these only provide a qualitative assessment of fibre organisation.

(3b) The molecular organisation is mainly studied using biochemistry techniques or x-ray diffraction

It was at this third level of structure that I applied polarised light methods The optical properties of materials when viewed with polarised light can be used to measure fibre orientation and the interaction of polarised light with a material can be used to reveal molecular organisation Quantitative polarised light microscopy can therefore link two apparently different aspects of structural organisation and so provides a biophysical bridge between biochemical and morphological methods

To appreciate how polarised light can be used to determine structure a brief discussion of some of the properties of light is required Light is a form of electromagnetic radiation Each light wave behaves as if it were a transverse oscillation, in an elastic medium, of an electric vector with an accompanying magnetic vector (Hecht and Zajac 1974) The magnetic vector has an equal amplitude and the same phase as the eleetric vector, but vibrates in a plane at right angles to the oscillation of the electric vector By convention, the discussion will consider only the electric vector Unpolarised light, e g., sunlight or the light from an ordinary light bulb, is made up of light waves whose electric vectors have no preferred orientation In perfectly polarised light however, all of the electric vectors are aligned in the same way The state of polarisation can take different forms Consider a polarised beam of light travelling along the z-axis of a right-handed coordinate system and viewed along that direction. If the electric vector is confined to one plane, then the sectional pattern of the beam will be a straight line (Figure 1). This represents linearly polarised light. The light may also be circularly or elliptically polarised.

The uniform alignment of the electric vector makes polarised light the simplest form of light and, as such, it can be used as a probe to determine structure If a material has an isotropic molecular organisation, then, a beam of polarised light passing through it is unaffected. If, however, the material has an anisotropic molecular

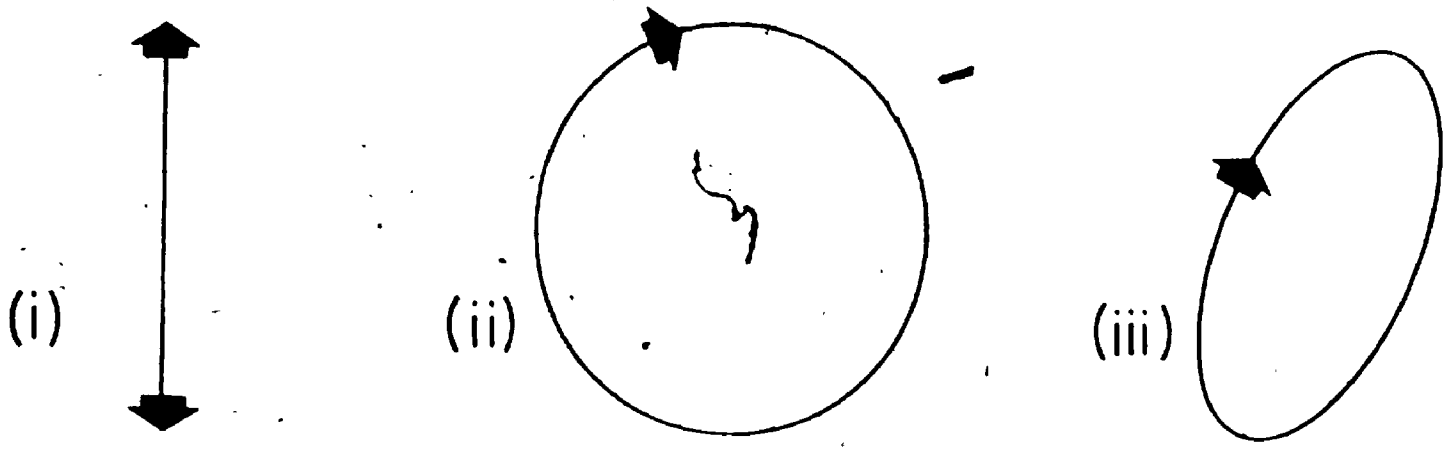

Figure 1: Sectional patterns of polarised light beams showing the vibration plane of the electric vector. (i) linearly polarised (ii) circularly polarised (iii) elliptically polarised light.

organisation then the interaction of the polarised light with the electrons in the material will be different in different directions. The net result is a change in the state of the beam's polarisation after it has passed through the material The molecular organisation of the material can thus be assessed by analysing the altered polarisation state

The understanding of polarised light has evolved relatively recently The use of polarised light effects, however, has a long history, with evidence that the Vikings used such effects as a navigational aid over 1000 years ago (Ramskou 1969, Gelsinger 1970ab) The light of the sky is partially polarised, with the maximum degree of polarisation 90 from the sun's position Sunstones, probably the mineral cordierite, which act as polarising filters were used to detect the sun's position even when it was cloudy In the Northern latitudes this would have been extremely useful

More recently, many branches of science e.g , Geology (Hartshorne and Stuart 1970), Physics (Booy and Fowler 1985), Astronomy (Hansen and Arking 1971) and also applied industrial sciences: textiles (Fatou 1978), ceramics (Roberts and Robinson 1985), and food science (Flint and Pickering 1984), and even Archeology (Montes et al. 1985) have all used polarised light methods; however, these methods are not used much in experimental biology and medicine There are perhaps two reasons for this. Table 1 (adapted from Frey-Wyssling 1974) shows some of the materials whose ultrastructure was discovered using polarised light. These discoveries were made before 1940, the date which coincides with the introduction of the electron microscope. There is no doubt that electron microscopy, because of its greater resolution, is a more effective tool in ultrastructure research. Polarised light microscopy can, however, reveal molecular changes invisible using electron microscopy. These capabilities appear to have been largely forgotten or ignored. Another reason for the neglect of polarised light methods in biology is that, although polarised light may be simple, the mathematics used in the past to describe it were complicated. More sophisticated techniques are now available

OBJECT	AUTHOR	YEAR
gel of cellulose	H. Ambronn	1916
lobster shield	A. Moehring	1922
muscle fibres	H. Stuebel	1923
scales of butterfly wings	F. Sueffert & H Zuchet	1924
tooth enamel	W.J. Schmidt	1925
collagen fibres	H. Kuentzel	1926
bone	W.J. Schmidt	1933
silk	K. Ohara	1933
myelin sheath of nerve	W.J. Schmidt	1935
axon of nerve	R.S. Bear et al.	1937
envelope of erythrocytes	F.O. Schmitt et al.	1938

Table 1: Materials whose ultrastructure was discovered using polarised light (adapted from Frey-Wyssling 1974, for the references see this paper).

which simplify the mathematics of polarised light. This advance coupled with the improvement of equipment since 1940 provide the potential for an increased use of polarised light methods in biology

In this thesis I will show that polarised light methods provide effective tools to study tissue structure at both the molecular and fibre level. I shall illustrate the practicality of the polarised light methods in the study of collagen and muscle in cardiovascular tissue. The versatility of the polarised light methods will be demonstrated by the diversity of the problems addressed. These projects were undertaken primarily for their clinical applicability because this provided an excellent demonstration of the value of polarised light microscopy

CHAPTER 2 METHODS

I used quantitative polarised light microscopy to determine macromolecular and molecular organisation in a variety of cardiovascular tissues: cerebral arteries, cardiac muscle and mitral valve chordae tendineae. The fibre organisation can be measured using the optical properties of materials when viewed with polarised light. The molecular organisation can be analysed by measuring the effect that the fibre's molecules have on linearly polarised light. The theory for each technique and the general methods used are described in this chapter, while methods specific to particular experiments are covered later in the appropriate chapters.

2.1. Polarised Light

2.1.1. Mathematical representation: Wave equations are used in the classical descriptions of polarised light. If the effect of a series of optical devices on polarised light must be calculated the wave equations become complicated. The process can be simplified, however, by using the matrix methods of Jones (1941) and Müller (1948, described in Collett 1968). For the applications discussed in this thesis the Jones method is preferred for its use of 2x2 matrices instead of the 4x4 matrices used in the Müller method.

In the Jones matrix algebra, a beam of linearly polarised light is represented by a two element column vector (called a Jones vector),

$\begin{bmatrix} E_x \\ E_y \end{bmatrix}$ where E_x and E_y are the instantaneous x and y scalar components of the beam's electric vector. Thus, a horizontally polarised beam (travelling in the z-direction) has a Jones vector of $\begin{bmatrix} 1 \\ 0 \end{bmatrix}$ i.e., $E_x = 1$ and $E_y = 0$ and a vertically polarised beam is

is represented by $\begin{bmatrix} 0 \\ 1 \end{bmatrix}$

Any optical device that the polarised light encounters can be represented by a 2x2 matrix. The Jones vector of the emerging beam is determined by multiplying the incoming beam's Jones vector by the matrix of the optical device (or devices) encountered. The usual right to left rule of matrix multiplication applies. The state of polarisation of the emerging beam can then be computed from its Jones vector. The Jones method is specific to polarised light and cannot be applied if there is any depolarisation. In the experiments considered here, polarised light was produced as follows. The polarising microscope is shown schematically in Figure 2. Unpolarised light, from the light source, is converted to linearly polarised light by a filter (called the polariser). The light then passes through a second filter (the analyser) and then to the eye. The polariser and the analyser are aligned prior to analysis such that their transmission axes are perpendicular. Thus, if the polariser permits only horizontally polarised light to pass and the analyser's transmission axis is vertical (matrix $\begin{bmatrix} 0 & 0 \\ 0 & 1 \end{bmatrix}$ Shurcliff 1962), the then the result is given by

$$\begin{bmatrix} 0 & 0 \\ 0 & 1 \end{bmatrix} \begin{bmatrix} 1 \\ 0 \end{bmatrix} = \begin{bmatrix} 0 \\ 0 \end{bmatrix}$$

i.e., no light passes through the analyser. Two different microscopes were used: a Nikon Optiphot and a Zeiss Universal Polarising microscope.

Materials can only be seen with the polarising microscope if they are birefringent i.e., if the material has an anisotropic molecular organisation and has two refractive indices. When linearly polarised light enters a birefringent material it is resolved into two rays which travel at unequal velocities because of the material's anisotropy (Bennett 1950). For collagen and muscle, the two materials studied, the slow ray travels parallel to

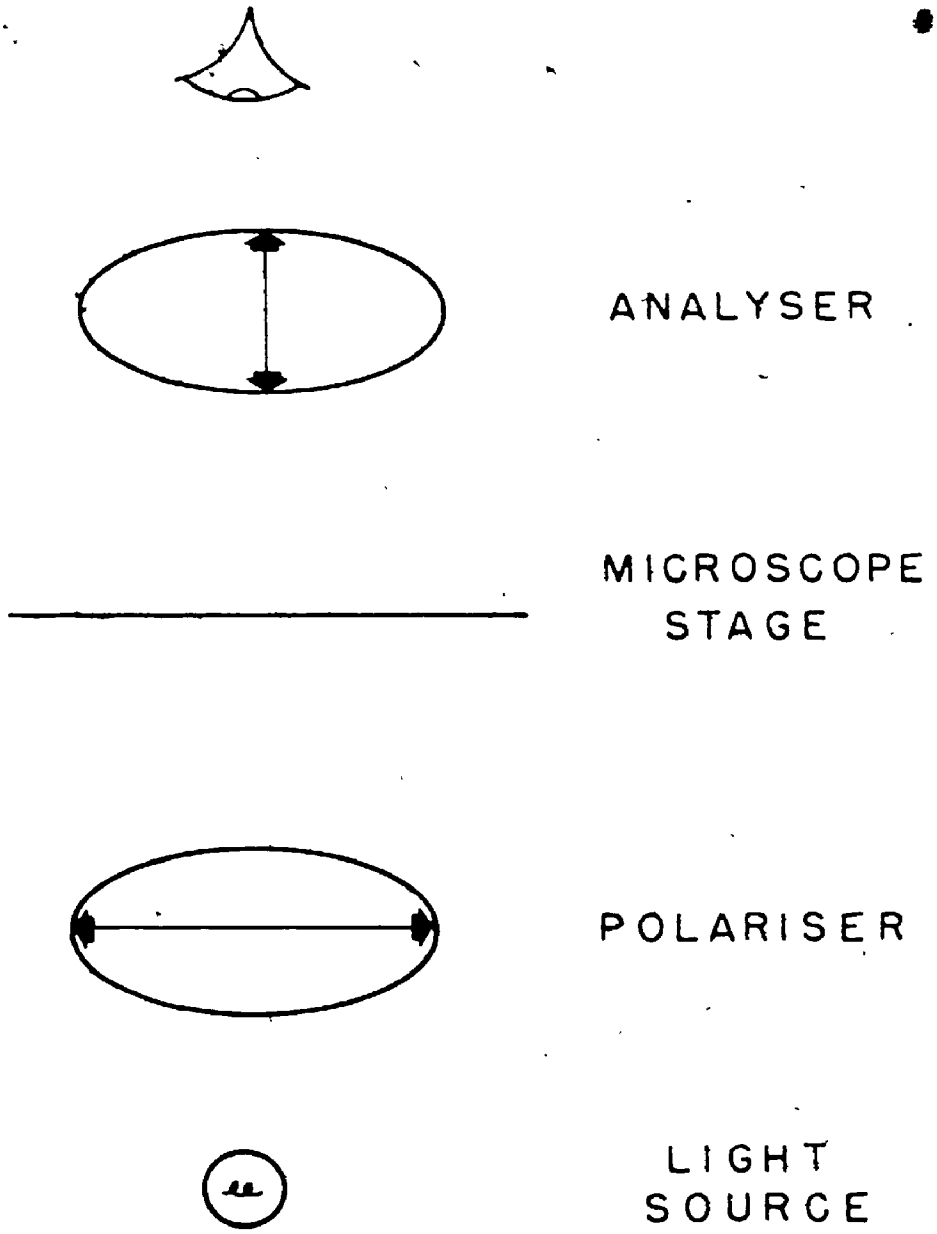

Figure 2: Schematic representation of the polarising microscope. The arrows on the polarising filters indicate their transmission axis.

the fibre's long axis and the fast ray parallel to the short axis (Bennett 1950, Fischer 1944). A birefringent material placed in the path of a polarised beam, can alter the beam's state of polarisation so that light passes through the analyser. The matrix for either a collagen or a muscle fibre, which can both be regarded as ideal homogeneous linear retarders with a phase shift, δ, is,

$$\begin{bmatrix} m_{11} & m_{12} \\ m_{21} & m_{22} \end{bmatrix}$$

where $m_{11} = \cos^2\theta + e^{-i\delta} \sin^2\theta$
$m_{22} = \sin^2\theta + e^{-i\delta} \cos^2\theta$
$m_{12} = m_{21} = (1 - e^{-i\delta}) \cos\theta \sin\theta$
θ is the azimuth of the fast axis (Shurcliff 1962)

If the birefringent material is placed between the polariser and the analyser the emerging beam's Jones vector is given by,

$$\begin{bmatrix} 0 & 0 \\ 0 & 1 \end{bmatrix} \begin{bmatrix} m_{11} & m_{12} \\ m_{21} & m_{22} \end{bmatrix} \begin{bmatrix} 1 \\ 0 \end{bmatrix} = \begin{bmatrix} 0 \\ m_{21} \end{bmatrix}$$

i.e., vertically polarised light. At certain orientations of the fast axis, however, no light will pass through the analyser. These are called extinction angles and will occur when $m_{21}=0$.

$$\text{i.e., } (1 - e^{i\delta}) \cos\theta \sin\theta = 0$$

$$\theta = 0°, 90°, 180°, 270°. \quad (\delta \neq 0)$$

As the fibres have no distinguishable heads or tails, the four extinction angles represent two equivalent orientations (Figure 3). Since the fibre's long axis is parallel to the path of the slow ray, it is more convenient to think in terms of the slow rather than the fast axis. The extinction angles for the slow and the fast axes remain the same because they are mutually perpendicular.

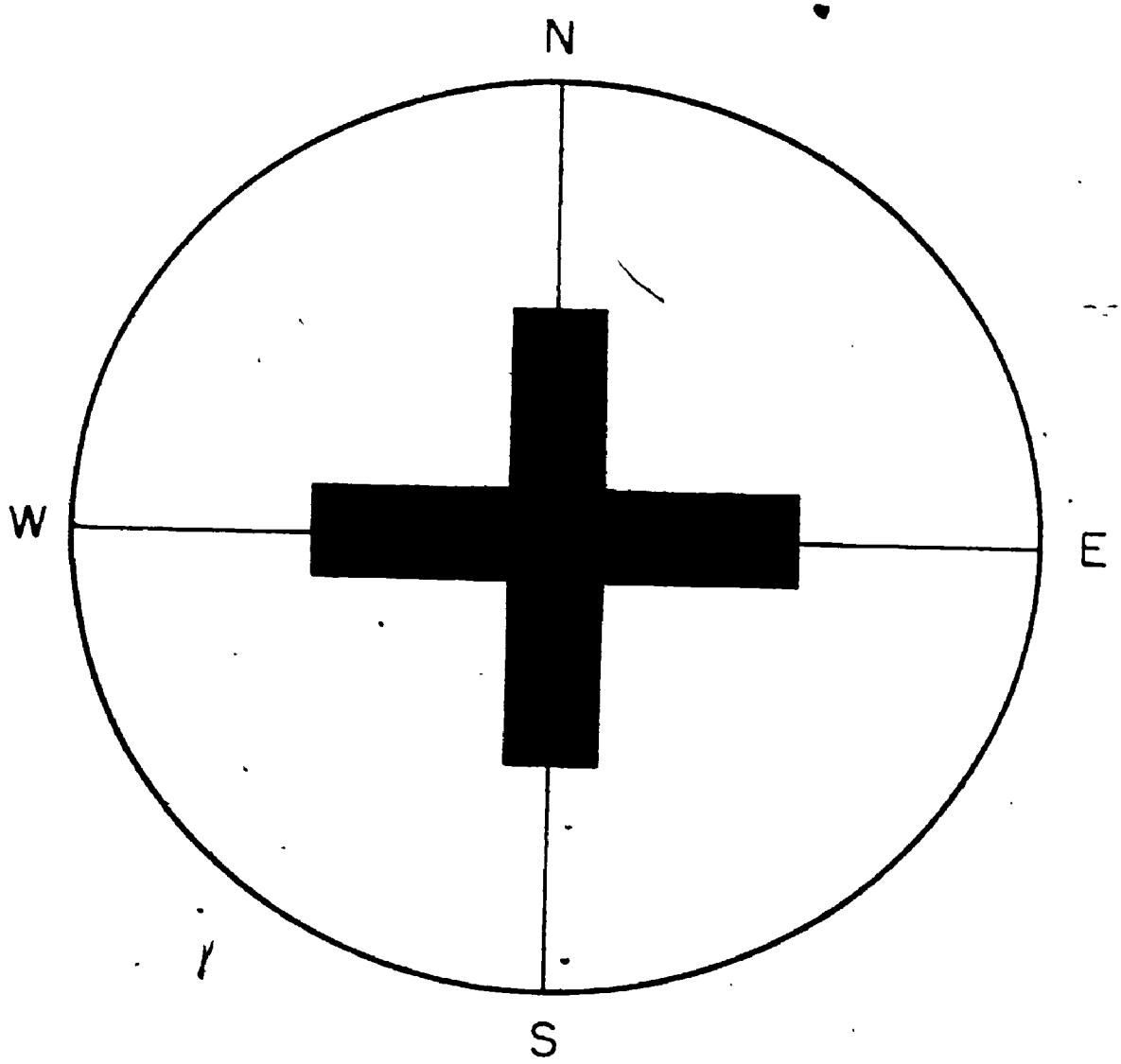

Figure 3: Schematic representation of the field of view in the microscope. A fibre will be at extinction (i.e., will be dark) when it is aligned parallel to either of the transmission axis directions of the polarising filters. The transmission axis of the polariser is aligned in the E-W direction and the transmission axis of the analyser is aligned in the N-S direction.

2.2. Two-Dimensional Orientation

The slow axis of collagen (Bennett 1950) and muscle fibres (Fischer 1944) are parallel to the fibre's morphological long axis, therefore the extinction angle can be used to determine the two-dimensional orientation of the fibre. The fibre whose orientation is to be measured is brought to the centre of the field of view and rotated on the microscope stage until the fibre is at extinction. The extinction angle is then read off the rotating stage. The orientations are measured relative to the eye piece cross-hairs, which are aligned parallel to the transmission axes of the polariser and the analyser (Canham et al. 1986).

Since there are two extinction positions care must be taken to ensure that the same one is found for each fibre analysed. By convention, I always used the extinction angle with the slow axis parallel to the polariser's transmission axis. It is often easy to confirm qualitatively that the correct extinction position has been chosen: if the fibre is viewed under bright field, it can be seen running East-West in the field of view i.e., parallel to the polariser's transmission axis (by convention the field of view is described according to map directions, with the top North (N), the bottom South (S), the left West (W) and the right East (E)). It is sometimes impossible to determine qualitatively that the correct position has been chosen, so the following quantitative method can be used. After extinction has been found, the fibre is rotated through +45°. A retarder (i.e., a birefringent material) is then placed between the fibre and the analyser with its slow axis aligned at +45°. The combined effect of the two retarders (the fibre and the added retarder) will depend on whether or not the correct extinction position has been chosen. If it has, then the fibre's slow axis will be aligned at +45° and will coincide with the orientation of the retarder's slow axis. The combined effect will be obtained by multiplying the matrices of the two together, giving a retarder with a combined retardation equal to the sum of the two individual retarders. For example, if we consider two retarders with phase differences between the two rays of ϕ and δ, with parallel slow

axes (Shurcliff 1962), then

$$\begin{bmatrix} e^{i\phi/2} & 0 \\ 0 & e^{-i\phi/2} \end{bmatrix} \cdot \begin{bmatrix} e^{i\delta/2} & 0 \\ 0 & e^{-i\delta/2} \end{bmatrix} = \begin{bmatrix} e^{i(\phi+\delta)/2} & 0 \\ 0 & e^{-i(\phi+\delta)/2} \end{bmatrix}$$

Thus the magnitude of the phase difference, γ, is $| \gamma | = (\phi + \delta)$

If the slow axes are perpendicular,

$$\begin{bmatrix} e^{i\phi/2} & 0 \\ 0 & e^{-i\phi/2} \end{bmatrix} \begin{bmatrix} e^{-i\delta/2} & 0 \\ 0 & e^{i\delta/2} \end{bmatrix} = \begin{bmatrix} e^{i(\phi-\delta)/2} & 0 \\ 0 & e^{-i(\phi-\delta)/2} \end{bmatrix}$$

the magnitude of the phase difference is $| \gamma | = (\phi - \delta)$.

If the wrong position was chosen then the slow axes of the fibre and the retarder are perpendicular and the result is a retarder with a combined retardation equal to the difference of the two individual components (as shown mathematically above). If the added retarder is a full wave plate with a retardation of 546 nm and the correct extinction is chosen then a shift towards the blue interference colours (from the Fabry colour chart, which can be found in most books on crystallography e.g., Phillips 1971) will be seen i.e., a combined retardation of 546 nm plus the retardation of the fibre. If the wrong position was chosen then the shift will be towards yellow interference colours i.e., 546 nm minus the retardation of the fibre. The exact colours seen will depend on the retardation of the material studied (the above colour descriptions apply to collagen stained with haematoxylin and eosin)

The two-dimensional orientation method may be carried out on either stained or unstained tissue. The advantage of staining is to provide differentiation between different tissue elements. Also, appropriate staining enhances birefringence and makes the precise measurement of extinction angle easier to obtain. Thus, two dimensional fibre orientation can be determined by measuring the extinction angle.

2.2.1. Statistical analysis: The data obtained in this manner deal with two-dimensional orientation and so cannot be analysed using ordinary statistics. Instead circular statistics are used; these have been reviewed by Batschelet (1981) and will be briefly discussed here. The mean direction of a sample of orientations is calculated as follows. The orientation angles are represented by points on the perimeter of a circle with a radius of unit length. Each point is assigned a mass, M. The centre of mass, C, is then calculated. If C is different from the centre of the circle, O, the line OC defines the mean direction of the points. A rectangular coordinate system is used (Figure 4). Let θ_i be one of n observed orientation angles and $\mathbf{a}_i$ the corresponding unit vector. Let x_i and y_i be the rectangular components of $\mathbf{a}_i$.

$$x_i = \cos \theta_i \qquad y_i = \sin \theta_i$$

Let X and Y be the coordinates of the centre of mass of the distribution. Then,

$$X = (x_1 + x_2 + \ldots + x_n) \quad n$$

$$Y = (y_1 + y_2 + \ldots + y_n) \quad n$$

Substituting for x and y,

$$X = (\cos \theta_1 + \cos \theta_2 + \ldots + \cos \theta_n) / n$$

$$Y = (\sin \theta_1 + \sin \theta_2 + \ldots + \sin \theta_n) / n$$

Let R be the length of the resultant vector with components Σx_i and Σy_i, and r be the length of the mean vector with components X and Y. Then

$$r = \sqrt{(X^2 + Y^2)}$$

$$R = \sqrt{[(\Sigma x_i)^2 + (\Sigma y_i)^2]}, \quad R = nr$$

$$r = \frac{1}{n} \sqrt{[(\Sigma \cos \theta_i)^2 + (\Sigma \sin \theta_i)^2]}$$

The mean angle of the sample,

$$\Phi = \arctan (Y/X) \quad \text{if } X > 0$$

$$\Phi = 180^\circ + \arctan (Y/X) \quad \text{if } X < 0$$

The concentration of points is given by r. This term can vary from 1 (if all the points

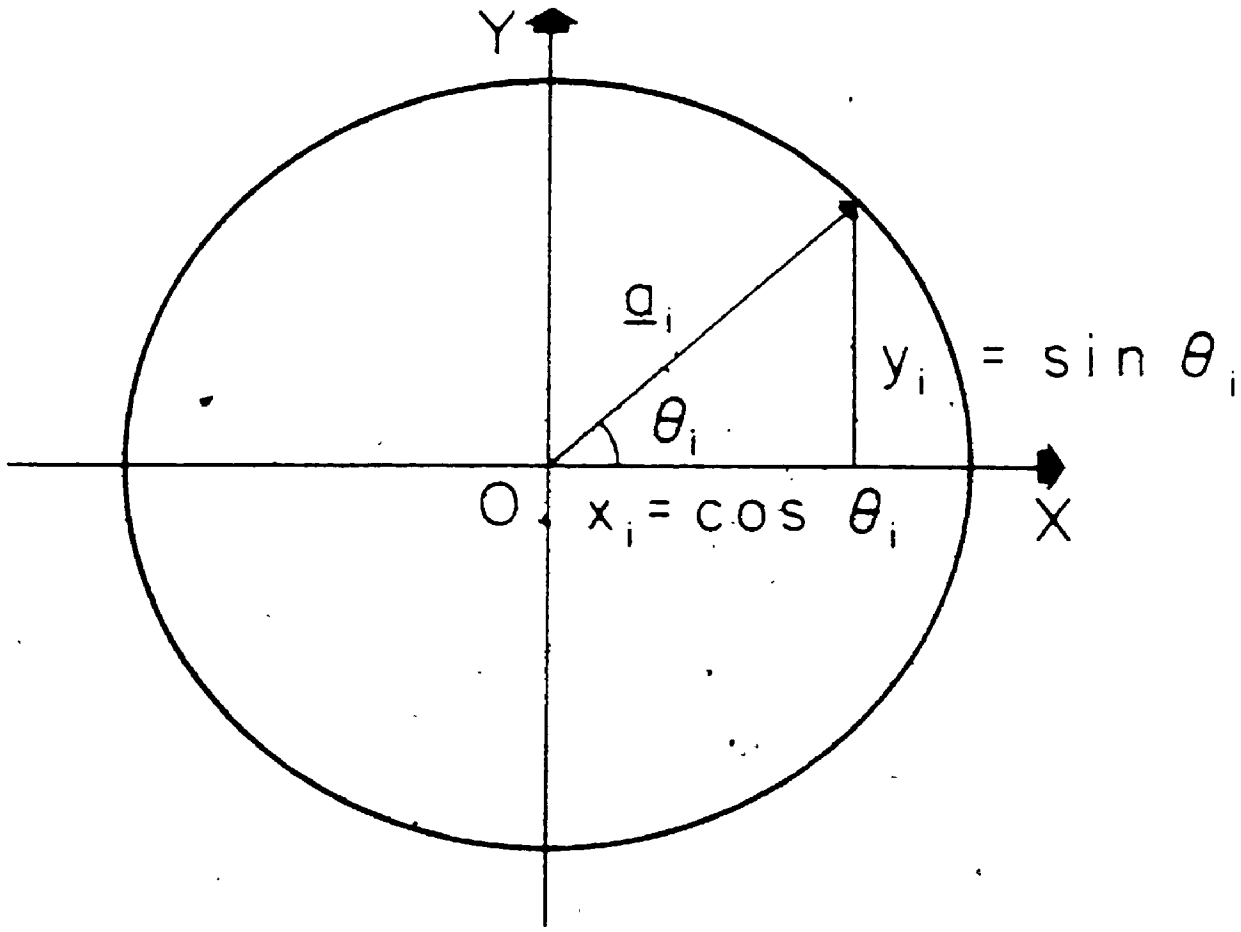

Figure 4: The rectangular components of a unit vector (redrawn from Batschelet 1981, p.10). Each measured orientation is resolved in this manner. The summation of all of the individual components is then used to calculate the mean orientation of each group of orientation angles.

have the same orientation) to 0 The angular variance, s^2, $s^2 = 2 (1 - r)$ (Batschelet 1981), represents the dispersion of the data. The mean angular deviation, s is given by, $s = \sqrt{[2(1 - r)]}$ As a general rule, if the range of orientations is less than 60°, and if the distribution is symmetric, then the mean angular deviation differs from the standard deviation (calculated in the usual way) by less than 1°

2.3. Three-Dimensional Orientation

The methods used are similar to those of the two-dimensional method The same optical properties are exploited, except that, instead of treating the fibre as a projection on the section plane the actual three-dimensional orientation can be determined The same equipment is used as for the two-dimensional study except that a four axis universal stage, with a 20x long working distance objective, is mounted on the rotating stage of the microscope. The universal stage, shown schematically in Figure 5, allows the specimen to be rotated freely in three dimensions

The three-dimensional orientation method derives from structural geology where it is used to measure crystal orientation. The use of the universal stage in Geology (Emmon 1943) and the pioneer work in Biology (Smith 1980, Smith et al. 1981) has been well documented, and will be covered briefly here The optical properties of the birefringent material are used such that the material's optic axis is aligned either parallel or perpendicular to the microscope's stage. For collagen and muscle, the optic axis is parallel to the slow axis and hence parallel to the fibre's long axis. Therefore, the angles through which the stage must be rotated to achieve the alignment of the optic axis give the orientation of the fibre with respect to the section plane. A fibre's three-dimensional orientation is completely defined by two angles: the azimuth angle which gives the orientation in the section plane (the azimuth angle was the only angle measured in the two-dimensional method), and the inclination angle which gives the orientation out of the

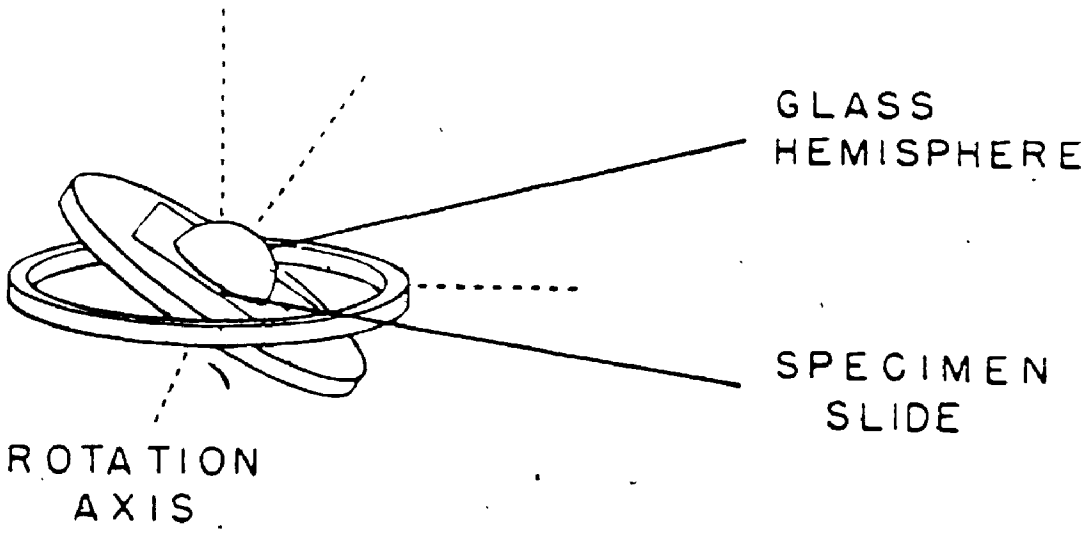

Figure 5: The universal stage. The four rotation axes of the stage are shown. The glass hemispheres above and below the slide ensure that no matter what angle the stage is positioned at, the light rays will always be normal to the surface.

section plane These two angles are read directly off the universal stage

While the universal stage method can be applied to biological tissues, it is much more difficult to obtain an orientation measurement from these tissues than from crystals. Biological tissue is generally less birefringent and often lacks the coherent organisation of crystal samples. To obtain an orientation measurement with the universal stage, an area of >2x2 μm of material must have a uniform orientation (Roubault 1963), a requirement that is often too rigorous for biological samples. This is probably the reason why Bennett (1950, p.639) stated that the universal stage could not be used for the study of biological material

As was the case with the two-dimensional method, the ability to make measurements in three dimensions can be improved by staining the tissue so that its birefringence is enhanced

2.3.1. Statistical analysis: The three-dimensional data obtained are presented in two dimensions using stereographic projections. A Lambert equal area projection was used. The projection is constructed using a reference sphere and is drawn in the plane tangent to the sphere at point A, shown in Figure 6(a). A fibre whose orientation is to be plotted, is hypothetically placed at the centre of the sphere. The fibre is extended until it intersects the surface of the sphere at point B (by convention the projection is done from the lower hemisphere), and is projected to a point C such that AB=AC. Figure 6(b) shows the Lambert projection looking from above, each division shown represents 2° and hence the difference between the centre and the poles is 90°. The three dimensional orientation of a fibre is represented by a point on the Lambert projection.

A plot of the individual data points on a projection is called a scatter diagram. Reference directions are needed to interpret a scatter diagram. For brain arteries, the long axis of the artery provides a convenient reference direction. The scatter diagram is plotted so that a longitudinal fibre (denoted by L and aligned parallel to the artery's

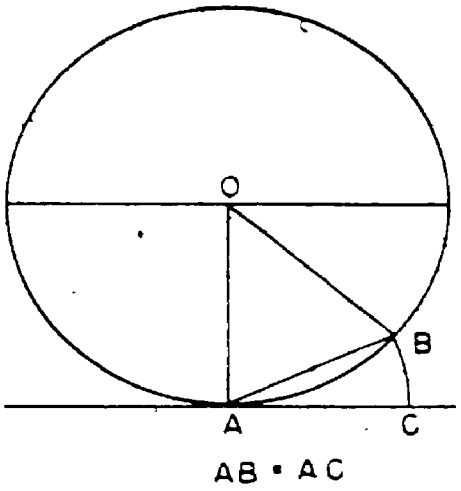

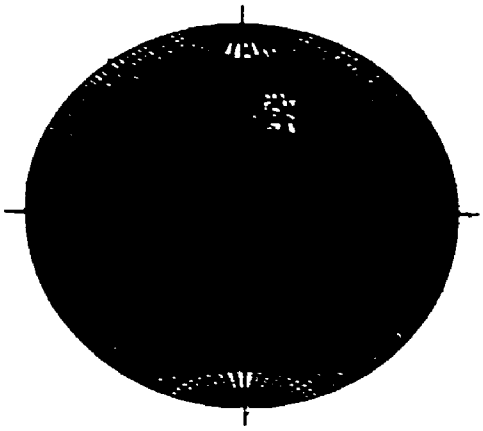

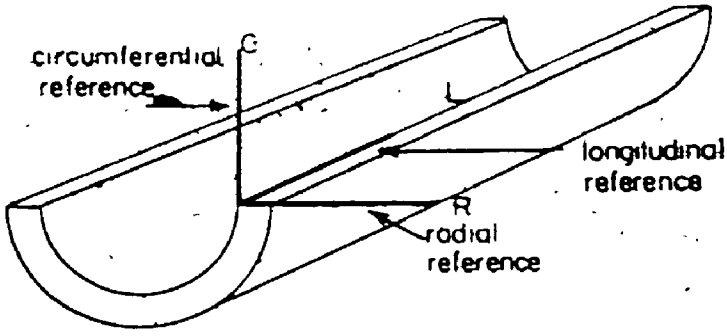

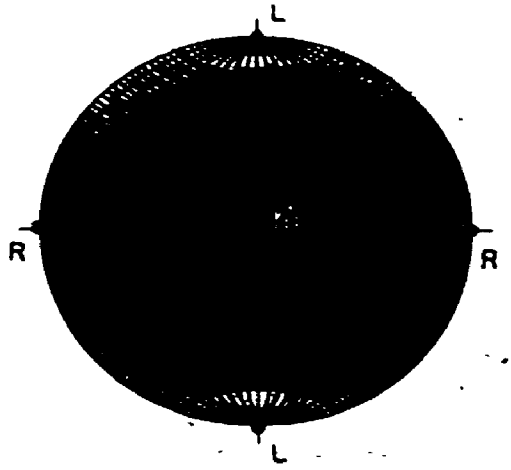

Figure 6: (a) The construction sphere used for the Lambert equal area projections. The fibre whose orientation is to be plotted is "placed" at the centre of the sphere, O, and extended until it cuts the surface of the sphere, B. Point B is then projected onto the plane tangent to the sphere at A, such that AB = AC.
(b) A fully constructed Lambert projection, the point C is shown.
(c) Schematic representation of an artery showing the reference directions that I used on the Lambert projections shown in the rest of the thesis.
(d) The location on the Lambert projection of fibres having orientations parallel to the arterial reference directions is shown.

long axis) appears as a point at either the north or south pole of the Lambert projection. Therefore, a circumferential fibre (C) will appear as a point at the centre and a radial fibre (R) as a point at either the east or west "pole". This is shown in figure 6(c) (d). Dispersion of data along the N-S axis represents a variation in the helical pitch of fibres, while dispersion of data along the E-W axis represents variation in the radial direction this will be referred to as spiral variation. It should be noted that the points on this scatter diagram only show orientation, they do not carry any information about the location of any measurement or the distance between measurements

In this thesis the three-dimensional orientation data are analysed using the statistical parameters k, α_{95} and circular standard deviation (c.s.d.) (Fisher. 1953). Figure 7 shows four separate groups of points analysed using Fisher statistics. The precision parameter, k, varies from zero for a perfectly random distribution, to infinity for a set of identical directions. The parameter α_{95} gives the radius of a circle on the surface of the sphere within which there is a 95% probability of the true mean lying The circular standard deviation is the circle of radius θ about the mean that encloses 63% of the points and is used to calculate the circular standard error (c.s.e.),

c.s.e. = $\theta_{63}/N^{\frac{1}{2}}$, where N is the number of data.

2.4. Retardation Measurements

The second aspect of this thesis is the study of molecular organisation When linearly polarised light passes through a birefringent material, a phase difference is introduced between the two components of the wave. This property forms the basis of the methods of examining molecular organisation. The phase difference is due to the unequal velocities of the two rays passing through the anisotropic material. The difference in the two velocities depends on the material's molecular organisation. Hence, by measuring the retardation, which is proportional to the phase difference, the

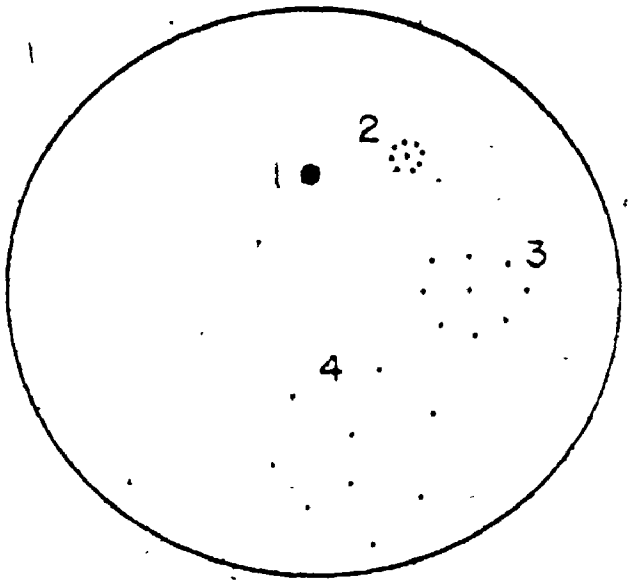

	K	α_{95}	C.S.D.
1	9906	1·7	2·7
2	347	2·8	4·4
3	32	9·2	14·4
4	10·6	16·6	25·1

Figure 7: Lambert projection showing 4 groups of data with the corresponding statistical analyses below: k is the precision parameter, α_{95} gives the radius of the circle in which there is a 95% probability of finding the mean orientation, CSD is the circular standard deviation for each group (redrawn from Tarling 1971, p.78).

molecular organisation of different materials may be compared. The retardation, Γ, is given by the formula $\Gamma = t\,(n_e - n_o)$ (Bennett 1950, p.611), where t is the section thickness and n_e and n_o are the refractive indices of the two rays called the extraordinary and the ordinary ray respectively. The term $n_e - n_o$ is called the intrinsic birefringence of the material. Besides the contribution of the intrinsic molecular organisation to retardation, there is another contribution called form birefringence. Form birefringence arises from the difference in refractive index between the material being studied and the surrounding medium. The contribution of form birefringence, $(n_e - n_o)_f$, to the retardation is given by $(n_1^2 - n_2^2)^2 F$, where n_1 is the refractive index of the material, n_2 the refractive index of the mounting medium, and F is a form factor (Bendet and Bearden 1972), which depends on volume fractions of the different components and the nature of the fibres. The mathematics developed to calculate F assume that a two component system is being studied i.e., the surrounding or imbibing medium and the material. Collagen, however, because of its attendant ground substance is more complex, and the equations cannot be rigorously applied. But when $n_1 = n_2$ the form birefringence will be zero regardless of the value of F, and so only the intrinsic birefringence will contribute to the retardation. Therefore, if collagen's retardation is measured in a series of different media with different refractive indices the retardation at the minimum of a retardation versus refractive index graph will be proportional to the intrinsic molecular organisation. This procedure is called imbibition analysis. Graphs of retardation versus refractive index are called form birefringence curves (an example is shown in Figure 8).

Molecular organisation has been shown, using X-ray diffraction (Sinex 1968), to increase as collagen matures. This increase in molecular organisation will change the optical properties of the collagen and increase its intrinsic birefringence. The method of imbibition analysis has been used to detect increasing collagen molecular organisation in scar tissue (Mello et al. 1975). It is important that the fluids chosen for this technique are able to imbibe fully the collagen but not react with it. My choice of fluids was

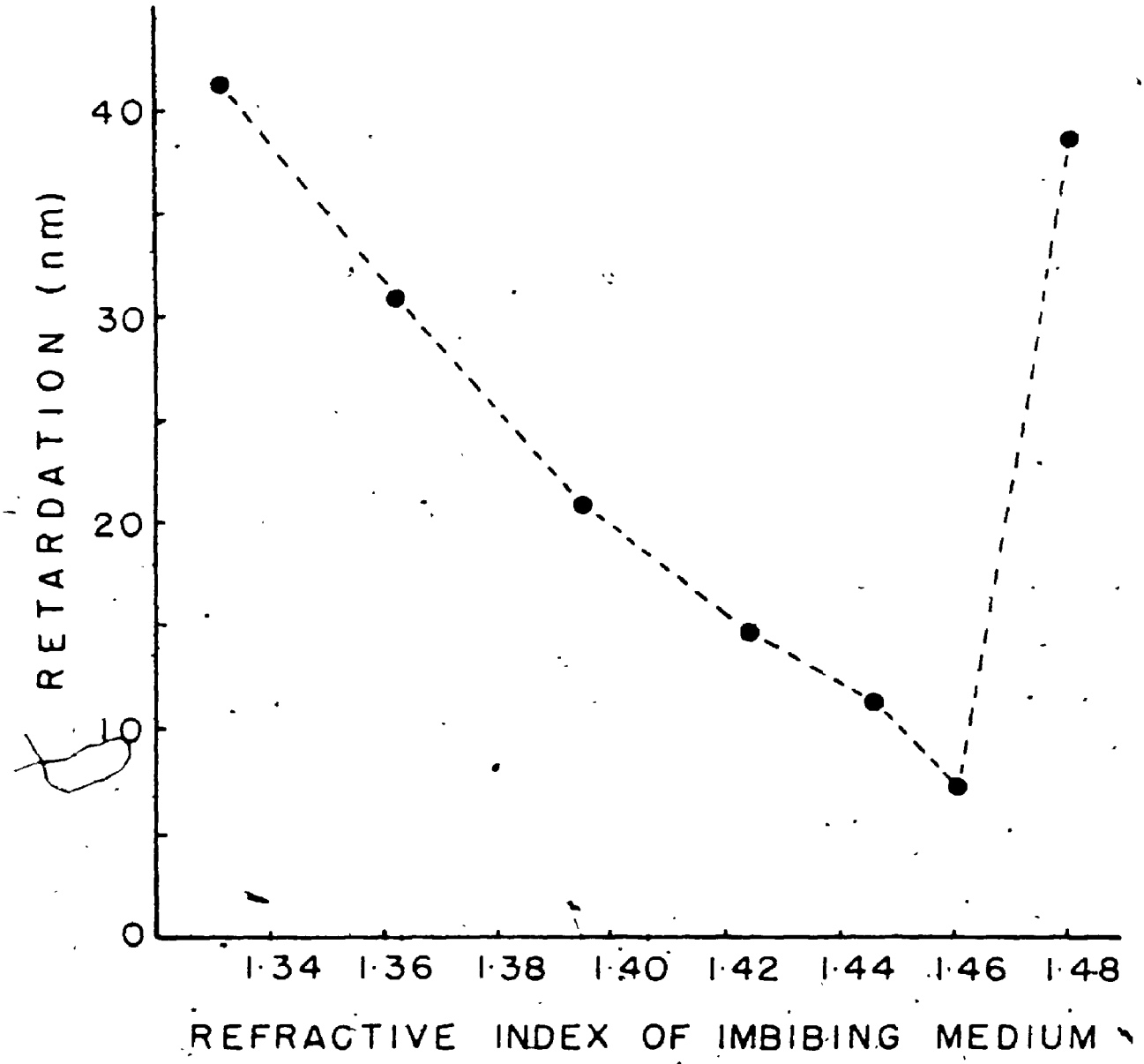

Figure 8: Example of a form birefringence curve for collagen. The collagen is from a 7 μm section of normal human mitral valve tendon. The retardation of linearly polarised light by collagen was measured in a series of fluids with different refractive indices (shown on the x-axis). Each point on the curve represents an average of ten measurements. The minimum of the curve, which was used to calculate the intrinsic birefringence of the collagen, occurs at a refractive index of 1.46.

determined by the work of Mello, Vidal and co-workers (e.g., Vidal 1980). The fluids used are shown in Table 2 with their refractive index (measured using an Abbe refractometer). Collagen's form birefringence curves cannot be quantitatively analysed (because collagen is not a simple two component system), however, qualitative interpretation of the form birefringence curves can be used as a guide to the nature of the system.

2.4.1. Imbibition analysis: Sections cut at 7 μm thickness were cleared of paraffin embedding wax by immersion in xylene. If cholesterol was also present in the section, it was removed by placing the section in hot acetone for thirty minutes (Drury and Wallington 1967, p.299). These two substances must be removed because they are strongly birefringent and overwhelm the weaker birefringence of the collagen. The acetone treatment did not affect the optical properties of the collagen. The sections were then hydrated through graded alcohols and soaked in water until fully imbibed i.e., further soaking in that fluid will produce no change in retardation (details of the actual retardation measuring procedure will be given later). Figure 9 shows how retardation varied with time for human mitral valve tendon collagen in 20% glycerol solution. The retardation stabilised after about one hour. I therefore used one hour as the time for imbibition in all the glycerol solutions. After imbibing in water, the first solution, a coverslip was placed over the section to prevent it from drying out and the retardation measured. This procedure was repeated through the series of imbibing media. After the 100% glycerol solution, the sections were washed with distilled water before imbibing for two hours in paraffin oil. Form birefringence curves were then constructed. The refractive index at the curve's minimum gives the refractive index of the collagen. The refractive index of collagen is often quoted as 1.53 (e.g., Hutschenreiter and Scheuner 1970), whereas I consistently found the minimum to occur at a refractive index of 1.46, agreeing with the imbibition analysis studies of Mello and Vidal (e.g., Vidal 1980, Mello et al. 1979). A possible explanation relates to the preparation of the tissue. To resolve

IMBIBING MEDIUM	REFRACTIVE INDEX
water	1.33
20% glycerol	1.36
40% glycerol	1.39
60% glycerol	1.42
80% glycerol	1.44
100% glycerol	1.46
paraffin oil	1.48

Table 2: The media used in the imbibition analysis and their refractive indices.

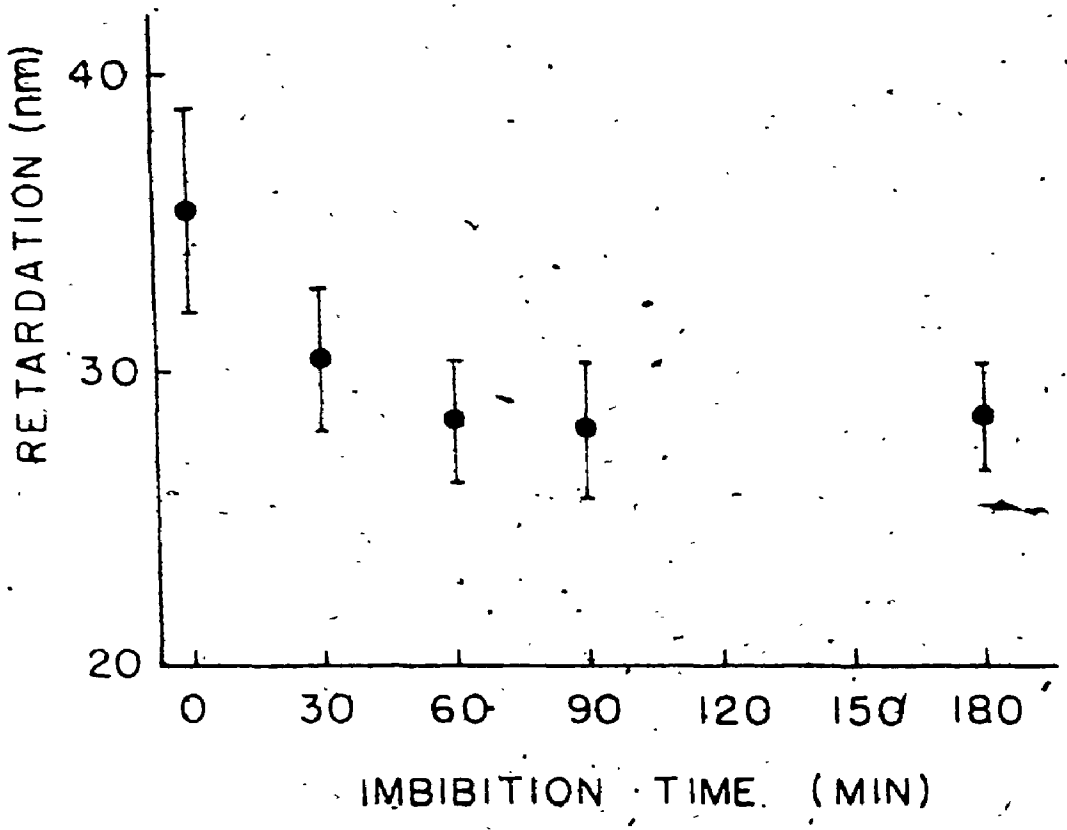

Figure 9: Determination of imbibing time. The retardation was measured in a human mitral valve tendon imbibed in a 20% glycerol solution. The retardation measured at zero time was the retardation measured in water. After 60 minutes the tissue was fully imbibed ie, further soaking produced no significant change in retardation. Each point on the curve is the average of ten retardation measurements. The standard deviations are shown by the bars.

the issue, I analysed reconstituted collagen in the same manner (Figure 10) and found the minimum of the form birefringence curve to be between 1.52 and 1.53 in agreement with the literature. The reconstituted collagen is essentially pure, the ground substance having been removed. This is not the case for the tendon collagen. The intrinsic birefringences calculated for biologic tissues should be regarded as that of the molecular organisation of the whole collagen matrix i.e., collagen plus ground substance. It should also be noted that the tissue has been fixed in formalin, a process which tends to increase the molecular organisation by the formation of cross links. Since all the tissue was fixed in the same way, the results can be compared quantitatively.

The retardations were measured using the method of de Senarmont with monochromatic light (λ = 546 nm) (Bennett 1950). The correct extinction position was found and the fibre rotated through +45°. A quarter wave plate (a device that introduces a phase difference of $\pi/2$ between the ordinary and the extraordinary rays) was inserted above the fibre with its slow axis parallel to the polariser's transmission axis. The elliptically polarised light emerging from the fibre is converted to linearly polarised light by the quarter wave plate. The azimuth of the linearly polarised light emerging from the quarter wave plate depends on the retardation of the fibre. The analyser is then rotated until its transmission axis is at right angles to the azimuth of the emerging beam (i.e., no light passes through the analyser and the fibre is dark). The angle, θ, through which the analyser was rotated to achieve this extinction was recorded and the retardation, Γ, was calculated from the formula, $\Gamma = (546/180) \times \theta$ (Bennett 1950, p 657). The mathematical confirmation of this method is outlined below.

quarter wave plate fibre

$$\begin{bmatrix} 1 & 0 \\ 0 & i \end{bmatrix} \begin{bmatrix} m_{11} & m_{12} \\ m_{21} & m_{22} \end{bmatrix} \begin{bmatrix} 1 \\ 0 \end{bmatrix} = \begin{bmatrix} m_{11} \\ im_{21} \end{bmatrix}$$

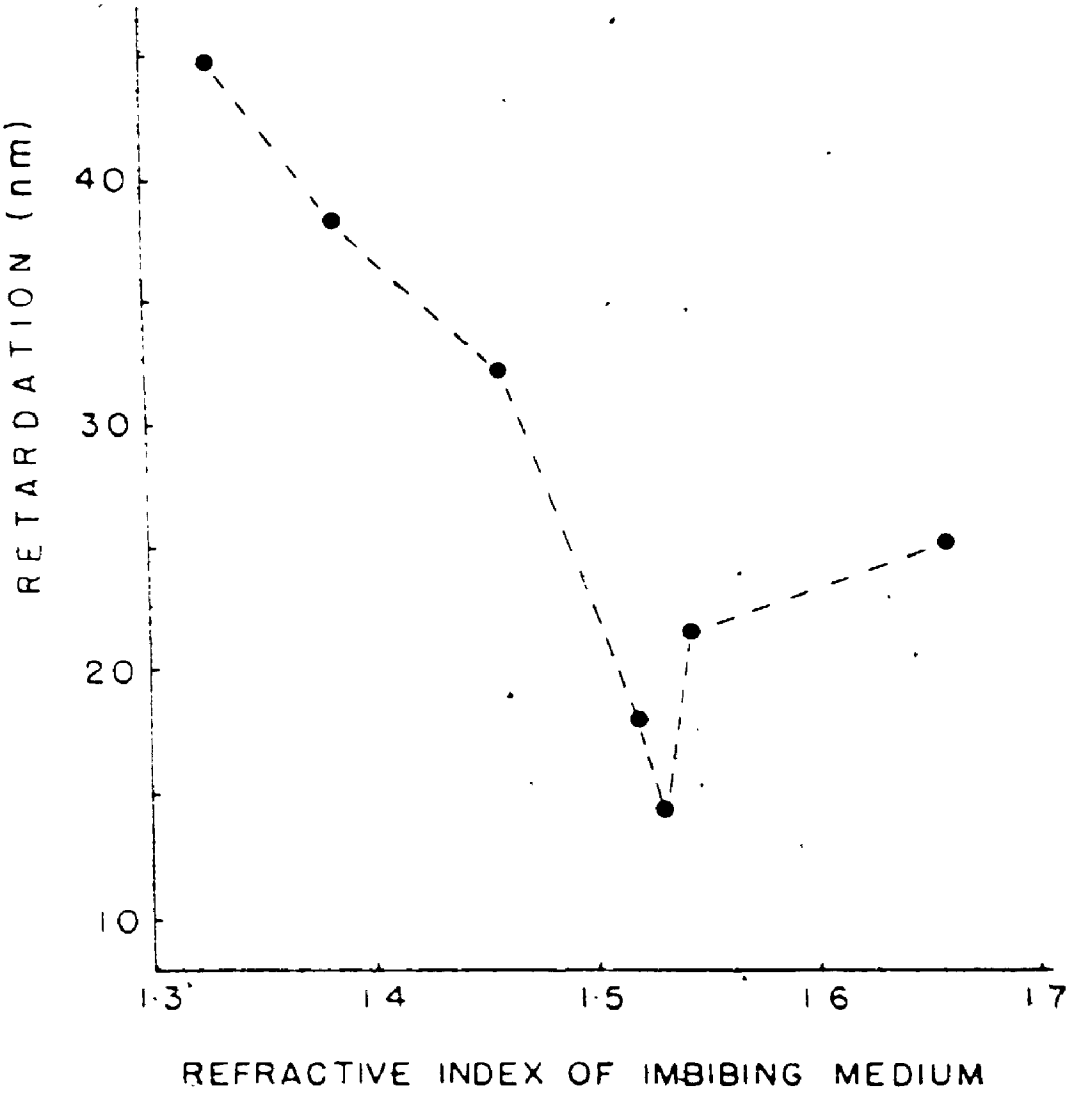

Figure 10: Form birefringence curve for reconstituted collagen (provided by Dr. M. H. Sherebrin, Department of Biophysics, U.W.O.). The minimum retardation occurs at a refractive index of ≈ 1.53. Compare this with Figure 8, where the minimum occured at a refractive index of 1.46. The reason for the difference relates to the preparation of the tissue. The reconstituted collagen has had its ground substance removed.

Substituting for m_{11}, m_{21} from Shurcliff (1962),

$$\begin{bmatrix} m_{11} \\ im_{21} \end{bmatrix} = \begin{bmatrix} \cos^2\theta + e^{-i\delta}\sin^2\theta \\ i\cos\theta\sin\theta\,(1 - e^{-i\delta}) \end{bmatrix}$$

Since $\theta = 45°$, a factor of $\cos^2\theta$ can be removed,

$$\equiv \begin{bmatrix} 1 + e^{-i\delta} \\ i\,(1 - e^{-i\delta}) \end{bmatrix}$$

taking out a factor of $e^{-i\delta/2}$, and substituting the identities

$$2\cos\theta = e^{i\theta} + e^{-i\theta} \qquad 2i\sin\theta = e^{i\theta} - e^{-i\theta}$$

$$\equiv \begin{bmatrix} \cos\delta/2 \\ -\sin\delta/2 \end{bmatrix}$$

This is linearly polarised light with an azimuth proportional to δ, the phase difference

2.4.2. Measurement of retardation in stained tissue: The natural birefringence of tissue can be enhanced by staining with dyes which have an anisotropic molecular structure Light passing through such dyes interacts with electrons oscillating in their chemical bonds, thus affecting the light's velocity If the dye molecules are aligned in a preferred manner they will be birefringent. Therefore, if positively anisotropic dye molecules are bound parallel to well aligned fibres, the anisotropy of the dye will be added to the anisotropy of the fibre. The increased birefringence produced by this addition will be proportional to the amount of dye bound in an oriented manner (Puchtler et al. 1973) If the dye molecules are bound at right angles to the fibre then the fibre's birefringence will be diminished or possibly made negative. Randomly bound dye molecules will not enhance the birefringence of the fibre (Figure 11). Therefore, information about the molecular structure of birefringent material can be gained by observing the retardation changes that occur following staining with anisotropic dyes. Such techniques have been used in the textile industry for many years with the results confirmed by X-ray diffraction (e.g., Preston and Tsien 1950). Enhancement of birefringence by staining

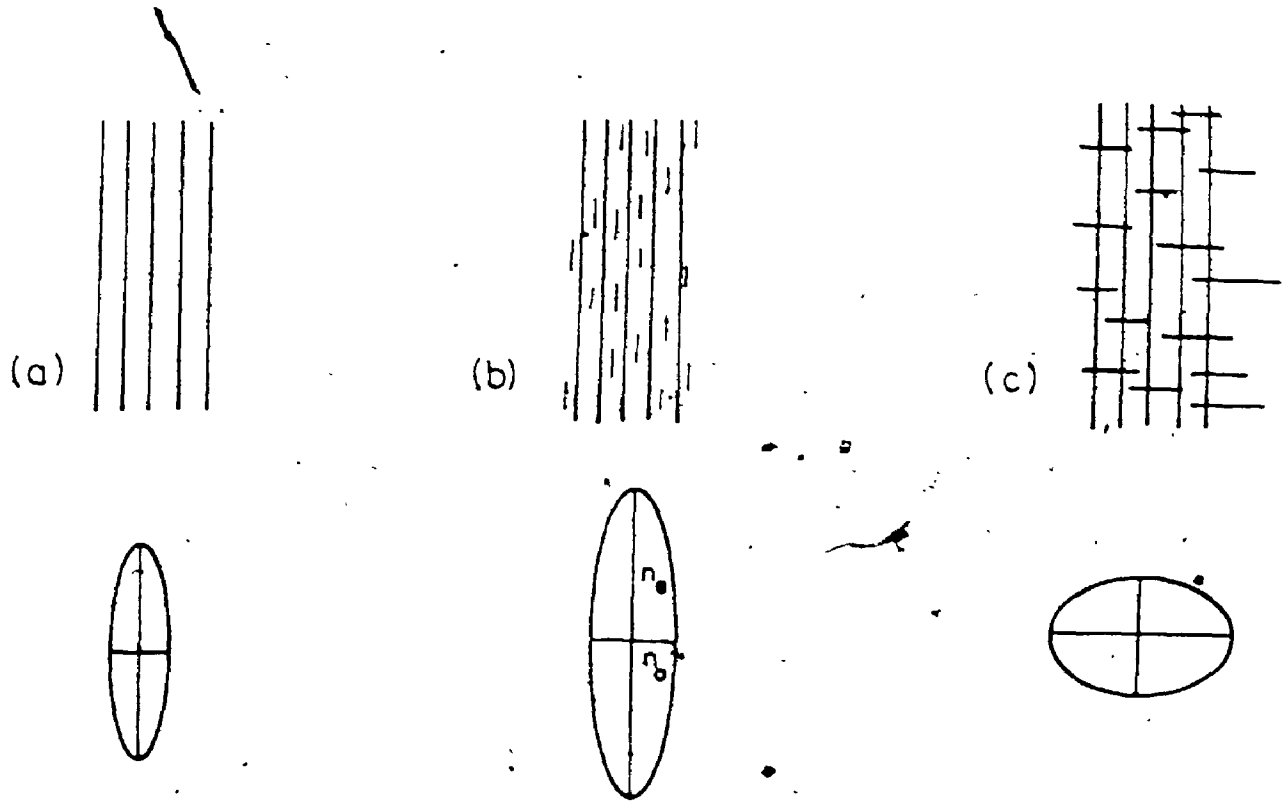

Figure 11: Schematic diagram showing how the alignment of collagen fibrils and stain molecules contribute to birefringence.
(a) The difference between the axes of the ellipse represents the intrinsic birefringence, ($n_e - n_o$), of the collagen. The two axes of the ellipse represent the refractive indices of the ordinary and extraordinary rays ($n_e > n_o$).
(b) The birefringence is increased when anisotropic dye molecules are bound parallel to the collagen fibrils ($n_e >> n_o$).
(c) If anisotropic dye molecules are bound at right angles to the collagen. The combined birefringence may be diminished, or even become negative as shown ($n_e < n_o$).
Therefore, by measuring the retardation of collagen fibres after staining with anisotropic dyes one can obtain information about the orientation of the bound dye and hence, indirectly, about the molecular organisation of the collagen.

to reveal molecular organisation was not used in biology until the late 1960s, when it was found that the azo dye picrosirius red increased the birefringence of collagen (Constantine and Mowry 1968). Collagen is rich in basic amino acids and reacts strongly with acidic dyes. Sirius red is an elongated molecule containing six sulphonic acid groups as shown in Figure 12. The sulphonic acid groups may react at low pH with the amino groups of lysine and hydroxylysine and the guanidine groups of arginine (Junqueira et al 1979). Collagen stained with picrosirius red exhibits positive linear dichroism i.e., linearly polarised light for which the vibration plane is parallel to the stained fibres will be absorbed far more than when the two are at right angles (Puchtler et al. 1973). Thus one may assume that the dye molecules' long axis are mostly parallel to the collagen fibres (Vidal et al. 1982). It has been shown that the ability to bind dye depends on the molecular state of the collagen (Joiner et al. 1968). Immature collagen which has a lesser degree of molecular organisation than mature collagen cannot bind as many dye molecules in a preferred way. Instead of using picrosirius red, eosin was used for the retardation measurements (with eosin it was easier to judge when the birefringence of the collagen had been compensated). The eosin molecule, although anisotropic, is smaller than the sirius red molecule, and therefore does not produce as much enhancement of the collagen's birefringence. Comparison of tissue from different specimens may be achieved by staining them at the same time. Simultaneous staining of tissue sections is not always possible and because there are other factors which determine the amount of dye bound e.g., time spent in the dye solution and the duration of the wash, comparison of tissue stained at different times would be difficult. But if two different "kinds" of collagen occur on the same slide (e.g., normal and pathological) then both will have been subjected to the same staining conditions. Therefore, variability of retardation introduced by staining at different times can be eliminated by expressing the retardations of the two "kinds" of collagen as a ratio. Thus samples stained at different times may be compared. Hence, retardation measurements can be used to determine if different collagen

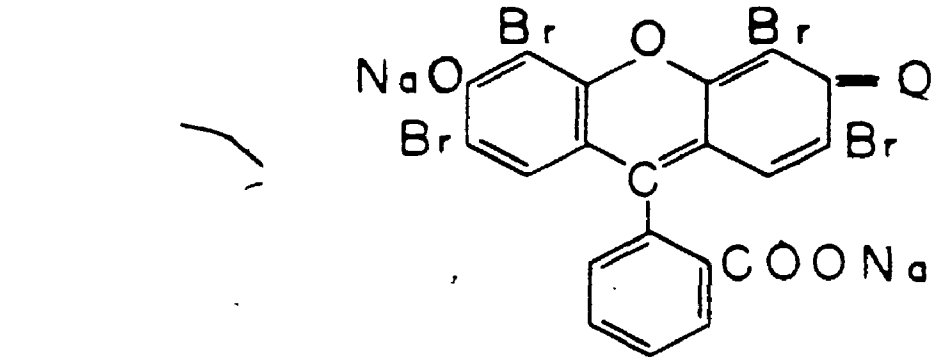

EOSIN

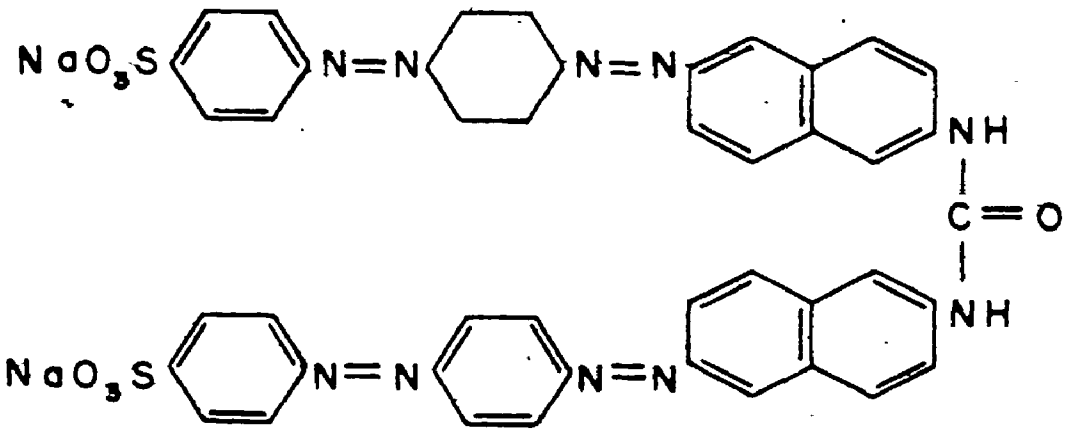

SIRIUS RED F3B

Figure 12: Schematic representation of the molecular configuration of eosin (Lillie 1977, p.342) and picrosirius red (*ibid*. p.199). The picrosirius red molecule is larger and therefore produces a greater increase in the birefringence of collagen than eosin.

fibres have different dye binding characteristics and hence different molecular organisations.

Retardation also depends on the thickness of the sample. To determine the relationship between retardation and section thickness, the following blinded study was done. Three chordae tendineae were sectioned (by J.G. Hicks, Biophysics Department U.W.O.) longitudinally at 4, 5, 6, 7, 8, 10, and 12 μm and all stained with eosin at the same time (I assumed that collagen occupied the entire section thickness). Without knowing the section thickness, I measured the retardation at ten different positions on each section. This procedure was done for all three chordae. For each of the three chordae the results were expressed as a percentage of the retardation of the 12 μm sections. These percentages were plotted as a function of section thickness (Figure 13). The high correlation coefficient ($r = 0.969$) indicates that there is a linear relationship between thickness and retardation.

The advantage of measuring the retardation of the stained tissue over the imbibition analysis of unstained tissue is that the larger retardations create the possibility that more subtle changes in molecular organisation might be detected. It is much quicker because only one set of measurements is made and is also easier because the retardations are greater.

2.5. Tissue Staining

2.5.1. Picrosirius red staining method: Picrosirius red has a qualitative use in polarised light microscopy. Collagen stained with picrosirius red has been observed to show different interference colours (Junqueira et al. 1978). These colours depend on the thickness of the fibres (Junqueira et al. 1982). The different interference colours can be used to detect fibres that have been degraded and also to distinguish between Type I and Type III collagen. In 7 μm sections, normal mature Type I collagen fibres stained with picrosirius red appear red or orange when viewed with polarised light. If a fibre has been

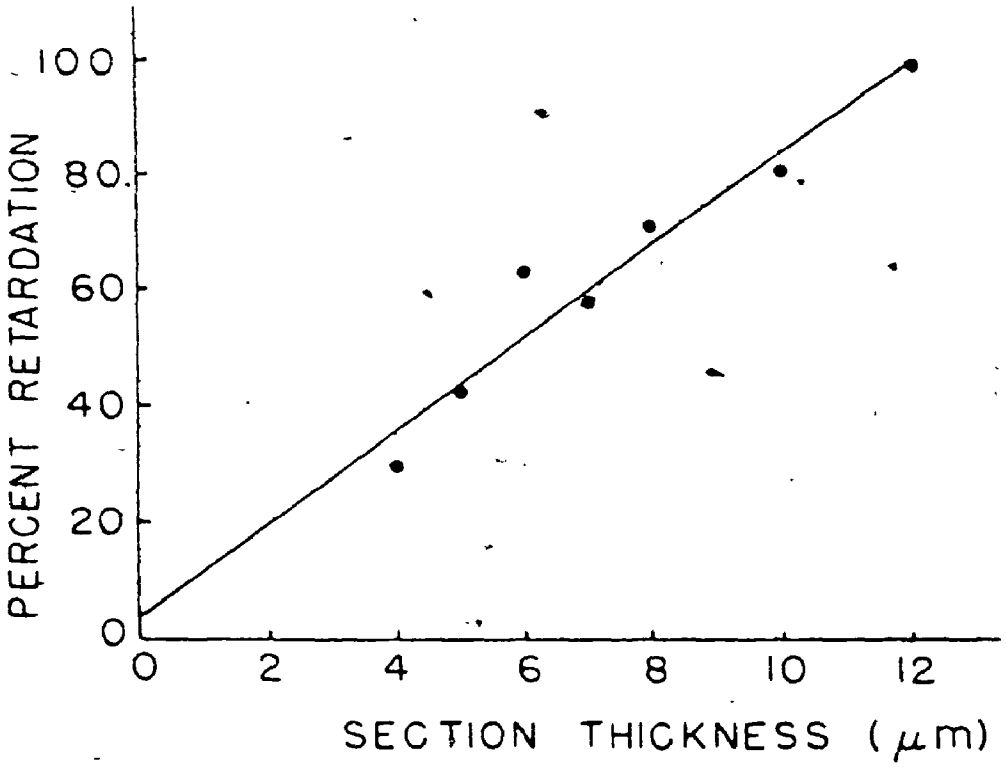

Figure 13: The relationship between retardation measured in tendon collagen and section thickness (r=0.969). The retardation is expressed as a percentage of that in 12 μm eosin stained sections. Each point represents the average of measurements taken on three different sections.

degraded, then the colour changes from red/orange to yellow to green as the fibre gets thinner. Such changes have been observed in vivo (Junqueira et al. 1980) and in vitro (Perez-Tamayo and Montfort 1980) in sections prepared in the same manner as in this thesis. If the degradation proceeds further, then even though dye may be bound to the collagen, it may not be bound in an oriented way and so the fibre will not be birefringent.

Type III collagen fibres are thinner than Type I fibres, so in 7 μm sections they appear either yellow or green. Differentiation between Types I and III can be clearly seen in brain arteries: the collagen in the tunica adventitia (Type I) is orange, while the collagen in the tunica media (Type III) is yellow or green (see Plate 1).

2.5.2. Other stains: Picrosirius red and haematoxylin and eosin were the stains of preference used most frequently to enhance birefringence in the orientation experiments; however, two other stains, Gomori silver impregnation and Masson's trichrome, were also used. The former is especially useful since it enhances the birefringence of both collagen and smooth muscle and permits their differentiation.

2.6. Orientation Measured by Retardation

The orientation of birefringent material can be determined by measuring the retardation produced at different fibre orientations. I did not make extensive use of this technique, but it is of interest because it combines the two main methods of the thesis. If an orientation reading cannot be made using the universal stage (because the coherent zone is too small), then a retardation measurement is taken instead. First, the retardation is measured with the slide parallel to the microscope stage and then the retardation is measured at different inclination angles of the universal stage. A graph of retardation versus inclination is plotted (a correction for the retardation must be made

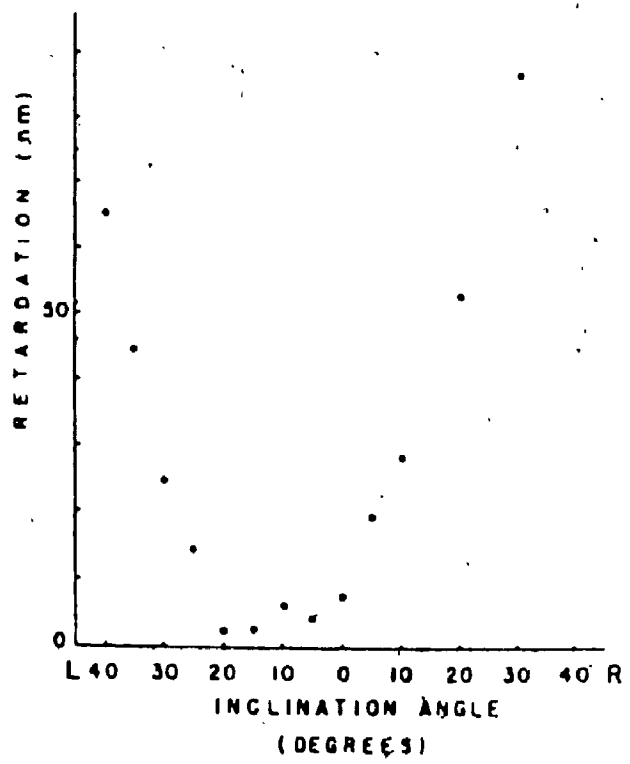

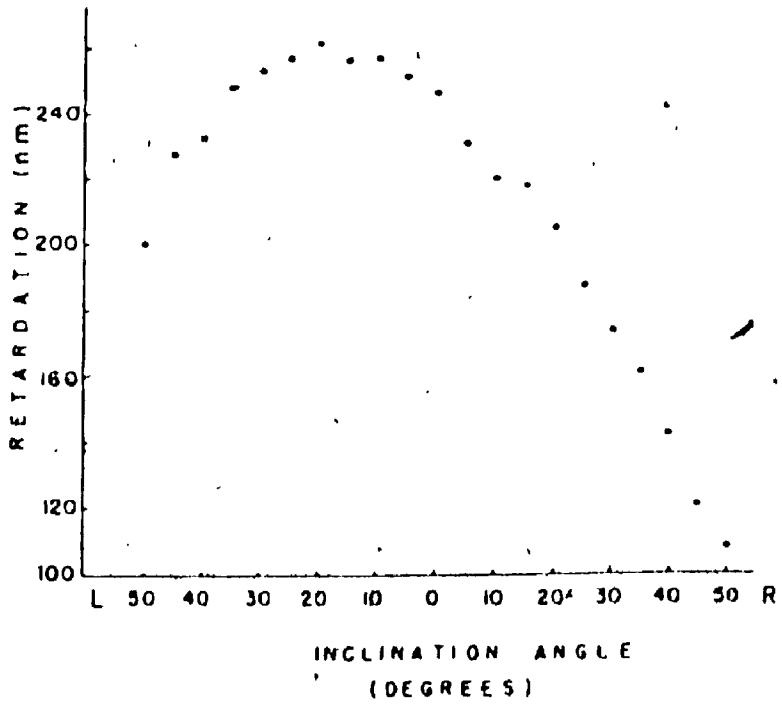

Figure 14:(a) Graph showing how retardation varied as a function of the inclination of the Universal stage for a single collagen fibre bundle in the apex of a mid-plane longitudinally sectioned cerebral artery bifurcation. The minimum of the curve will occur when the collagen fibres are aligned parallel to the tube of the microscope. No orientation measurement could be made with the universal stage. However, the shape of this curve was expected because the electron microscopy study of the bifurcation indicated that the collagen is aligned at right angles to this section plane. Therefore, a minimum retardation would be expected around 0°. The section was stained with picrosirius red.
(b) Obliquely sectioned mitral valve tendon stained with picrosirius red. Retardation measurements were made on the same zone of collagen at different inclinations of the Universal stage. The location of the maximum is in good agreement with the orientation angle of 15° measured on the Universal stage.

because as the inclination is increased then so does the apparent section thickness). The inclination angle at which the maximum retardation occurs (or the minimum, depending on whether the fibre is aligned horizontally or vertically) will give the fibre's orientation (Figure 14). This method is not as accurate as the universal stage but does provide an approximate measurement of the orientation when a measurement cannot be taken with the universal stage.

2.7. Tissue Preparation

All of the tissue used was fixed in 10% neutral buffered formalin. The artery samples were perfusion fixed at a range of physiological pressures so that the tissue's in vivo geometry and architecture could be maintained (method of Hassler 1961). All of the tissue was embedded in paraffin wax, sectioned at 7 μm and mounted on strain free glass slides. The latter are important because strained glass is birefringent and can easily overwhelm the weak natural birefringence of biological tissue. Prior to mounting the sections, albumin fixative was smeared on each slide to deposit a thin film. This helped the sections to lie flat, a necessary condition when three dimensional orientation was measured, and also helped the sections to adhere to the slide during imbibition analysis. The mounting media used were Permount (refractive index 1.52) and Depex (refractive index 1.53). Special features of tissue preparation are covered in the appropriate chapters.

In summary, the different techniques used and the information that each provides is shown in Figure 15.

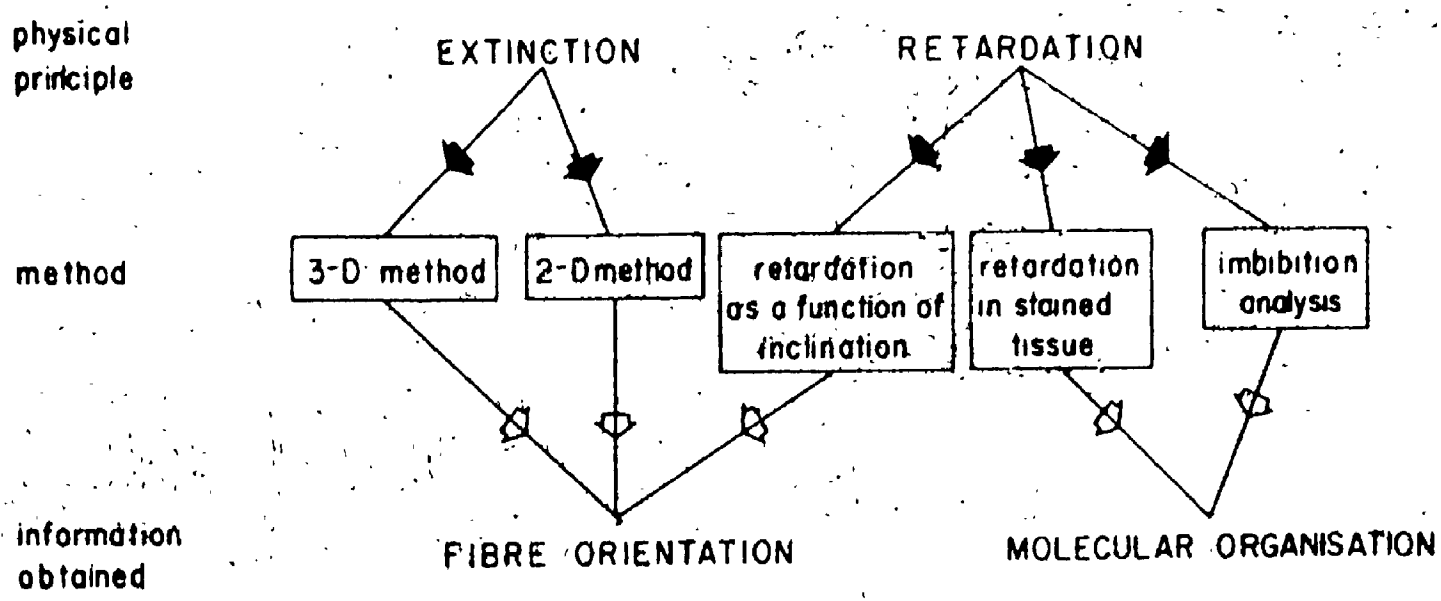

Figure 15. Summary of the methods used.

CHAPTER 3 TWO DIMENSIONAL ORIENTATION METHOD

3.1. Introduction

This chapter illustrates the use of the two dimensional orientation method, applied to the study of cardiac muscle fibre organisation in the interventricular septum of the heart. The interventricular septum divides the left and right ventricular chambers and when sectioned transversely it appears as a trilayered structure (Figure 16). In the outer two layers, the muscle fibres are obliquely aligned, but in the central layer the fibres lie predominantly in the section plane (Maron and Roberts 1981). In normal hearts the muscle fibres in the central layer generally run parallel to each other and are aligned circumferentially in the septum. Teare (1958) first described a heart muscle disorder that primarily involved the muscle cells within the septum. In this disorder the septum is abnormally thick in proportion to the remaining myocardium and produces clinical problems by obstructing the left ventricular outflow tract. This disorder is called hypertrophic cardiomyopathy (HCM). The pathologic features described by Teare consisted of a bizarre and disorganised arrangement of muscle bundles in the asymmetrically hypertrophied septum. Since then many criteria have been used to describe the presence of HCM, but it is the disorganisation of the cardiac muscle fibres in the septum that has been most commonly used to make a diagnosis at autopsy. Originally, it was thought that cardiac muscle fibre disorganisation was unique to HCM (Ferrans et al. 1972). Later work has shown, however, that muscle disorganisation is present in other heart diseases such as cor pulmonale and pulmonary and aortic atresia (Van der Bel-Kahn 1977, Bulkley et al. 1977a). In fact, fibre disarray has even been observed in normal hearts (Bulkley et al. 1977b, Becker and Caruso 1982). These findings have led to concern about the importance of fibre disorganisation as a reliable morphological marker for HCM. Davies (1984) suggested that if the extent of the muscle disorganisation is taken into account, then a

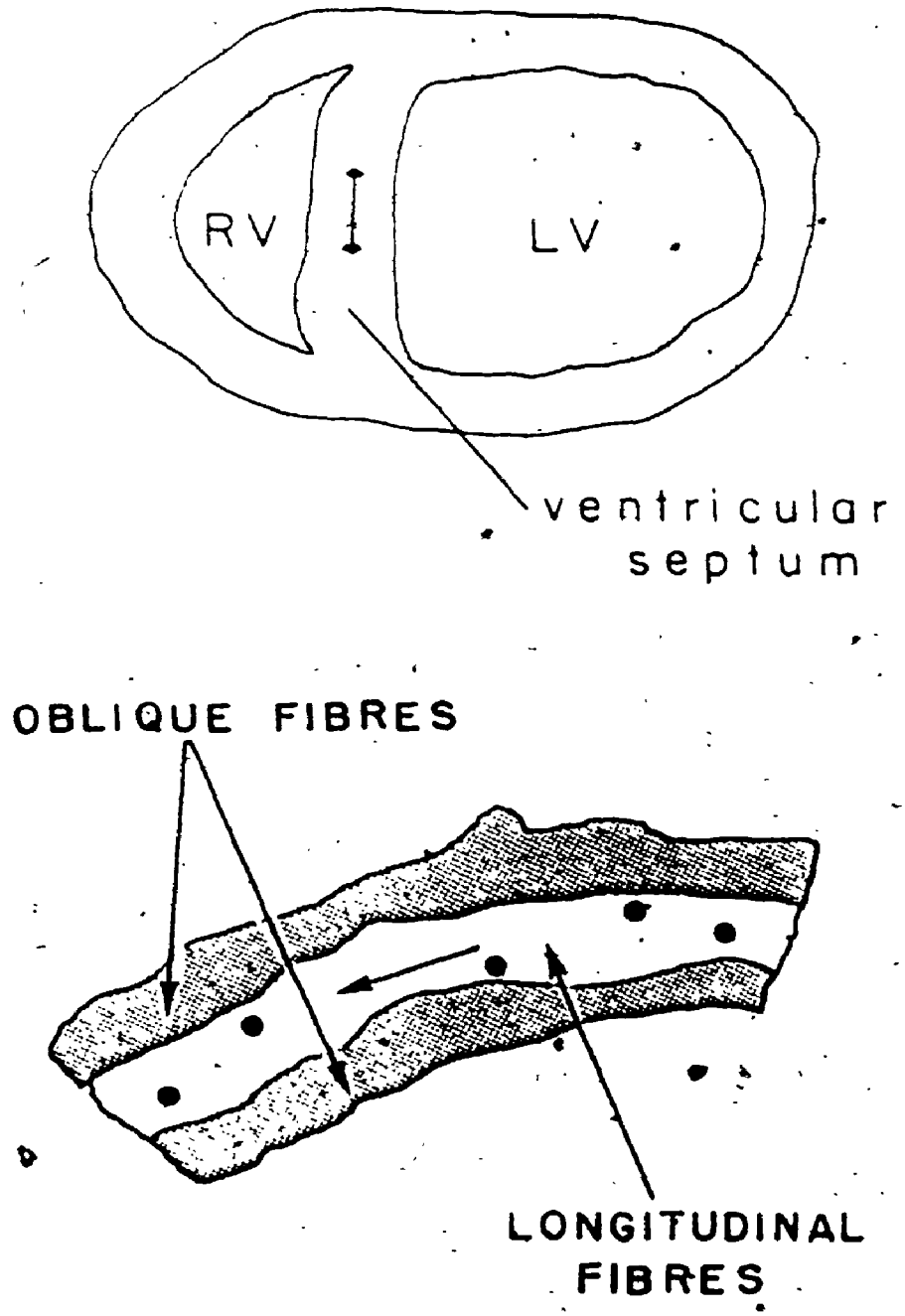

Figure 16: Transverse section of the heart showing the left (LV) and right (RV) ventricles and the interventricular septum (IVS). The septum is shown enlarged in (b). The location of the longitudinal (i.e., fibres that run circumferentially in the septum) and oblique fibres is indicated. The arrows indicate the circumferential direction.

diagnosis of HCM could be confidently made The extent of disorganisation may, however, only be determined if disorganisation itself can be recognised.

There is no standard definition of what constitutes muscle fibre disorganisation Therefore, each investigator must make a subjective assessment of what muscle is disorganised and what muscle is organised. Several methods of categorising different kinds of fibre disorganisation have been developed, ranging from purely qualitative descriptions, to the semiquantitative assigning of type numbers based on the pattern of disorganisation (Van der Bel-Kahn 1977, Maron and Roberts 1979) The current definition of normal fibre organisation derives from anatomical descriptions given by Streeter (1979) and Greenbaum et al. (1981). But such gross descriptions are inadequate to detect subtle changes in muscle organisation. Thus, a precise definition of normal organisation is essential for an appreciation of disorganisation.

Muscle organisation is inherently defined by the fibre orientation Quantitative polarised light microscopy is ideal for studying the two dimensional orientation of cardiac muscle since the contractile proteins of the muscle have an anisotropic molecular organisation making the fibres birefringent.

3.2. Methods

Sections from twelve ventricular septa were examined. Six samples were from patients with HCM (supplied by Dr. M.D. Silver, Dept. of Pathology, U.W.O.), and six were from patients who had died of non-cardiac causes and whose hearts were normal. The transverse 7 μm sections were all taken approximately midway between the ventricular base and apex, so that the septum appeared as a trilayered structure (Figure 16b). All of the sections were stained with haematoxylin and eosin, which enhances the birefringence of the cardiac muscle. Five regions (each $\approx$ 0.7 mm^2) from the middle layer of each section were photographed. The micrographs, printed at a magnification of 280x,

were taken using a Nikon FX-35A camera mounted on a Nikon polarising microscope fitted with a strain free Achromat 10x 0.25 objective. So that all the muscle fibres could be clearly seen on the micrograph, and to provide contrast, the polarising filters were aligned with their transmission axes at ≈ 80° to each other when the sections were photographed. For the HCM samples, I photographed one region that qualitatively appeared to be the most disorganised, and a second the least disorganised. The other three regions were randomly chosen. For the normal samples all five regions were randomly chosen.

A 65 point rectangular grid was then superimposed on each micrograph. The muscle fibre at each grid point was located on the section, brought to the centre of the field of view and rotated on the microscope stage until the correct extinction (and hence orientation) angle was determined. To permit comparison among the samples, the orientations were measured relative to the circumferential direction in the septum (one sample could not be measured in this way because it had been trimmed to fit on the slide, making it difficult to judge the circumferential direction). For each of the regions photographed the mean orientation angle, the angular deviation (the circular statistics equivalent of standard deviation), and the relationship to the circumferential direction were calculated. Circular histograms, which show the distribution of fibre orientations were also drawn. To test the repeatability of the measurements, fibre orientations from two of the regions (one normal and one HCM case) were measured at two different times.

Finally, a blinded study was done using the same sections as in the previous study to determine if HCM tissue could be accurately distinguished from normal tissue. The same sections that were used in the initial experiment were covered with masking tape except for a region ≈ 0.7 mm². Fibre orientations were measured as before except that a 100 point grid was used.

3.2.1. Statistical analysis: Analysis of the orientation data was done using methods

described by Batschelet (1981). The Rayleigh test (Batschelet 1981, p.54) was used to check for randomness of organisation in the HCM cases. For the repeatability test, the distributions obtained were compared using Kuiper's modification of the Kolomorgorov-Smirnov test (*ibid*, p 112)

3.3. Results

3.3.1. Descriptive results: In addition to the quantitative assessment of fibre organisation provided by the two dimensional method, polarised light also provides a qualitative method of assessing muscle organisation. If a uniform extinction pattern is seen when the stage is rotated (i.e., if all fibres appear dark at a certain angle) then the muscle is coherently organised. In contrast, the multidirectional HCM organisation gives a patchy extinction pattern when the stage is rotated (Plate 1)

3.3.2. Quantitative results: The orientation distributions of muscle from the normal hearts were unimodal and sharply peaked at the mean orientation angle (Figure 17). Distributions obtained from HCM samples were more spread out, sometimes bimodal, but were never randomly arranged ($p<0.05$, Rayleigh test). For regions that were chosen at random, the angular deviations in normal septa were significantly lower than those from HCM cases (Figure 18). The mean orientation angle of all the normal regions did not differ significantly from the orientation of the circumferential direction in the septum (95% confidence limit, Batschelet 1981, p.84). Mean fibre orientation did, however, differ from the circumferential direction of the septum in several HCM cases (15 out of 25).

Some (8 out of 30) HCM distributions had angular deviations comparable to those observed in normal samples, and qualitatively appeared normal. Inspection of their orientation distributions indicated, however, that they were not the same as the normals.

From these results it can be seen that measurements of angular deviation and mean orientation were not definitive parameters for diagnosing HCM. Therefore, another

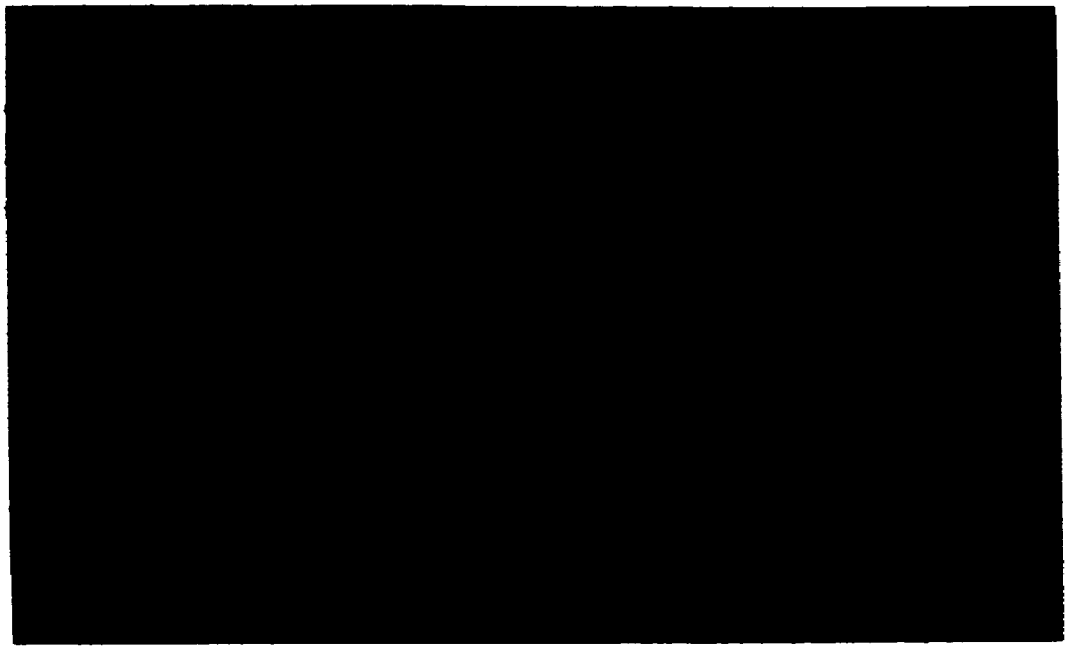

Plate 1: A region of the ventricular septum observed with ordinary light (left hand micrograph) and with linearly polarised light. The orientation of the transmission axes of the filters corresponds to the edges of the figure. The disorganisation of the muscle fibres can be seen with ordinary light, but, is much more evident with polarised light. If all of the muscle fibres had the same orientation then they would all have the same extinction angle. With polarised light a patchy extinction pattern is seen. (Magnification 50x)

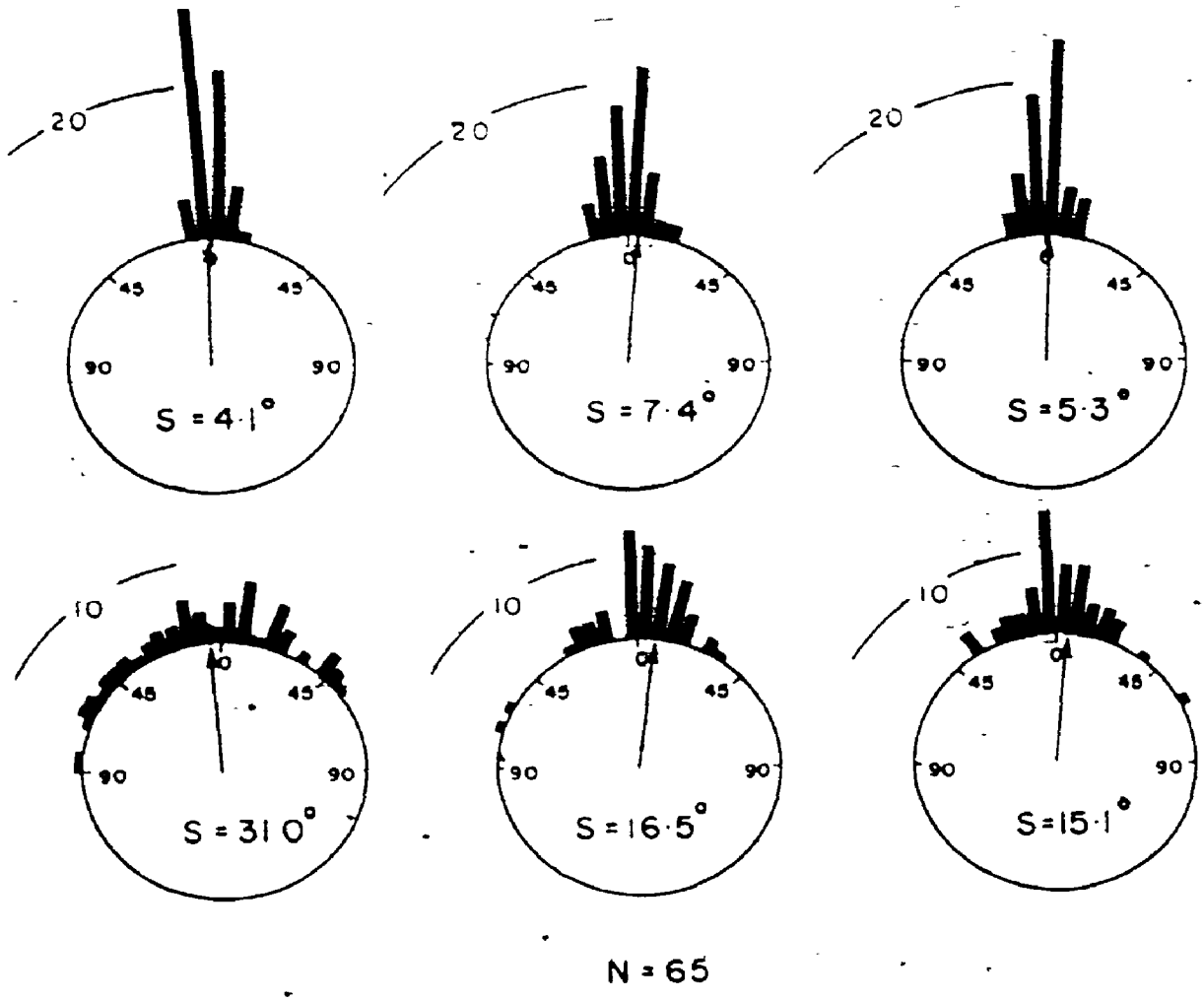

Figure 17: Circular histograms. The orientation distributions are divided into 5° intervals. The angular deviation, s, of each of the distributions is given. The mean orientation of each distribution coincides with 0°. The circumferential direction of the septum is indicated by the direction of the arrows. The upper three histograms are from normal hearts, and the lower three are from cases of hypertrophic cardiomyopathy (N=65).

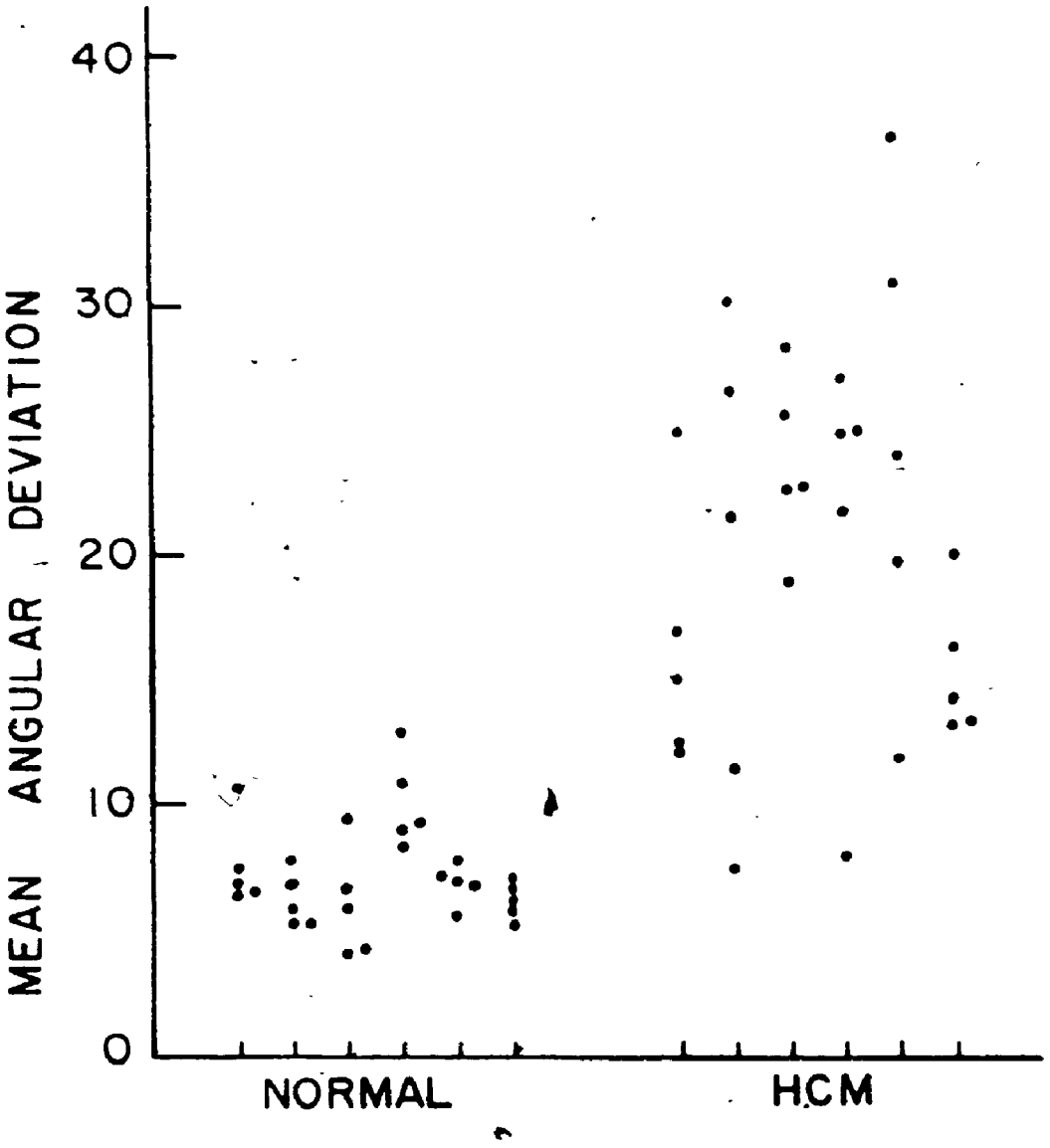

Figure 18: The mean angular deviation for the fibre orientation distributions from normal and hypertrophic cardiomyopathy samples. Each tick mark on the x-axis represents a single sample. The points vertically above each mark represent the five different regions analysed for each sample.

indicator was sought to distinguish normal from HCM muscle orientation in the blinded study. It was my qualitative impression that the orientation distributions of normal and HCM samples appeared to be different, especially around the mean orientation. The HCM distributions tended to be flatter, lacking the sharp peak seen in the normal distributions (Figure 19). To analyse this the following procedure was used. For each micrograph analysed in the blinded study, a graph of orientation angle versus cumulative frequency was drawn (Figure 20). An orientation distribution that is sharply peaked about the mean orientation will have an S-shaped cumulative frequency curve, while an orientation distribution that is flat topped will have a relatively linear cumulative frequency curve (Figure 20). To measure these differences, the slope of the line of best fit through the point representing the mean orientation and the three points above and below the mean was calculated. The slope was then plotted as a function of the angular deviation of the whole distribution. The results are shown in Figure 21. Maron and Roberts (1981) have shown that the normal muscle fibre organisation in the septum is disrupted around large blood vessels and where muscle bundles converge. The one point from a normal heart on the graph that overlaps the HCMs was taken from a section where it was obvious that muscle bundles were converging. This section was therefore excluded. All eleven remaining samples in the blinded study were correctly identified as representing either normals or HCM cases using this approach.

The reproducibility of the orientation measurements was tested by repeating a set of measurements from both normal and HCM cases. There was no significant difference between the distributions obtained in the repeatability test ($p>0.05$, Kuiper's modification of the Kolomorgorov-Smirnov test).

3.4. Discussion

As well as providing an excellent means of qualitatively identifying muscle

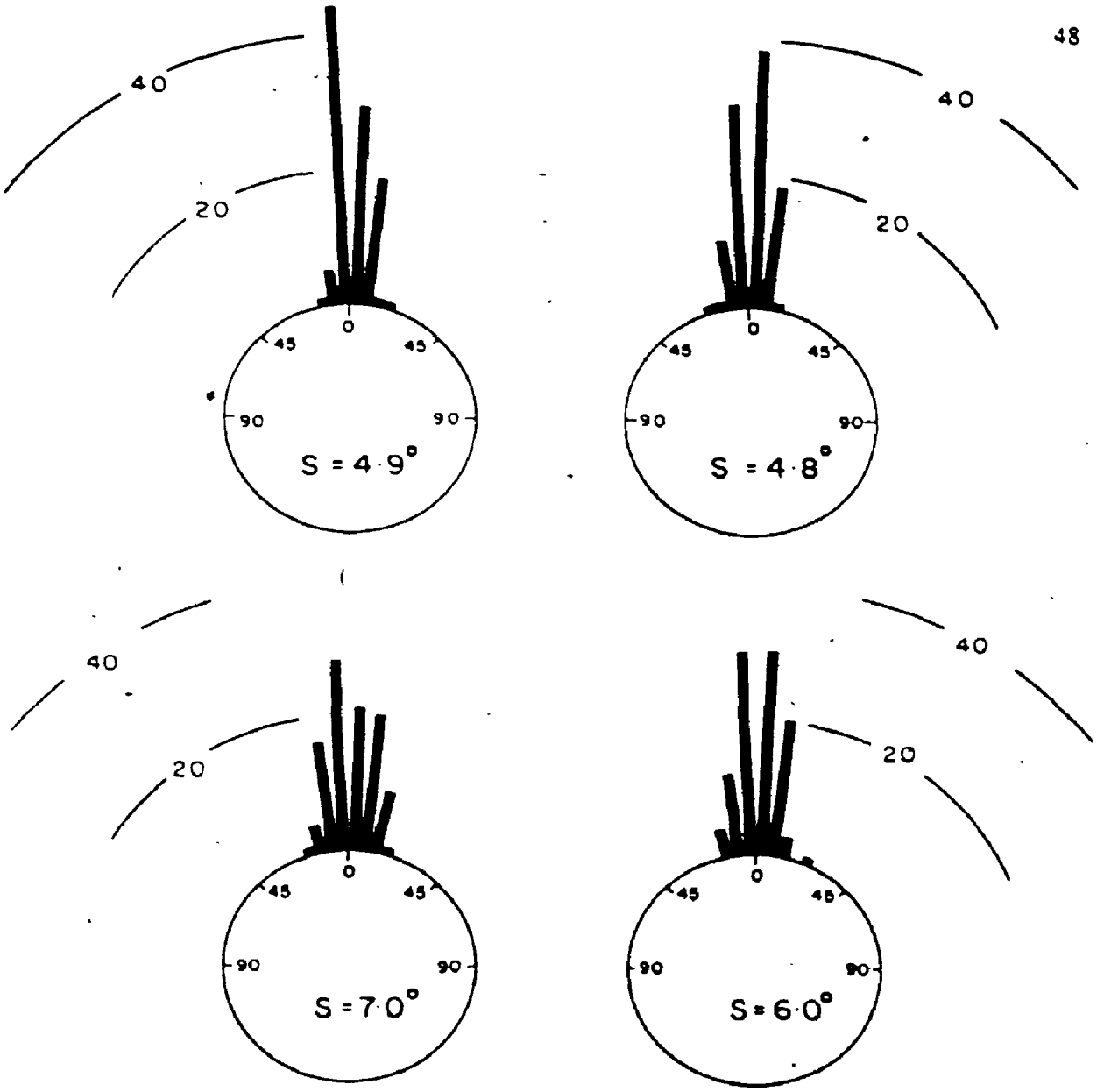

Figure 19: Circular orientation histograms from the blinded study (N=100). Angular deviations are indicated by s. The mean orientation of the distribution coincides with 0°. The distributions are plotted in 5° intervals. The upper two histograms are from normal samples, note the sharp peak at the mean orientation. The lower two are from cases of hypertrophic cardiomyopathy but were from regions where the muscle fibre organisation qualitatively appeared normal.

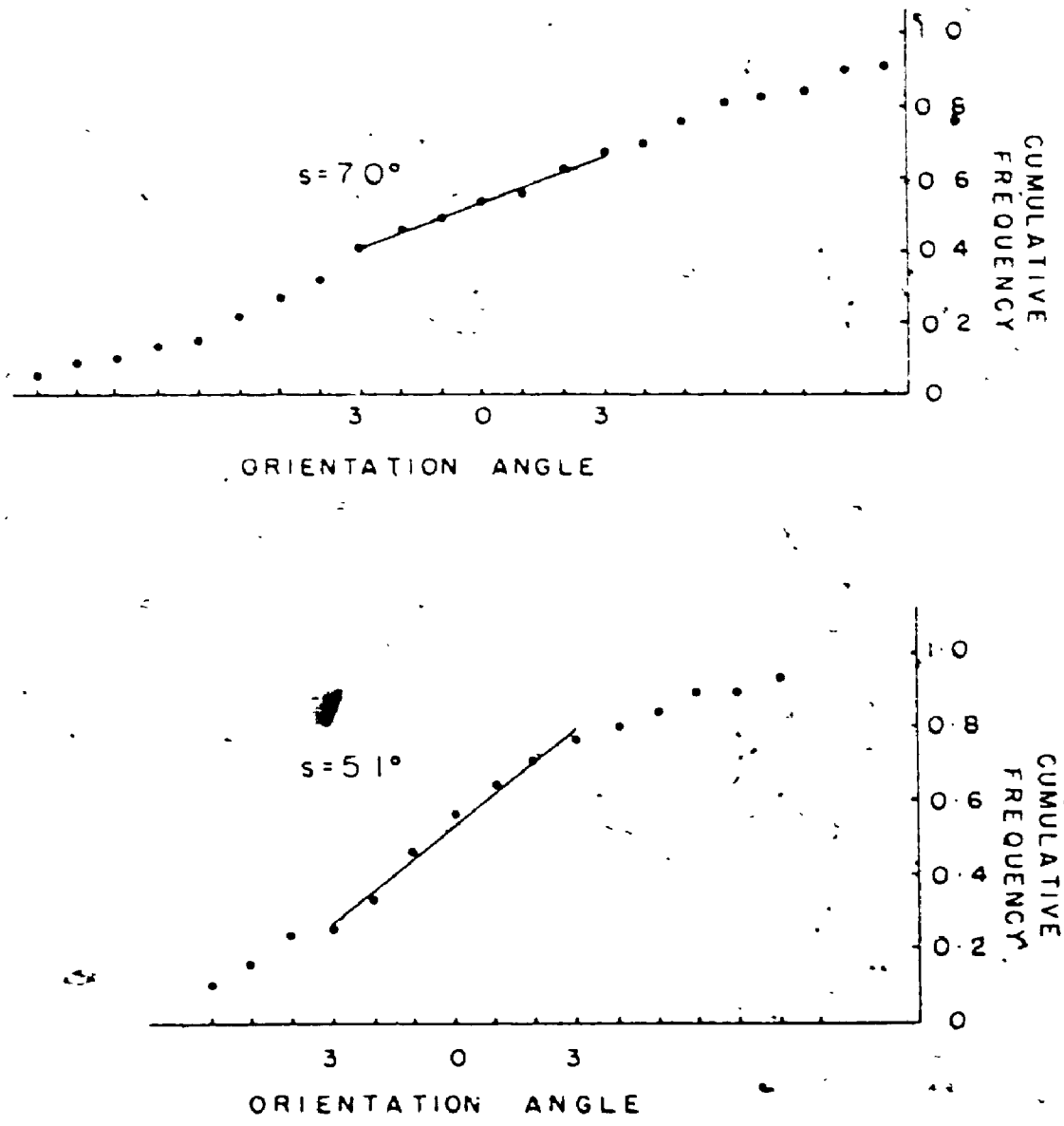

Figure 20: Cumulative frequency graphs. These illustrate the method used to differentiate between normals and HCM cases. The line of best fit was drawn through the central part of the distribution and its gradient calculated. The lower curve is from a normal septum and the upper curve from an HCM case. The angular deviation for each of the samples is shown. The central portion of the curve from the normal septum is steeper than that from the HCM case, indicating a more sharply peaked orientation distribution.

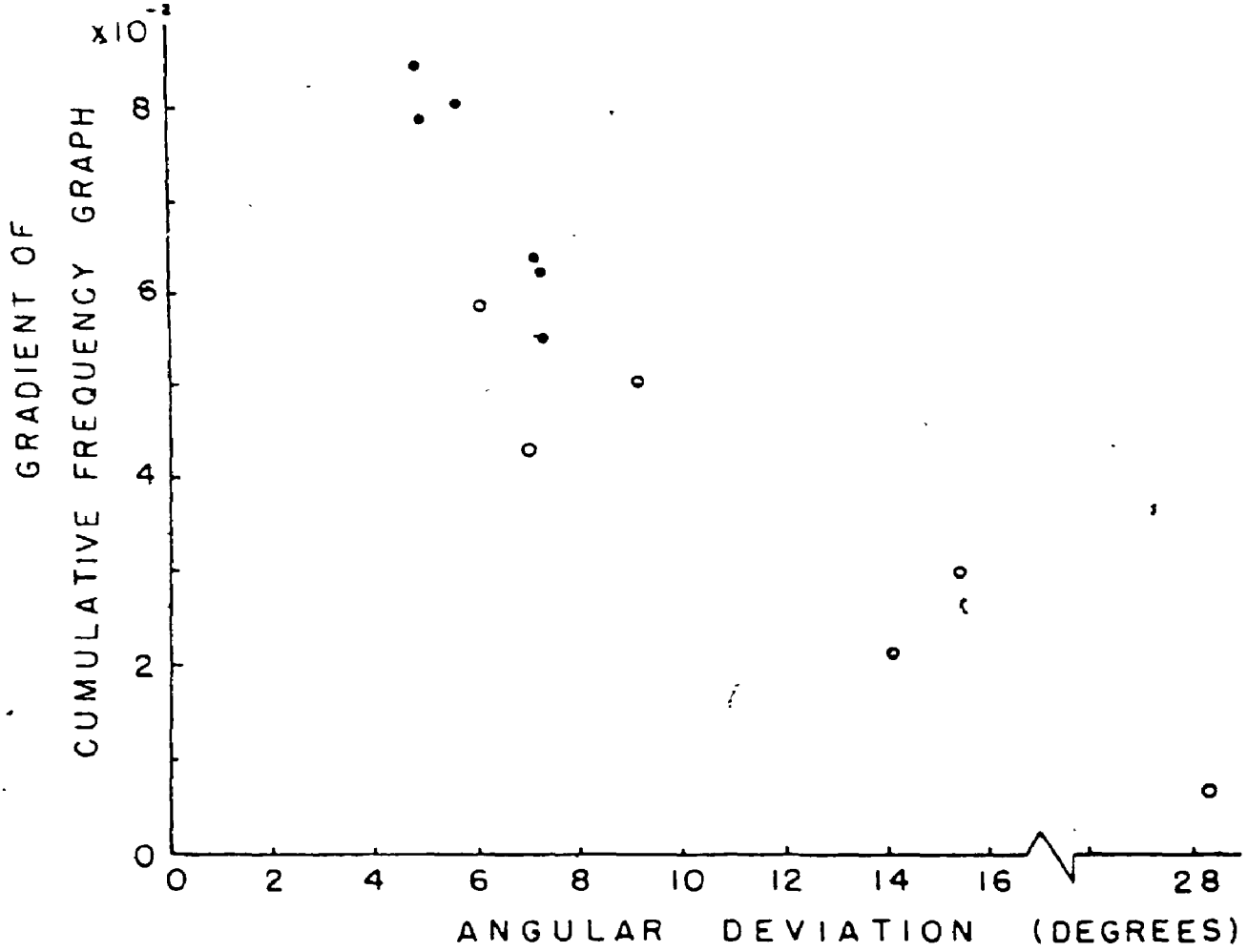

Figure 21: Gradient of cumulative frequency graph plotted as a function of angular deviation for the blinded study. Closed circles - normals, open circles -HCM cases. Inspection of the micrograph from the one normal sample that overlapped one of the HCM cases indicated that it coincided with a region where muscle bundles converged. Such locations are well known areas of abnormal organisation, even in normal hearts.

disorganisation, polarised light microscopy also provides a method for quantitative study of muscle organisation. The data presented here indicate that muscle fibres in the middle layer of the normal septum tend to be aligned parallel to one another, and parallel to the cicumferential direction of the septum. This is consistent with earlier qualitative descriptions (Streeter 1979, Greenbaum et al. 1981), and is the most suitable arrangement to produce efficient left ventricular ejection during systole.

In all the HCM cases I found muscle fibre disorganisation, identified by orientation distributions with high angular deviations, which is consistent with previous work. I also observed fibres in the same regions aligned at right angles to each other, and perpendicular to the circumferential direction, as had been seen by Fujiwara et al. (1982). The distribution of the muscle fibre orientations, however, was never random. The assumption, based on qualitative observation, that runs through all the previously published work is that, while there may be focal areas of disarray in HCM, the rest of the muscle has a normal organisation. Indeed, I did find areas of tissue in HCM patients that appeared qualitatively normal. Although the angular deviations from such regions were similar in magnitude to normal, the nature of the distributions was not. The results suggest that no region in the central portion of the septum in HCM cases is normal and that the qualitative assessment of muscle organisation can be misleading.

The mechanical consequences of fibre disorganisation in HCM are unlikely to be significant, unless a large percentage of fibres deviate substantially from the circumferential direction. The component of force generated along the circumferential direction will be proportional to the cosine of the angle the fibres make with this direction. Even in HCM regions with large angular deviations, the majority of fibres lie within 20° of the circumferential direction, so that the force generated will be only slightly less than normal.

Fibre disorganisation will probably be of greater consequence in the propagation of the depolarisation wave (the electric signal that travels through the myocardium

producing regular contraction of the muscle fibres). Disorganisation will retard the signal, but because the disorganisation is not uniform the retardation will not be uniform and asynchronous contraction may result.

An animal model of HCM has recently been developed (Olsen 1985), so the ability to quantify the extent of disarray could be very useful, especially with regard to testing the efficacy of different methods o. treatment.

In summary, polarised light microscopy provides a method of qualitatively identifying muscle disarray by observing the extinction pattern produced when the microscope stage is rotated. Use of the two dimensional orientation method enables a quantitative assessment of orientation to be made. In normal septa, cardiac muscle is highly aligned, producing a sharply peaked orientation distribution. In HCM tissue, two different muscle populations were observed. In one population, disarray is obvious, with fibres sometimes oriented perpendicular to each other, but never randomly aligned. In the other population, the muscle orientation appears qualitatively normal, but is not and the orientation distribution tends to be flat topped. While muscle fibre disorganisation may not be a definitive marker for HCM, it appears that normally organised muscle is never found in the septum of HCM patients.

CHAPTER 4 THREE DIMENSIONAL ORIENTATION METHOD

4.1. Introduction

This chapter illustrates how polarised light and the universal stage can be used to measure three-dimensional orientation. I have applied the technique to the measurement of collagen's three-dimensional orientation in the wall of human cerebral arteries. This study is an extension of the work of Smith (1980), who studied collagen organisation in brain arteries perfusion fixed at normal physiological i.e., 120 mm Hg pressures.

Generally, arteries can be divided into two classes: (1) elastic arteries such as the aorta, where layers of elastin comprise a substantial part of the media, and (2) muscular arteries such as cerebral arteries, where smooth muscle is predominant in the media. The walls of brain arteries have three distinct layers. The innermost layer of subendothelial layer consists predominantly of smooth muscle. It is separated from the next layer, the *tunica media*, by a relatively thin band of elastin called the internal elastic lamina. The *tunica media* is composed of smooth muscle and Type III collagen (Carrasco et al. 1981). The outermost layer, the *tunica adventitia*, is predominantly Type I collagen (Carrasco et al. 1981). Brain arteries were chosen for this study because of two abnormalities, saccular aneurysms and vasospasm, that can occur in the cerebral circulation sometimes leading to stroke. Saccular aneurysms, are spherical bulges of the arterial wall that may rupture, while arterial vasospasm is an abnormal contraction of the arterial smooth muscle that reduces the cross sectional area of the artery and so reduces blood flow to the brain. The aetiology of these potentially life threatening abnormalities remains uncertain, but a relationship to the mechanical properties of the artery must exist. Collagen is the stiffest and strongest component of the brain artery wall, and its organisation will therefore be important in determining the mechanical properties of the artery. Since the mechanical properties are dependent on arterial structure, the measurement of collagen fibre

orientation in brain arteries is an ideal subject for study using the universal stage. Before one can consider what mechanical role collagen organisation may play in saccular aneurysms or vasospasm, the organisation of collagen in normal arteries and its relationship to the mechanical properties must be determined.

It is acknowledged that the non-linear elastic properties of arteries are derived from the complex arrangement of two fibrous proteins: elastin and collagen. It is also accepted that in compliant biological tissues such as arteries, connective tissue elements and muscular components become reoriented with tissue deformation. Roach and Burton (1957) explained the non-linear distensibility (stress-strain) curves of arteries in terms of structure. The shape of the curves is explained as follows: elastin fibres are responsible for the first part of the curve, the so called "toe region", and, as the elastin is straightened, the load is transferred to collagen fibres. Collagen fibres are then recruited to bear the increasing load; more and more of them become straight increasing the artery's stiffness. I shall refer to this explanation as the recruitment theory.

There are two paradoxes associated with this theory: (1) the recruitment of collagen would mean that some fibres would be straight while the artery is still being distended. Type I collagen, which makes up the bulk of the adventitia, is known to be intolerant of strain once it is straight (approximately 4% strain will produce irreversible plastic deformation (Wainwright et al. 1976)). Therefore, recruitment would result in fibres breaking. (2) arteries, tendons and skin collagen all give a stress-strain curve of approximately the same shape, yet tendon and skin (especially tendon) contain little or no elastin. How then is the toe-region of the stress-strain curves to be explained?

The recruitment theory makes the assumption that collagen fibres must be straight before they can make any contribution to the mechanical properties. Ling and Chow (1977), however, have shown that even wavy fibres provide resistance to tension. There is some evidence to suggest that collagen is straight at higher pressures in arteries (Wolinsky and Glagov 1964). This suggestion comes mainly from electron microscopy

observations, but, at the high magnifications used it is unlikely that one would be able to distinguish whether or not the fibres were truly straight. We have seen no evidence in our two dimensional measurement of fibre orientation to suggest that fibres are straight, even at 200 mmHg (unpublished data). Another shortcoming of the recruitment theories is that it is claimed that medial collagen is the major contributor to the mechanical properties (Dobrin and Canfield 1984). This statement is made even though medial collagen is predominantly Type III collagen. Since Type III collagen has never been isolated its mechanical properties are unknown. Circumstantial evidence (Park et al. 1976, Pierard and Lapiere 1976) indicates, however, that it is more compliant and weaker than Type I collagen.

In the present theories the tunica adventitia is regarded as merely a "safety device" to prevent rupture of the artery at high pressures. For this reason it has received little attention. The universal stage allows a quantitative measurement of tissue orientation to be made. With the hypothesis that adventitial collagen plays a greater role than has been believed, I measured the orientation of both adventitial and medial collagen, and analysed how the orientation changed as a function of pressure at the time of fixation.

4.2. Methods.

4.2.1. Tissue selection: Fourteen sections from eight different autopsies were studied. These were taken from twelve different vessels. The vessels were all from or near the circle of Willis. Vertebral, basilar, anterior cerebral and middle cerebral arteries were used in this study. All of the samples were from males (age 42-84). The study was divided into two parts (1) the orientation of medial collagen (2) the orientation of adventitial collagen.

4.2.2. Orientation of medial collagen: In part (1) four sections, all from different autopsies, were analysed. A range of pressures (60 to 190 mmHg) was studied with all

vessels cut in cross section. The sections were stained with picrosirius red, which enhances the birefringence of collagen allowing it to be clearly seen and does not enhance the birefringence of smooth muscle. Twenty measurements of three-dimensional orientation were taken on each section with the universal stage. In both parts of the study the orientation data obtained were presented as scatter diagrams on Lambert projections. The average spiral component of the orientation i.e., the deviation from circumferential alignment in the section plane, was calculated for each section. To compare the effect of distending pressure, the angular deviation of the distribution of spiral angles for each section was calculated using circular statistics. The same procedure was also carried out for the helical component of orientation.

4.2.3. Orientation of adventitial collagen: In part (2) ten sections were analysed, and fifty orientation measurements were taken on each section. Three enhancement stains were used: picrosirius red, haematoxylin and eosin and Gomori silver impregnation. The vessels were perfusion fixed at different pressures, and divided into three groups, 30-60 mmHg (low), 100-125 mmHg (average), 160-190 mmHg (high). The variation of the spiral component was calculated for the different pressure ranges.

4.3. Results

4.3.1. Medial collagen: The medial collagen, when stained with picrosirius red and observed with polarised light, appeared green or yellow compared to the orange of the adventitia (Plate 2), indicating that the medial collagen was Type III and the adventitial collagen was Type I (Junqueira et al. 1978). The orientation of the medial collagen is shown in the scatter diagrams (Figure 22) as a function of distending pressure. The analysis of the orientation data using Fisher statistics is shown in Table 3. These data indicate that collagen in the media tends to become more circumferentially aligned with increased distending pressure (the precision parameter k increases). In all four sections

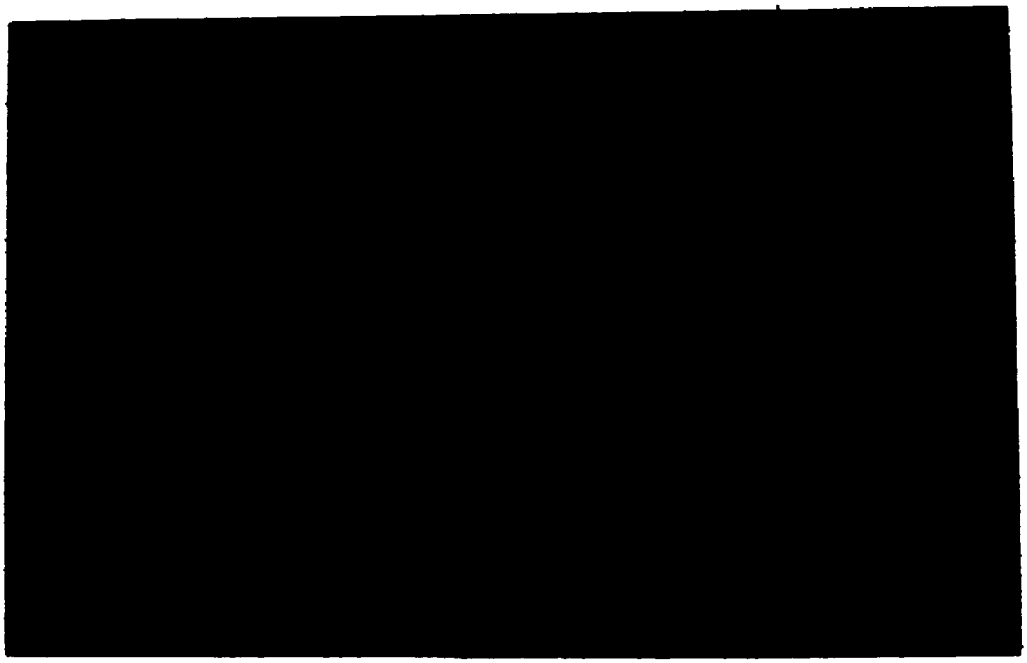

Plate 2: A region of a cerebral artery cut in cross section and stained with picrosirius red. In the tunica adventitia the collagen fibres appear red/orange, indicating the Type I collagen. In the tunica media the collagen fibres appear yellow/green, indicating Type III collagen. (Magnification 165x)

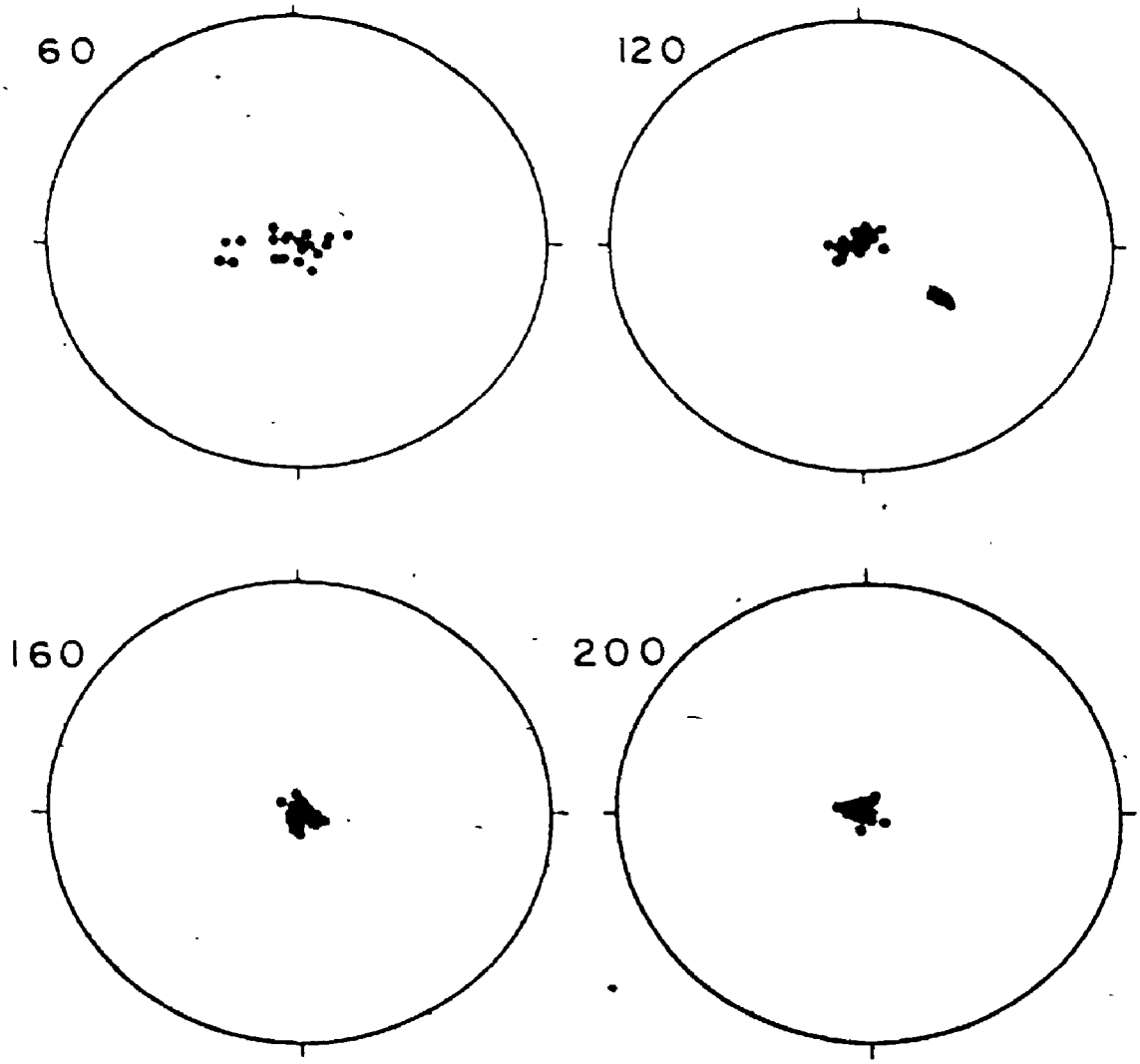

Figure 22. Lambert projections showing the organisation of medial collagen as a function of distending pressure (shown in mmH_g). At 120 mmHg the medial collagen has a coherent circumferential alignment. A circumferentially aligned fibre is represented by a point at the centre of the projection.

PRESSURE (mmHg)	ANGULAR DEVIATIONS		K
	SPIRAL	HELICAL	
60	11 4	4 1	44
120	5 0	2 9	199
160	3 3	3 3	285
200	3 6	2 8	304

Table 3. Statistical analysis of medial collagen orientation using Fisher statistics. The spiral and helical components (the definition of spiral and helical angles is shown in Figure 24) of orientation were separated and analysed. The trend is for the spiral component to decrease with increasing pressure. There was little variation in the helical component. The precision parameter, k, increased with increased distending pressure.

analysed, the longitudinal component of orientation is approximately the same (Table 3), it is only the spiral variation of orientation which changes with distending pressure, tending to increase.

4.3.2. Adventitial collagen: The data obtained from each of the ten sections were pooled according to the pressure range and statistically analysed in this form. A representative (unpooled) scatter diagram for each pressure range is shown in figure 23. The precision parameter k, which is a measure of the coherence of alignment, was greater in the 100-125 mmHg range than in the 30-60 mmHg. The helical component of orientation remained virtually the same. Therefore, the increase in k derives from the decrease of the variation of the spiral component of orientation (Table 4). In the 160-190 mmHg pressure range the distribution of collagen fibre orientations was resolved into three groups. In one group the fibres are aligned circumferentially around the artery. The rest of the fibres occur in two groups aligned with a mean orientation approximately + 60° and - 60° from the longitudinal direction along the N-S axis of the Lambert projection i.e., the mean orientation of the fibres corresponds to a left and a right handed helix with a pitch angle of ≈ 60° (relative to the artery's long axis).

4.4. Discussion

The use of the universal stage to measure the three dimensional orientation of birefringent material has been demonstrated. The medial collagen appears to be circumferentially aligned, and so is parallel to the smooth muscle (Canham et al. 1986). The medial collagen is more coherently aligned at high pressures than at low pressures. There is evidence that increased distending pressure produces a similar increase in the coherent orientation of the smooth muscle (Finlay personal communication). I found the medial Type III collagen to be highly aligned in the circumferential direction at the 100-

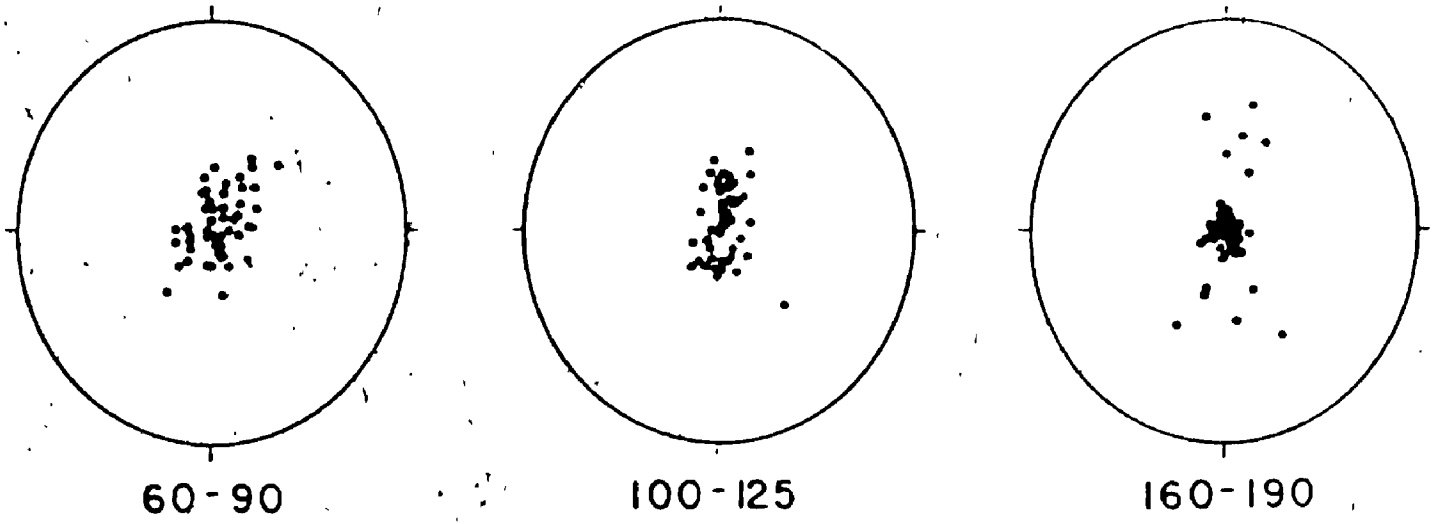

Figure 23. Lambert projections showing the three-dimensional organisation of collagen in the *tunica adventitia*. One scatter diagram representing data from a single section is shown for each of the pressure ranges studied (shown in mmHg). A circumferentially aligned fibre is represented by a point at the centre of the projection.

PRESSURE RANGE (mm Hg)	K	SPIRAL ANGULAR DEVIATION
30 - 60	21	10 0
100 - 125	34	6 8
160 - 190	94	4 7

Table 4. (a) Analysis of adventitial collagen orientation Fisher statistics were calculated from pooled data from all the sections for each pressure range (the fibres that had substantial longitudinal components in the high pressure range were omitted from this analysis). The precision parameter increased with increased distending pressure, while the spiral angular deviation decreased.

	K	HELICAL ANGLE	N
1	27	59 2	31
C	94	89·6	105
2	36	56·4	64

(b) Results calculated from Fisher statistics for each of the three groups in the high pressure range, N is the number of data in each group. C is the central group, 1 the upper and 2 the lower group shown on the Lambert projection in Figure 23. The average helical angle (see Figure 24), expressed relative to the long axis of the artery, of each of the groups is shown. Thus, group C is circumferentially aligned, while groups 1 and 2 have large longitudinal components.

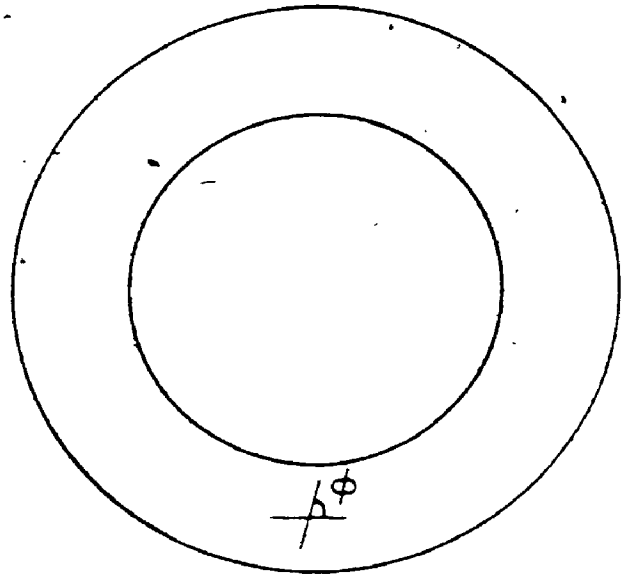

end view

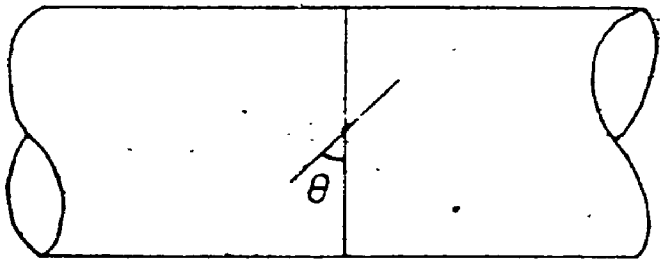

side view

Figure 24. End and side views of a cylindrical artery segment. The end view illustrates the spiral component of orientation. The angle ϕ that a fibre makes with the circumferential tangent gives the spiral angle. Therefore, a fibre with a 0° spiral angle is aligned circumferentially, while a fibre with a 90° spiral angle is aligned radially.
The side view illustrates the helical component of orientation. The angle θ that a fibre makes with the cross section gives its helical angle. Therefore, a fibre with a 0° helical pitch is aligned circumferentially, while a fibre with a 90° helical pitch is aligned longitudinally.

125 mmHg pressure range, but there was little increase in the coherence of organisation at higher pressures. If the medial collagen is responsible for the rapid increase in artery stiffness that occurs at these higher pressures then it would have to be quite stiff and inextensible. Type III collagen is never found alone, therefore, its mechanical properties have been indirectly investigated (Park et al. 1976). The mechanical properties may also be indirectly assessed from study of a tissue where the content of Type III collagen changes rapidly. The proportion of different types of collagen forming the dermis shifts during foetal development from a large proportion of Type III to increasing amounts of Type I collagen (Epstein 1974). This change occurs simultaneously with an increase in the stiffness of the collagen (Pierard and Lapière 1976). It therefore appears that Type III collagen is not as stiff as Type I collagen.

The second reason why the medial collagen seems inadequate to explain the mechanical properties is related to its three-dimensional orientation. It is known that in a cylindrical vessel there is a longitudinal stress as well as a circumferential stress (Burton 1962). In the sections examined, the longitudinal (i.e., helical) component of the medial collagen orientation was negligible, and so would be unlikely to provide longitudinal resistance to stress. There is a possibility that there are collagen fibres in the media that are longitudinally aligned, which would be difficult to detect in cross-sections. I have seen no evidence using polarised light microscopy for the presence of such a fibre population in longitudinally cut sections where these fibres would lie in the section plane and would be easily seen. Thus, it appears that the medial collagen cannot be responsible for the nature of the passive stress-strain curves of cerebral arteries.

Evidence to support the concept presented here that medial collagen plays only a small role in the artery's mechanical properties comes from interpretation of the results of Dobrin and Canfield (1984). These authors studied the biaxial elastic properties of canine carotid arteries before and after treatment with elastase and collagenase. The enzymes were delivered to the inner surface of the vessels, such that the *tunica media*

was affected rather than the *tunica adventitia*. Indeed, they found that if the adventitia was affected then the vessels leaked. Treatment with collagenase made no significant difference to the longitudinal mechanical properties, while the circumferential mechanical properties were slightly affected at pressures greater than 60 mmHg. Although they studied carotid arteries, which are elastic arteries, and not muscular brain arteries, their results suggest that the medial Type III collagen does not contribute to the longitudinal mechanical properties and makes only a slight contribution to the circumferential mechanical properties. In brain arteries where there is only a single band of elastin, the adventitial collagen may prove to be the main contributor to the mechanical properties of the artery.

The changes of collagen fibre orientation as a function of pressure that I have observed in the adventitia are compatible with data from circumferential stress-strain curves obtained by Roach and Burton (1957). At low pressures the fibres have relatively large spiral and helical components and so the artery is fairly distensible. With an increased distending pressure, however, the fibres become increasingly aligned in the circumferential direction, producing a rapid increase in stiffness.

The resolution of arterial collagen fibre orientation into different groups at high pressures is a finding not previously reported. This observation can perhaps be explained as a mechanism of structural reinforcement. Clark and Cowey (1958) developed a mathematical model to predict the orientation of fibres in the basement membrane of nemertean worms. At the maximum volume i.e., when the worm is cylindrical in shape the model predicts that the fibres in the basement membrane will be aligned at an angle of $\approx \pm 55°$ with respect to the long axis of the worm. It is tempting to apply a similar model to the artery; assuming that the maximum volume of the artery occurs at high pressure, then the predicted orientation of 55° is close to the average values of orientation that I measured in the 160-190 mmHg pressure range (59.2° and 56.4°, Table 4b).

In conclusion, the universal stage provides an effective method of measuring the three dimensional organisation of tissue elements. From the evidence presented here I conclude that the medial Type III collagen in brain arteries is highly aligned even at normal systolic pressure. Its circumferential organisation and the suggestion that Type III collagen is not very stiff compared to Type I collagen (Park et al. 1976, Pierard and Lapière 1976), indicate that it plays a minor role in determining the mechanical properties of brain arteries. In many histology texts the *tunica adventitia* is often described as consisting of a loose network of collagen fibres (e.g., Leeson and Leeson 1981, p.270, Fawcett 1986, p.371), which implies that it does not contribute to the mechanical properties of the artery. My results show that the adventitial Type I collagen of brain arteries is not loose, but is highly organised and appears to play a major role in determining the passive mechanical properties of the vessel wall. The orientation data presented here may be used as a reference for a comparison of collagen fibre orientation in pathological arteries.

CHAPTER 5 MOLECULAR ORGANISATION METHODS

5.1. Introduction

This chapter illustrates the quantitative polarised light techniques that can be used to determine changes in molecular organisation. The greatest change in collagen's molecular organisation probably occurs as the collagen is maturing. Such an increase in molecular organisation can be observed in two slightly different ways by measuring the retardation of linearly polarised light passing through the collagen.

(1) *Imbibition analysis*. This method involves the measurement of the retardation of unstained collagen in a series of imbibing media with different refractive indices (Bennett 1950, p.666). From the minimum of the form birefringence curve the intrinsic birefringence of the collagen can be calculated. The intrinsic birefringence is determined by the molecular organisation of the collagen.

(2) *Measurement of retardation in stained collagen*. The retardation values obtained from stained tissue will depend on how the stain's molecules bind to the collagen. That in turn depends on the molecular organisation of the collagen (Joiner et al. 1968). If the collagen has a high degree of molecular organisation then the molecules of the stain will be bound in a preferred orientation and the retardation will be increased. With less molecular organisation the molecules of the stain do not have a preferred orientation and so the retardation will be only slightly increased.

It is known that changes in the molecular organisation and cross linking of collagen occur throughout its life (e.g., Nimni 1980). These changes are most pronounced in the early stages of maturation, but later the changes are more subtle with slight modifications in the nature of the intermolecular cross links occurring (Light and Bailey 1980). The following experiment was designed to examine the extent to which the polarised light techniques can detect these changes. To examine the two retardation

methods I analysed maturing collagen of known age. For this research I had the opportunity of analysing tissue provided by Dr. R.A. Kloner (Wayne State University).

The collagen studied was from scar tissue formed following an experimentally induced myocardial infarction in dogs. When a coronary artery is occluded, the blood flow to the region of the myocardium served by that artery is greatly diminished or, in some cases, stopped completely. The muscle's oxygen supply is therefore severely reduced, the myocardium is rendered ischemic and, if the occlusion persists, the muscle dies. If the healing process proceeds normally, the necrotic muscle is gradually resorbed and replaced by collagen fibres. These fibres mature until a firm, fibrous scar is formed.

In addition to providing data establishing the two retardation methods, the scar tissue experiments illustrate a potentially important clinical application. Many recent studies of experimental ischemia have concentrated on efforts to reduce the area of necrosis (e.g., Maclean et al. 1978). Little or no consideration has been given to how such efforts might affect the quantity or quality of collagen in the scar. Some of the drugs given to reduce infarct size are antiinflammatory agents e.g., methylprednisolone, which appear to affect the normal healing of the scar (Hammerman et al. 1983). An effective method to test for such possibilities would be useful.

5.2. Methods

The surgery described was performed by Dr. H. Hammerman in Dr. Kloner's lab. Twelve mongrel dogs of either sex were anesthetized with sodium pentobarbital (30 mg/kg IV), intubated, and ventilated with room air. A left thoracotomy was performed through the fifth intercostal space, the heart suspended in a pericardial cradle, and the left anterior descending (LAD) coronary artery isolated proximal to its first major diagonal branch, usually within 1 cm of its origin from the left main coronary artery. The LAD was then permanently occluded with a double ligature. Thirty minutes post-occlusion, the

incision was sutured, the chest evacuated, and the dogs allowed to recover from anesthesia. Tissue from the region of the scar was obtained from dogs sacrificed at one week (n=4), three weeks (n=3) and six weeks (n=4) post-occlusion. In addition tissue was obtained six weeks post-occlusion from four animals treated with methylprednisolone (MP: 50 mg/kg IV at 15 mins, 3, 24, 48 hours post-occlusion).

Formalin fixed tissue blocks, containing both scar tissue and visceral pericardial collagen, were taken from the centre of the scars. The tissue blocks were embedded in paraffin wax and sectioned at 7 μm. I analysed the sections, blinded, using a combination of, imbibition analysis of unstained tissue and measurement of retardations produced in eosin stained sections. In all sections the visceral pericardium, which surrounds the heart, was used as the control tissue, representing normal mature collagen. Fibres that appeared thinner due to sectioning artefacts were avoided. Also, because retardation is dependent on orientation, fibres that appeared to have been sectioned obliquely were avoided. With these restrictions, measurements were taken throughout the scar. For the imbibition analysis ten measurements were taken from both the pericardium and the scar collagen in each imbibing medium. The media used were those listed in Chapter 2. The intrinsic birefringence (IB) of each of the samples was calculated from the form birefringence curves according to the relationship,

$$IB = \text{minimum retardation} / \text{section thickness}.$$

For the eosin stained sections, ten retardation measurements were taken from each region. To eliminate bias produced by different staining conditions, the average retardation from the scar was expressed as a percentage of the average pericardial retardation. I compared the results obtained for the different post occlusion times and treatments using one way analysis of variance. Pairwise comparisons were then performed using Tukey's test (Zar 1984, p.189).

5.3. Results

The combined form birefringence curves from each of the groups are shown in Figure 25. The intrinsic birefringence for each of the samples is shown in Figure 26. The intrinsic birefringence of the pericardial collagen was significantly greater than that of collagen from the six week scar tissue, which in turn was significantly greater than the one week scar. There was no significant difference between the methylprednisolone treated and the untreated specimens at six weeks post-occlusion.

The results from the analysis of the eosin stained tissue are shown plotted as a function of time in Figure 27. The six week scar had a significantly greater value of retardation than three week scar, which in turn was significantly greater than the one week scar. Again no difference was found between the methylprednisolone treated, and the untreated collagen scar tissue at six weeks.

The possibility exists that the observed retardation differences between normal collagen in the pericardium and that of the scar tissue was due to the collagen not occupying the full 7 μm section thickness. Using the formula $\Gamma = t\,(n_e - n_o)$ the value measured for the one week scar could have been produced if the collagen was $(35/100 \times 7) = 2.45$ μm thick. When stained with picrosirius red the collagen, if it were 2.45 μm thick, should have appeared green (Junqueira et al. 1982). In fact, the collagen in these scars appeared orange, indicating that the decreased retardation was not due to decreased collagen thickness.

These retardation measuring methods can detect the changes in molecular organisation that occur during early maturation. The changes that occur after that, such as the increased cross linking processes that lead to increased stiffness of collagen in later life, may not be able to be detected. To investigate this possibility the following experiment was done. The intrinsic birefringence for normal chordae tendineae (the tendons that are attached to the mitral valve in the heart, *see Chapter 9*) obtained at

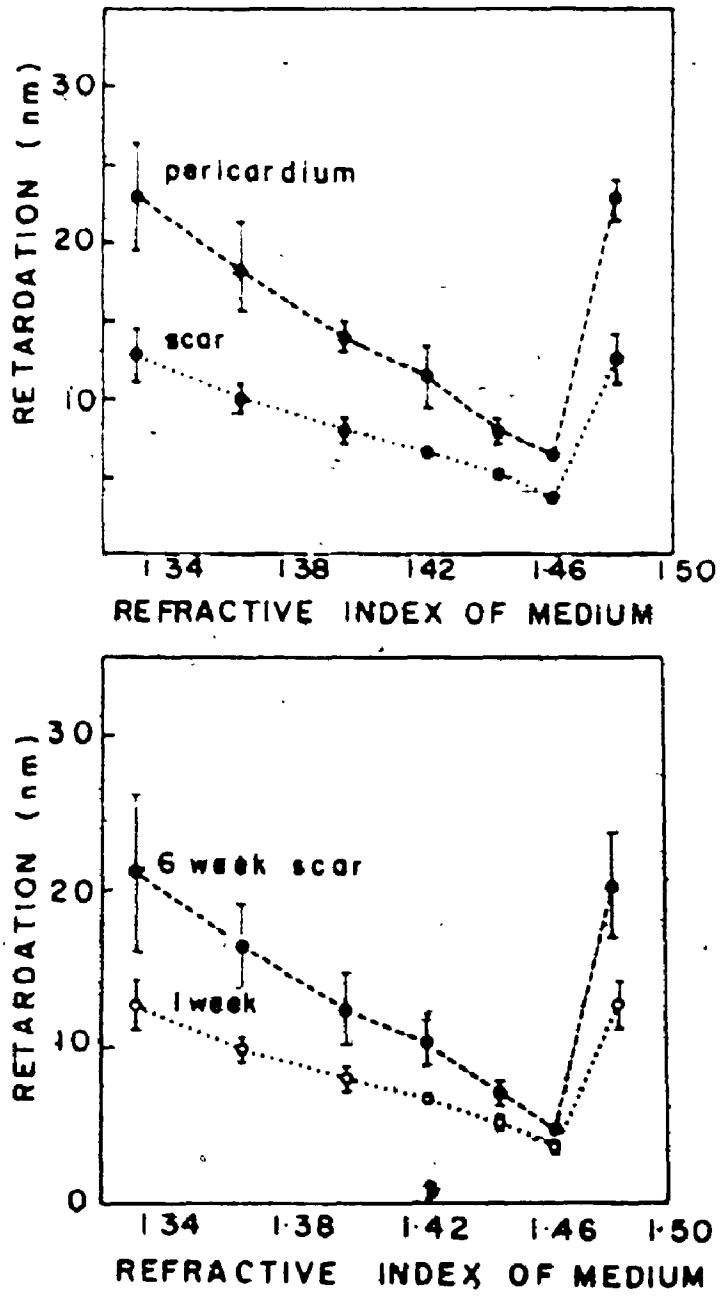

Figure 25: Form-birefringence curves of the myocardial collagen. The upper panel shows the curve for visceral pericardium (the control) and the curve for the one week scar. Each point represents the average of ten retardation measurements. The standard deviations are also shown except where they are smaller than the points. The lower panel shows the difference between the one and six week scars.

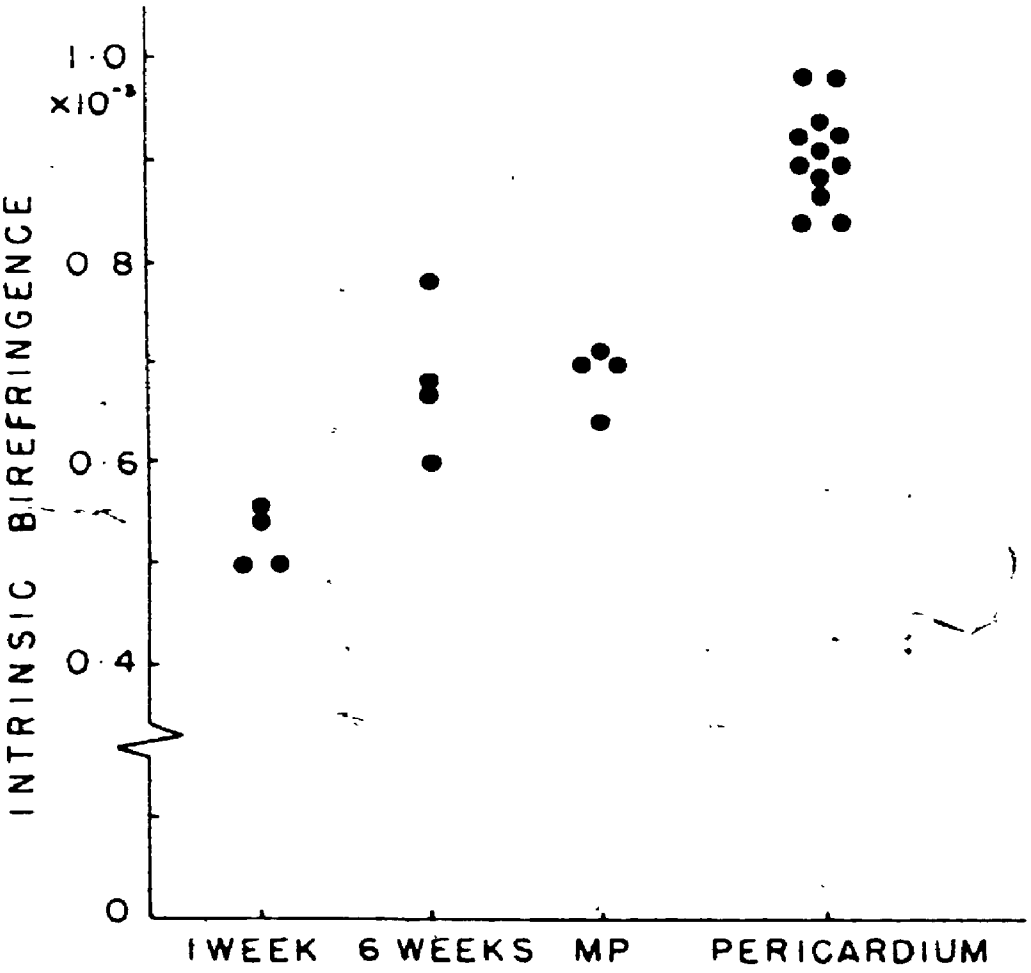

Figure 26: The intrinsic birefringence, calculated from the minimum of the form birefringence curves, for each of the samples analysed. The methylprednisolone (MP) treated group was also analysed at six weeks and was not significantly different from the six week control.

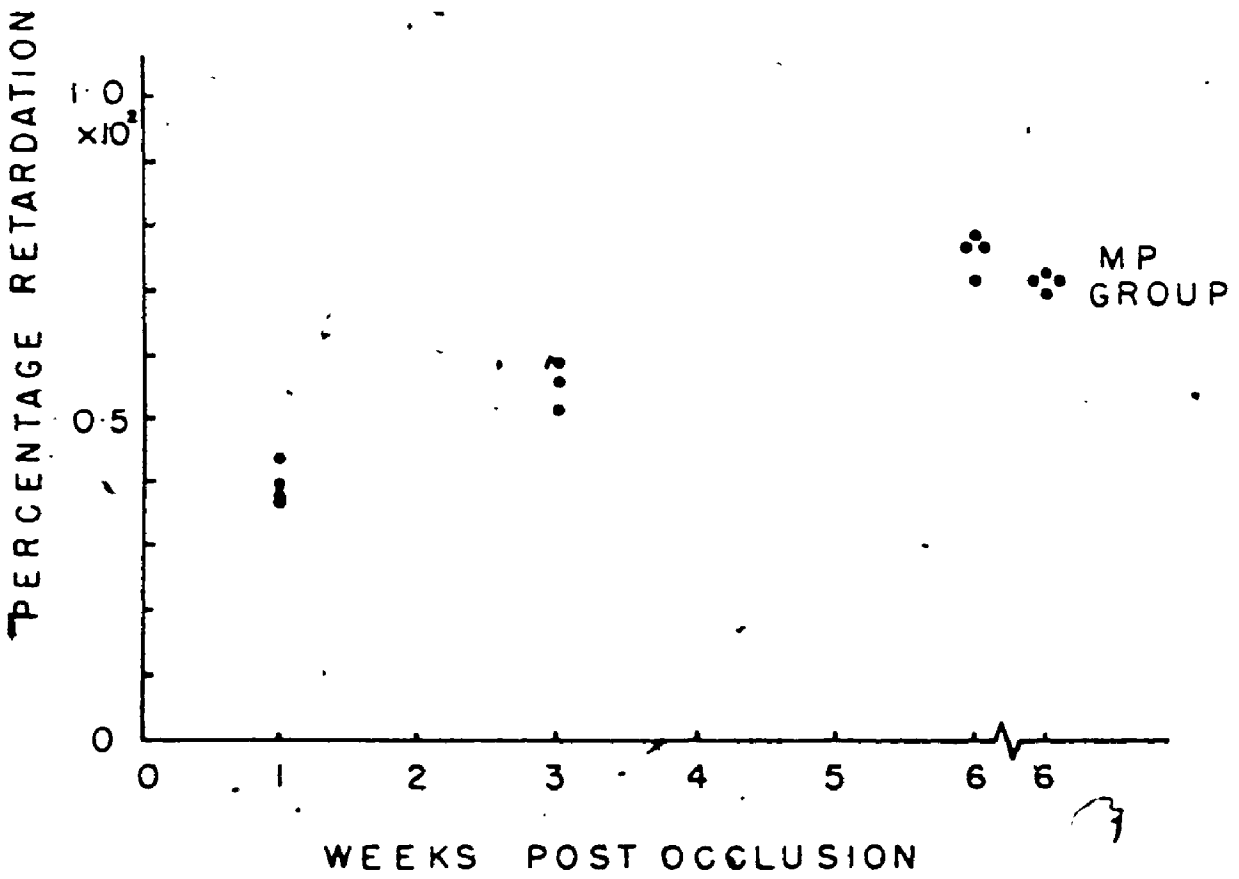

Figure 27: The retardation of eosin stained tissue expressed as a percentage of the retardation of the visceral pericardium and plotted as a function of the "age" of the scar i.e., the number of weeks post-occlusion. The retardation increased as a function of time. The MP treated group was not significantly different from the untreated group at six weeks.

autopsy was calculated from imbibition analysis and plotted as a function of the patient's age (Figure 28). There was no apparent change in intrinsic birefringence even though samples covering a large age range were analysed (r = -0.0004). The values of intrinsic birefringence were similar to those obtained from the mature canine pericardium.

5.4. Discussion

These data demonstrate that changes in collagen's molecular organisation during the first six weeks of its development can be detected by retardation measurements. In addition, it appears that methylprednisolone does not alter collagen's optical properties at six weeks post occlusion, and thus does not hinder the maturing process. Biochemical findings from a study of the effect of methylprednisolone on myocardial scar maturation in rats support this conclusion (Vivaldi et al. personal communication). They found no significant differences between the concentration of hydroxypyridinium cross links in methylprednisolone treated and untreated rats at four weeks post-occlusion. The retardation measurements that I obtained from both the stained tissue and the imbibition analysis revealed the increase in molecular organisation in the maturing collagen. Each method has its own advantages. Imbibition analysis, although it cannot be rigorously applied to collagen, because collagen and its attendant ground substance do not constitute a two component system, can give information about the system by the qualitative interpretation of the form birefringence curves. The stained tissue method, because of the higher retardations, should provide a greater ability to discriminate between different degrees of organisation than the imbibition analysis. Measurement of retardation from stained tissue is also more quickly and easily done. Both methods have advantages over biochemical techniques. First, the tissue is not destroyed and measurements can be repeated and confirmed if needed. In addition, it is also possible to detect localised differences in the tissue which would not be discerned if the tissue had

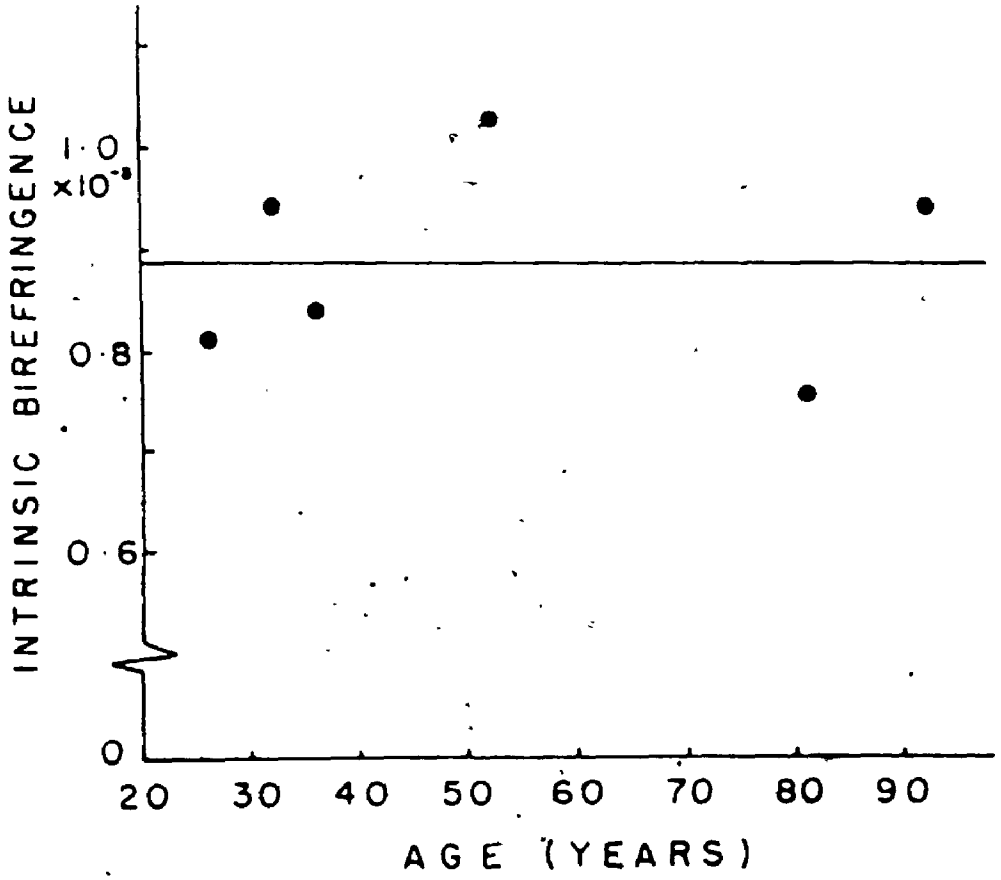

Figure 28: Intrinsic birefringence of normal mitral valve tendons plotted as a function of the patients age (r=-0.0004). The values are similar to those found in the visceral pericardium of the dog (*see Figure 26*). This finding indicates that imbibition analysis is unable to detect the subtle changes that occur in the molecular organisation of collagen during long term ageing.

been homogenised. A further advantage over a biochemical assay method such as the assay for hydroxyproline content (which is used to determine total collagen content), is that, while the assay will reveal the total concentration of hydroxyproline in the sample, it cannot distinguish between hydroxyproline present in functional, intact collagen and hydroxyproline from collagen which is being degraded. Degraded collagen fibres, analysed using the retardation methods, will have diminished birefringence when compared with intact nondegraded fibres and so may be easily distinguished.

The methods used in this experiment cannot be used to detect the presence and relative amount of different kinds of cross links. Therefore, the methods could not detect molecular organisation differences in mature collagen from patients of very different ages. In this respect the polarised light techniques are inferior to the biochemical tests. The retardation methods do, however, provide a way of comparing overall molecular organisation and should be regarded as a complement and not an alternative to biochemical analysis.

In conclusion, measurement of the retardation of linearly polarised light in collagen can be used to detect the early changes in molecular organisation that occur as collagen matures.

CHAPTER 6 STRUCTURE OF CEREBRAL ARTERY BIFURCATIONS

6.1. Introduction

The following three chapters show how a combination of the quantitative polarised light techniques, illustrated in the preceding three chapters, can be used to investigate a particular pathological problem - cerebral saccular aneurysms. Saccular aneurysms are balloon like distensions of an artery arising from the tissue at the apex of arterial bifurcations. Although not particularly common, aneurysms have the potential for producing devastating effects. Aneurysm rupture usually produces a major stroke. Aneurysms are principally made of collagen (Stehbens 1975). The development, growth and rupture of saccular aneurysms is paradoxical:- collagen is a relatively stiff material and yet aneurysms grow, - collagen has a relatively high tensile strength and yet aneurysms rupture. These paradoxes concern collagen structure and the mechanical properties that derive from the structure. Since collagen is birefringent, it may be analysed at both the molecular and fibre levels using the polarised light methods that I have described in the preceding chapters. Such a study could resolve the paradoxes, and, by providing a greater understanding of the structure lay the foundation for improved clinical and surgical management of saccular aneurysms.

This chapter deals with the development of cerebral saccular aneurysms. Saccular aneurysms develop predominantly at the apex of human brain artery bifurcations (Hassler 1961). The first question to consider is why does such a preference for one particular site exist? Perhaps the most obvious possibility is that the structure at the bifurcation is conducive to aneurysm formation. In spite of this, the structural organisation of human brain artery bifurcations has received little attention. The studies that have been done have largely ignored collagen and have concentrated instead on the internal elastic

lamina and the presence of medial gaps (reviewed by Sekhar and Heros 1981).

Forbus (1930) proposed that the frequent presence of medial gaps, an absence of the *tunica media* muscle layer from the apex of the bifurcation, represented a congenital structural defect. Subsequent studies, however, have shown no correlation between the distribution or incidence of aneurysms and the presence of medial gaps (e.g., Stehbens 1959). Stehbens (1981) gave an alternative explanation for the presence of medial gaps: that the collagen in the muscle layer gap constitutes a "raphe" (a seam or join) between the muscle fibres of the adjoining daughter branches, providing a structural anchor during vasoconstriction. An implication of Stehbens' proposal is that the collagen in the medial gap performs a specific function and should therefore have an organisation consistent with this function. Macfarlane et al. (1980), in a study of the mechanical properties of brain artery bifurcations, found that the apex of the bifurcation was relatively stiff compared to the rest of the artery. The stiffness of the apical region indicates that it would be unlikely to bulge outwards, a necessary requirement for aneurysm formation. The muscle is replaced in the medial gap by collagen. The presence of a much stronger and stiffer material tends to discount the possibility that the medial gap represents a congenital defect. In view of the above evidence, the paradox of aneurysm formation may be stated as follows; saccular aneurysms develop at regions where the principal structural component is a material with a high tensile strength (relative to the other materials in the artery wall) and a relatively high stiffness. Such a paradox could be explained if the collagen laid down to replace the smooth muscle at the bifurcation apex had an organisation that made it unable to resist aneurysm formation. Therefore, the aim of this study was to determine the organisation of collagen in the medial gap and assess its relationship to the different proposals regarding the significance of the medial gap.

6.2. Methods

Collagen organisation was studied at two structural levels. The alignment of fibres was studied using polarised light and the three-dimensional orientation method, while fibril organisation was examined using transmission electron microscopy (TEM). Segments of eight brain arteries with bifurcations were obtained from six autopsies (males and females, age range 42-92). After perfusion fixation at a pressure of 120 mmHg the arteries were processed as described in Chapter 2.

I studied five of the arteries using polarised light. Three were embedded so that the parent vessel was cut in cross section, and two were sectioned longitudinally. The sections were stained with silver impregnation, picrosirius red or Masson's trichrome. The arteries cut in cross section were analysed using the universal stage. Measurements of fibre orientation were taken in two regions: from where the daughter vessels touched, and at sites distant from the gap (Figure 29). For each section, ten three-dimensional orientation measurements were taken in each region.

The sectioning, embedding and microscopy for the TEM study was done by Dr. R.C. Buck (Department of Anatomy, U.W.O.). Three vessels from two different autopsies were pressure fixed in the same way as the others, except that Karnovsky's perfusion fluid, rather than formalin was used. The vessels were trimmed so that only the apex and some tissue from the daughter branches remained. The samples were osmicated in 1% osmium tetroxide in a 0.1M s-collidine buffer, pH 7.4, for one hour at 4°C, immersed in 2% aqueous uranyl acetate for one hour, dehydrated in alcohol, and embedded in Epon 812. The sections were cut on a Sorval MT 1 ultramicrotome using glass knives, mounted on unfilmed grids, stained with lead citrate and examined with an AEI 801 or JEOL 100CX electron microscope at 80 kV. The sections were taken mid-plane longitudinally through the apex. Longitudinal sectioning cut the fibrils in cross section. Fibril diameters were measured from micrographs of the section (magnification 60,000x).

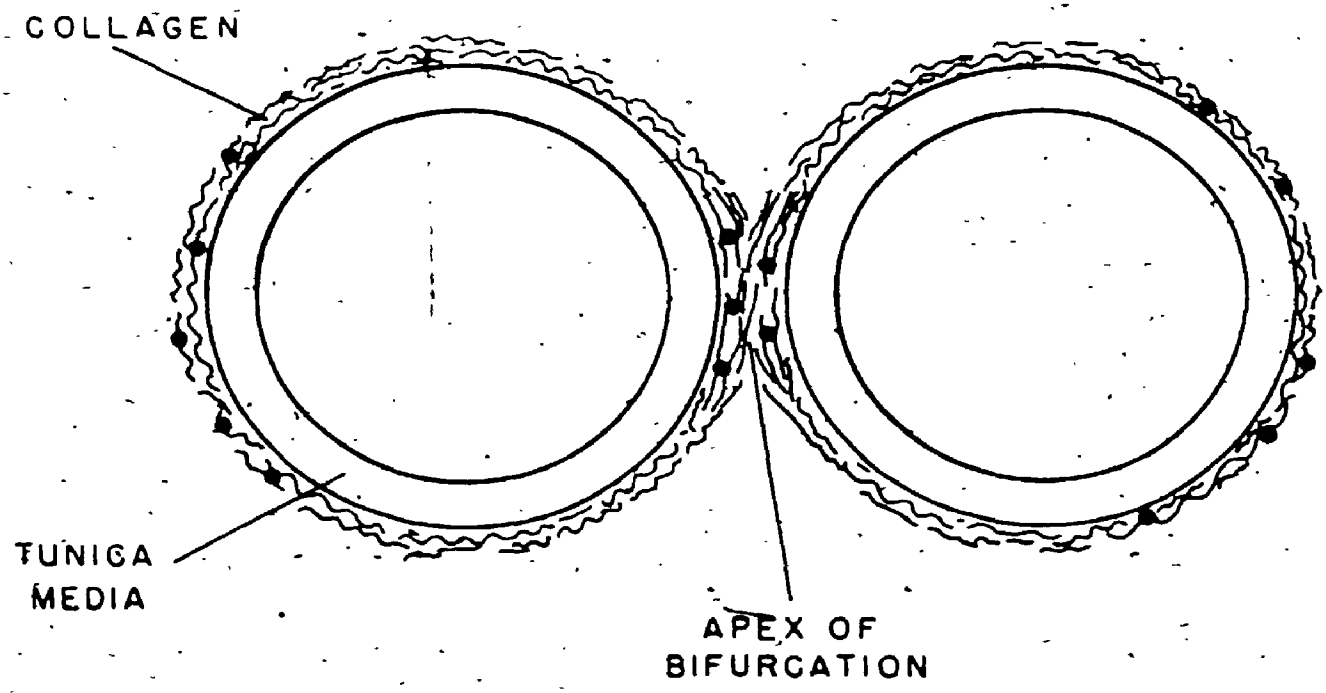

Figure 29: Schematic representation of a cerebral artery bifurcation cut in cross section. The dots show schematically where orientation measurements were taken. Collagen fibres at the apex of the bifurcation are drawn according to the results of this study i.e., they are relatively straight and are aligned at right angles to the long axis of the parent artery.

Measurements were taken from two regions: in the medial gap, and from the adventitia at sites distant from the gap. The size of the sections meant that the latter region was still close to the medial gap, but such regions were adjacent to medial smooth muscle cells, and therefore, not part of the gap. The measurements from the three vessels were pooled, 1100 fibril diameters were recorded in both regions.

6.3. Results

The data obtained from each of the vessels cut in cross-section were plotted on Lambert projections (Figure 30). The collagen fibres from the apex of the bifurcation were more coherently aligned, having a greater precision parameter and smaller helical components, than the rest of the adventitial collagen. Confirmation of the highly aligned circumferential fibres in the medial gap came from gross inspection of mid-plane longitudinal sections of bifurcations viewed with polarised light. Although I was unable to obtain universal stage measurements in this plane, because of the small size of the coherent zones, I observed that the collagen in the medial gap remained at extinction for all planar rotations of the stage. The only circumstances in which birefringent materials do not display their birefringence is when they are observed along their optic axis (Bennett 1950). Collagen's optic axis is parallel to the long axis of the fibre (Wolman 1975). If collagen fibres do not appear birefringent, then they must be aligned at right angles to the section plane. Therefore, at the apex of the bifurcation, in mid-plane longitudinal sections, the collagen fibres are aligned at right angles to the long axis of the parent artery.

Qualitative assessment revealed that the fibril organisation was the same as that of the fibres (Plate 3). At the apex of the bifurcation the collagen fibrils all appeared to have approximately the same orientation. Away from the apex the fibrils were aligned at a variety of oblique angles and some fibrils were even longitudinally aligned. Fibril

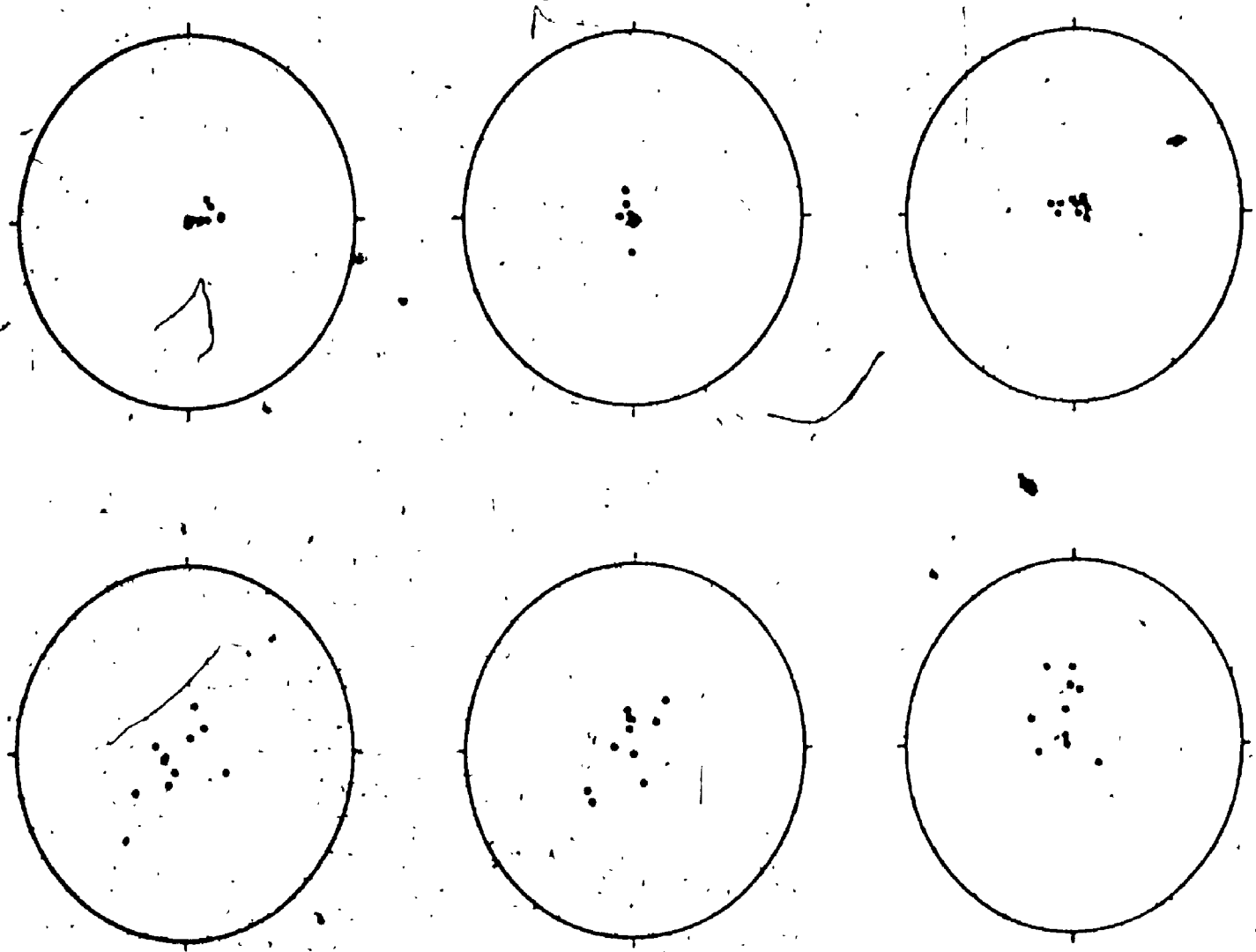

Figure 30: Scatter diagrams showing collagen orientation in the apex of the bifurcation (upper three) and in the rest of the adventitia of the same section (lower three). All samples were fixed at a perfusion pressure of 120 mmHg. Ten orientation readings were taken in each region (a circumferential fibre would be represented by a point at the centre of the projection).

2 OF DE 2

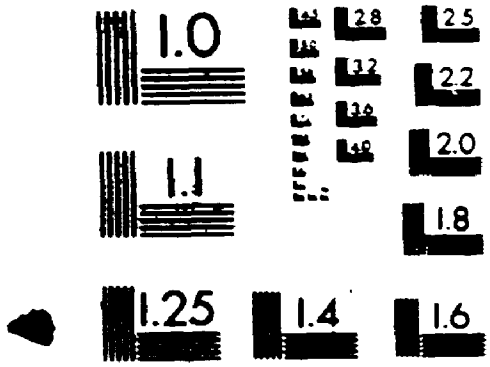

MICROCOPY RESOLUTION TEST CHART
NATIONAL BUREAU OF STANDARDS
STANDARD REFERENCE MATERIAL 1010a
(ANSI and ISO TEST CHART No. 2)

Plate 3: Photomicrographs from transmission electron microscopy showing the orientation of collagen fibrils. The upper figure is from the apex of a cerebral artery bifurcation, and the lower one from a region of the adventitia away from the apex. The orientation of fibrils in the apex is very uniform compared to the three-dimensional weave of fibrils seen elsewhere in the adventitia. (Magnification 19,000x)

diameters were examined from both regions and their distribution is shown in Figure 31 The combined mean fibril diameter in the medial gaps (49.9±7.2 nm, mean ± S.D.) was not significantly different ($p>0.05$) from the mean diameter in the rest of the adventitia (52.3±8.4).

6.4. Discussion

The striking feature of collagen in the medial gap of brain arteries is its highly aligned organisation, with fibres and fibrils running parallel to each other and perpendicular to the long axis of the parent artery. In contrast, the collagen in the rest of the adventitia is not as organised, having a larger helical component of orientation. Stehbens and Ludatscher (1973), in an electron microscopy study, qualitatively assessed the organisation of collagen in rabbit renal artery bifurcations. This artery, like brain arteries, is a muscular artery. They stated that the bundles of collagen appeared at times to be "criss-crossed" and that collagen in the medial gap was the same as that in the rest of the adventitia. The "criss-crossed" fibre organisation in the adventitia is indicative of a helical component of orientation, which agrees with my results. The organisation of the collagen in the medial gap may not be revealed using electron microscopy because it will only be evident at specific locations in mid-plane longitudinal sections. Ordinary light microscopy is also unsuited to detect the organisation providing, at best, only an approximate measure of alignment. The use of polarised light with the universal stage enables fibre orientation to be assessed quantitatively, and, because of the relatively low magnifications used, the orientation measurements can be easily related to the overall geometry of the bifurcation.

The orientation of collagen in tissues is a key determinant of mechanical properties. For example, collagen fibres in tendon are highly aligned and relatively straight. The straighter the fibres are, the greater the stress required to straighten them further,

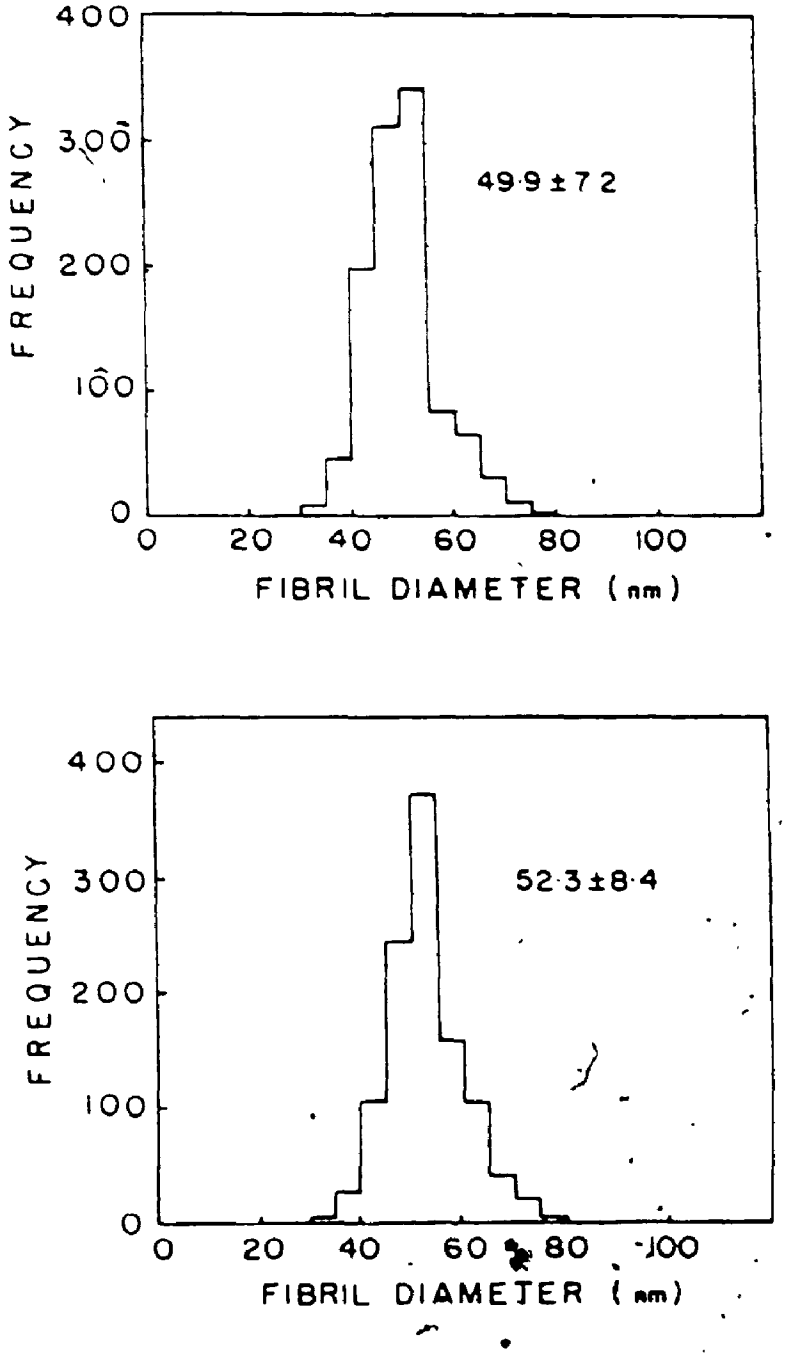

Figure 31: Frequency distributions of fibril diameters from the apex (upper graph) and away from the apex (lower graph). The average fibril diameters were not significantly different. The means ± S.D. are shown.

thereby accounting for tendon's relative stiffness (Rigby et al. 1959). I found that collagen fibre orientation in the medial gap is similar to that in tendons i.e., the fibres run approximately parallel to each other. This suggests that, at any given pressure, the medial gap will be stiffer than the rest of the adventitia. Macfarlane et al. (1980) reported that the apex of the bifurcation was able to maintain its shape even at negative pressures, and that the radius of curvature of the apex did not change appreciably as the pressure increased. These findings would be expected if the collagen in the medial gap was similar to that of tendons. The stiffness provided by the organisation of the collagen would make distension, which is a requirement for aneurysm growth, difficult.

The tensile strength of collagen is the other important factor in determining the mechanical properties of the medial gap. Based on a survey of the literature, Parry et al. (1978) proposed that a positive correlation exists between collagen fibril diameter and tensile strength. Comparing the diameters we found (30-90 nm range) with those of Parry's literature survey, the arterial collagen is smaller than skin (100-200 nm), which has a tensile strength of 12 MPa and is comparable to cartilage (40-100 nm), which has a tensile strength of 1.2 MPa. Cartilage is, however, composed of Type II collagen, which has different mechanical properties compared to Type I collagen (Kenedi et al. 1966). Unfortunately there was no arterial collagen included in the study of Parry et al. (1978). Carrasco et al. (1981) in a study of collagen fibril diameters in the aortic adventitia from different species (excluding humans) found that in dogs, rats and pigs the mean fibril diameter was around 75 nm with a standard error of the mean around 12 nm. Since the aorta is an elastic artery it is probably invalid to make a direct comparison with the brain arteries, which contain less elastin. Even if there is a direct correlation between fibril size and tensile strength, I found no significant difference in fibril diameter in the medial gap compared to the rest of the adventitia, and fibril diameter would therefore not appear to be a source of weakness at the bifurcation. This is consistent with the finding that bifurcations could withstand high pressure without rupture (Glynn 1940).

Thus, it appears that the organisation of collagen is likely to make the medial gap a region of strength, a finding incompatible with the idea that the medial gap represents a congenital defect.

Stehbens (1981) has suggested that the collagen in the medial gap provides a structural anchor during vasoconstriction. To perform this function the medial gap should be stiff, a requirement satisfied by the parallel alignment of the collagen fibres. Thus, my findings are consistent with the hypothesis that the medial gap forms a raphe between the muscle fibres of the adjoining daughter branches.

I conclude that the medial gap contains highly aligned, parallel collagen fibres and fibrils that run circumferentially in the apex and perpendicular to the long axis of the parent artery. This organisation should make the medial gap a region of stiffness and strength which is not conducive to aneurysm formation.

CHAPTER 7 MOLECULAR ORGANISATION OF COLLAGEN IN SACCULAR ANEURYSMS

7.1. Introduction

Despite the evidence, based on the organisation of the collagen fibres, that the medial gap of cerebral artery bifurcations appears to be a region of strength there is no doubt that aneurysms do develop at that point. Once an aneurysm has developed its growth is unpredictable (Allcock and Canham 1976), but its chance of rupture increases with increasing diameter (Crompton 1966). The mechanism of aneurysm growth and rupture illustrates two paradoxes. The first concerns mechanical stiffness. The work of Scott et al. (1972) showed that aneurysms are less distensible than normal cerebral arteries. That is, the aneurysm which has very low elastic deformation when tested in the laboratory must have undergone substantial plastic deformation in the process of enlargement. The second paradox concerns mechanical strength. Ferguson (1972) examined how wall stress in aneurysms of different wall thickness changed as a function of pressure. For pressures in the physiological range the calculated wall stress in the aneurysm ($\approx$ 1 MPa) is much less than the breaking stress of collagen (60-100 MPa, based on the strength of tendon collagen, Harkness 1961, Wainwright et al. 1976), and yet aneurysms do rupture.

The presence of immature collagen in the aneurysm wall provides a possible explanation for these apparent paradoxes. Immature collagen is more extensible than mature collagen (Harkness and Harkness 1973, Torp et al. 1975) and has a lower tensile strength (Gillman 1968). This would make an aneurysm more likely to enlarge and rupture. Theoretically it may be possible to account for the collagen in a uniformly thin walled aneurysm using collagen already present at the apex of the bifurcation (Canham and Ferguson 1985). The majority of aneurysms, however, are not thin walled but have

widely varying wall thicknesses (Suzuki and Ohara 1978). Thus, I propose that in most cases the total quantity of collagen in the aneurysm cannot be derived solely from the previously existing arterial collagen and the production of new collagen is required.

In Chapter 5 I demonstrated that immature collagen can be detected using the polarised light techniques of imbibition analysis and the measurement of retardation in stained tissue. I used both these methods to analyse collagen in the aneurysm wall and to compare it to the mature collagen in the *tunica adventitia* of adjacent arteries.

7.2. Methods

7.2.1. Tissue preparation: Six human cerebral saccular aneurysms and adjacent arteries were obtained at autopsy (5 males, 1 female ages 40 to 82). Three of the aneurysms used were not prepared specifically for the present study but were fixed by immersion (i.e., not by pressure perfusion) in 10% neutral buffered formalin. The freshly obtained samples were perfusion fixed at a pressure of 120 mmHg. The previously prepared sections were stained only with haematoxylin and eosin (H&E), while the "fresh" tissue sections were stained with H&E, picrosirius red, or left unstained for imbibition analysis.

7.2.2. Stained tissue: I took retardation measurements in two regions on each of the H&E stained sections: (i) From collagen in the tunica adventitia of the vessels adjacent to the aneurysm. This collagen was assumed to be normal, mature collagen.

(ii) From collagen in the aneurysm itself.

On average, I took 15 measurements in each region. The average retardations from the adventitia and from the aneurysm wall of each section were compared using student's t-test. To verify that the fibres selected for measurement lay mainly in the section plane, three dimensional orientation was measured using the universal stage.

7.3.2. Unstained tissue: Imbibition analysis was done on sections from three aneurysms.

For two of these, ten retardation measurements were taken randomly in each region in each of the imbibing fluids. For the third aneurysm, the readings were taken on the same fibres in each of the imbibing media. Form birefringence curves were then drawn and the intrinsic birefringence calculated for each sample.

7.3. Results

7.3.1. Stained tissue: Figure 32 shows the retardation readings from collagen in the aneurysm and in the *tunica adventitia*. I analysed 19 different sections, with an average of 110 readings taken from each aneurysm. The mean retardation of the adventitial collagen was significantly greater than that of the aneurysm collagen ($p<0.001$) for each section. Regional variation was seen in all of the aneurysms studied. Table 5 shows how retardation varied with radial position across the aneurysm wall for one of the samples. There was no clear trend seen in the distribution of the retardation values. One of the aneurysms had an obvious rupture site. Collagen close to this site was found to have the lowest retardation values, while collagen further away had progressively higher retardation.

7.3.2. Unstained tissue: Significantly lower values of retardation and intrinsic birefringence ($p<0.05$) were found in the aneurysm collagen (Figure 33). As with the stained tissue regional variations were observed throughout the aneurysm wall (Figure 34).

7.4. Discussion

How can a strong, inextensible material be the principal component of a saccular structure which undergoes substantial dilation and eventual rupture? Earlier studies have indicated that forces in the artery and the aneurysm wall produce stresses well below the

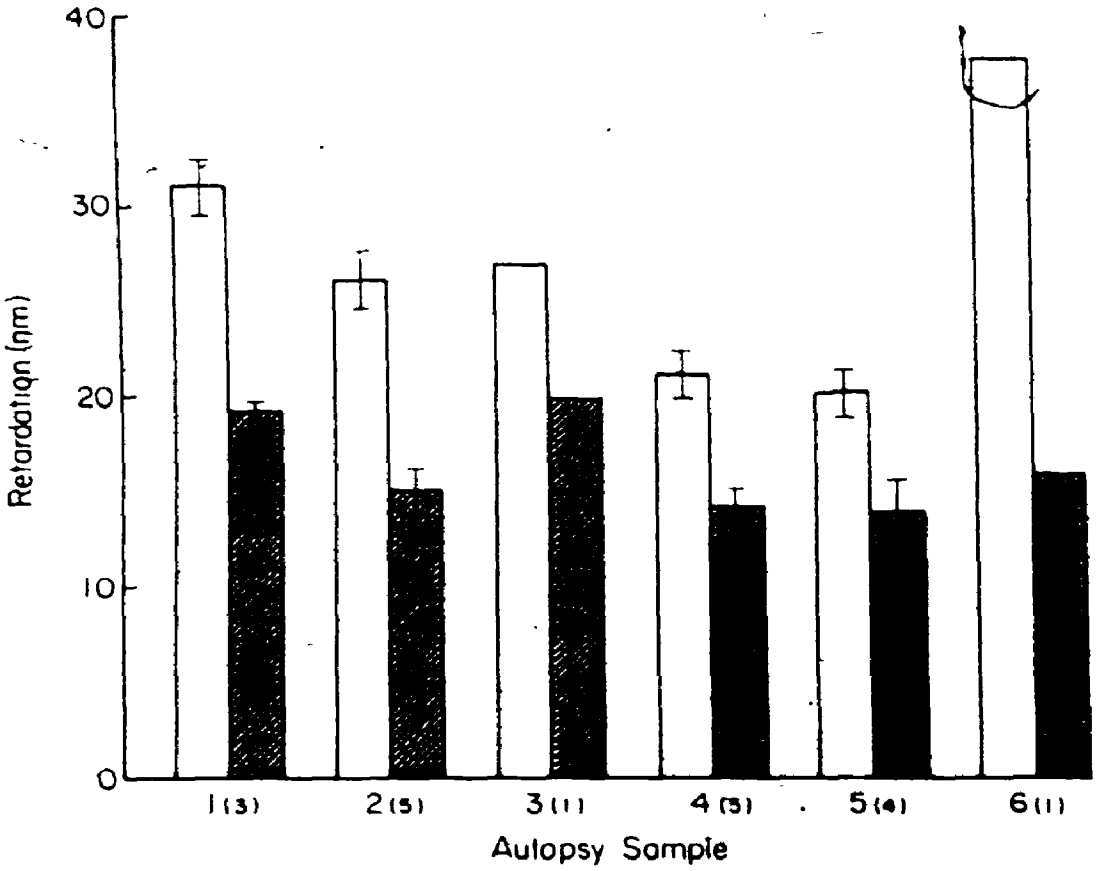

Figure 32: Bar graph showing the retardation found in the aneurysm collagen (stippled bars) compared to the adventitial collagen (open bars) for each of the 6 samples studied. The number in brackets after the autopsy sample number gives the number of sections analysed. All sections were stained with H&E. Where appropriate the standard error of the mean is shown. In all cases the aneurysm collagen has a significantly lower retardation than the adventitial collagen.

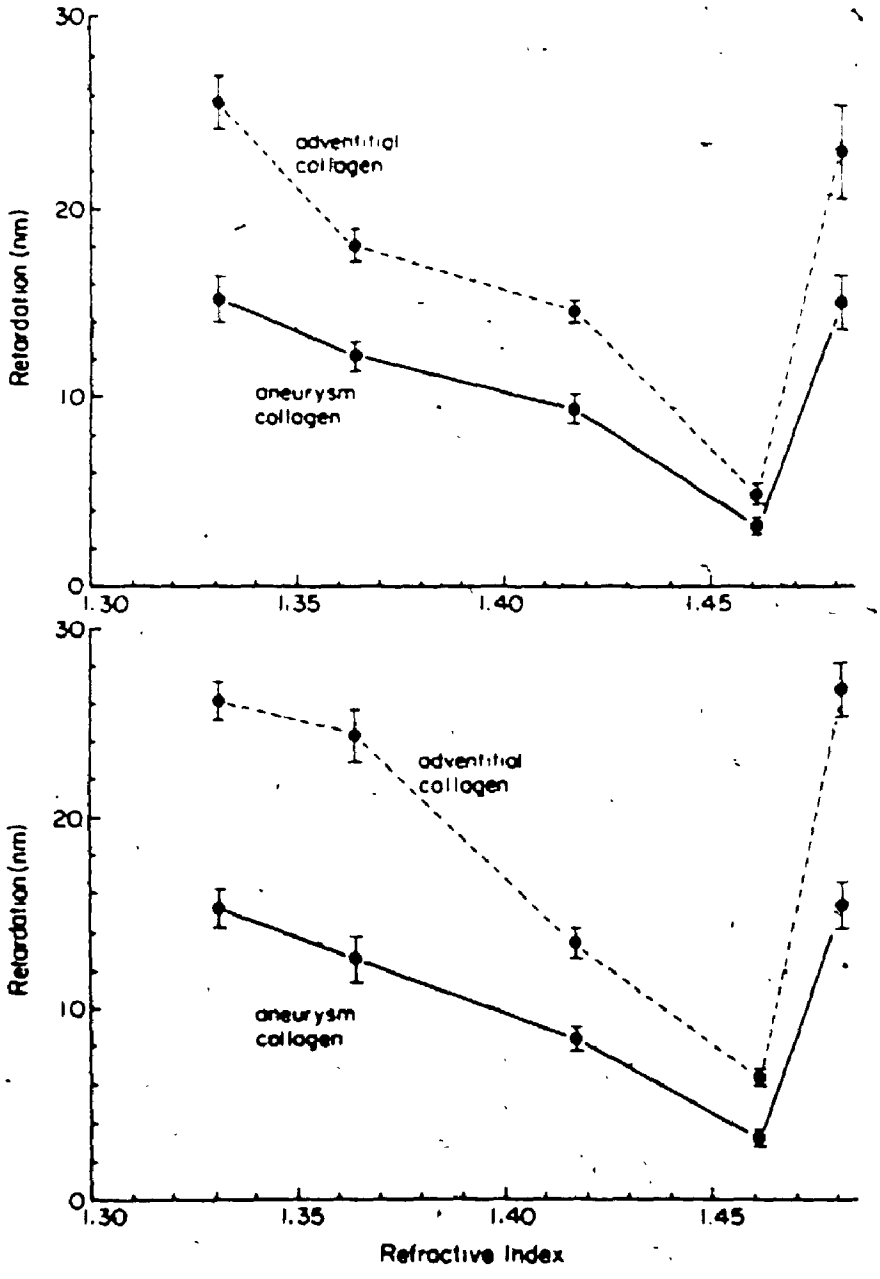

Figure 33: Form birefringence curves for sections from two of the aneurysms along with the curves for the corresponding adventitial collagen.

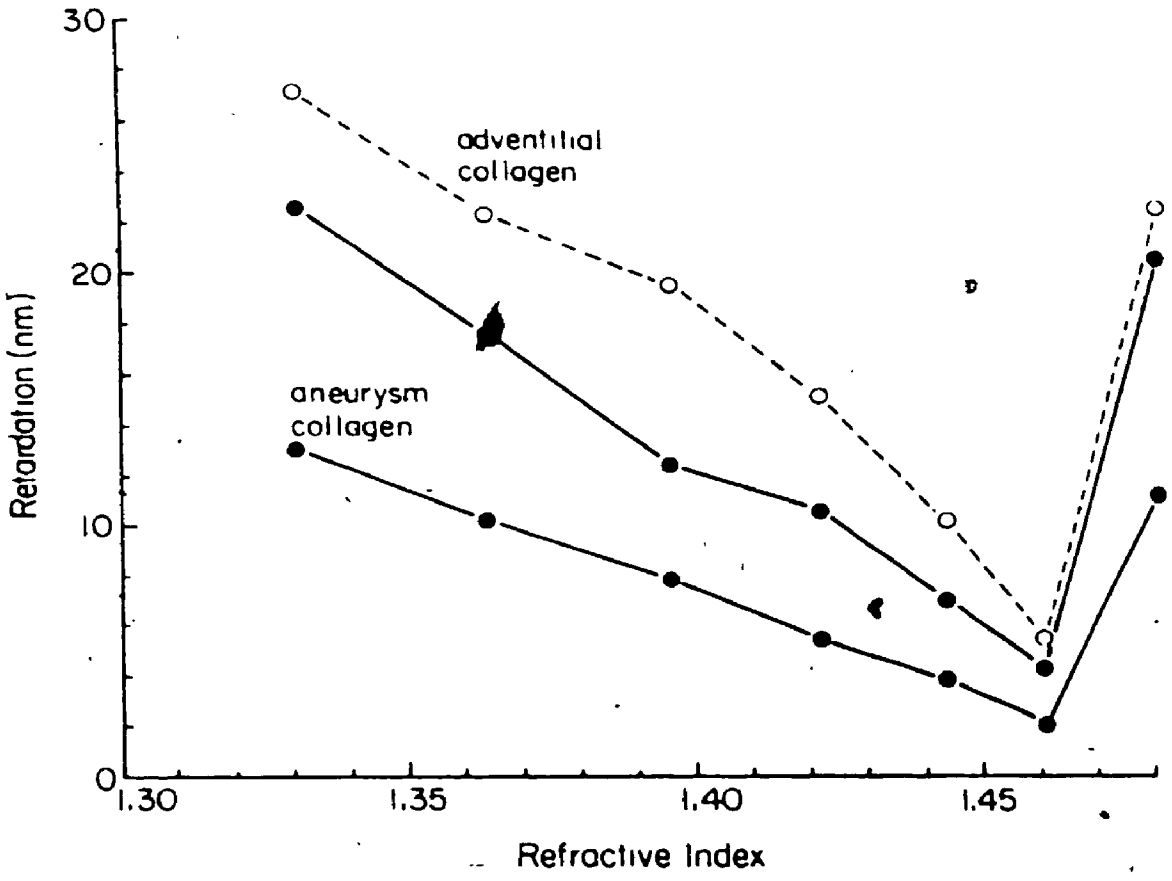

Figure 34: Family of form birefringence curves obtained from one of the aneurysms (sample 3). Collagen from different locations in the aneurysm wall had different curves. The two curves shown for the aneurysm (closed circles) represent the two extremes found.

	radial position expressed as a percentage of the distance across the aneurysm wall								
	0	10	20	50	60	80	90	100	%
1	10·6	14·2	10·0	9·1	18·5	14·2	10·3	23·6	
2	11·5	12·4	17·2	17·0	10·4	6·4	15 5	30·5	
3	10·6	7·9	13·6	18·0	12·8	20·8	15·4	20·9	
4	13·0	12·7	11·2	24·2	17·0	7·6	29·8	34·6	

Table 5: The regional variation in retardation through the aneurysm wall was illustrated by measuring the retardation (nm) as a function of radial position across the wall at four different positions around an aneurysm wall. No consistent trend was seen, although the highest readings were found at the outside of the wall.

magnitude necessary to cause collagen to exhibit this inelastic behaviour (Scott et al. 1972). It appears that the collagen in a developing aneurysm has different mechanical properties making it more tolerant of inelastic deformation.

There are two possible explanations for the different mechanical properties: (1) degradation of mature collagen in the aneurysm and (2) the predominance of immature collagen in the aneurysm wall. Degradation can result from enzymatic breakdown of the collagen's molecular structure. The action of enzymes has been thought to play a role in aneurysm formation in cases where there has been penetration of the wall by polymorphonuclear leucocytes and the subsequent release of their enzymes (Lazarus et al. 1972, Cajander and Hassler 1976). Although such deterioration of the collagen is physically possible, it does not appear to be a significant factor in the tissue studied here for the following reasons. Work in other laboratories has shown that a change in the interference colours is produced when linearly polarised light passes through collagen degraded in vivo by polymorphonuclear leucocytes (Junqueira et al. 1980), or in vitro by bacterial collagenase (Perez-Tamayo and Montfort 1980). In those studies, the collagen was prepared in the same way as in my study (picrosirius red staining of 7 μm sections). For Type I collagen fibres the observed interference colours would be orange/red but at more advanced stages of degradation, these colours change through yellow, to green. The colour is determined by the diameter of the fibres, with the largest appearing orange/red and the smallest green. The aneurysm tissue studied appeared as orange for the most part with a few isolated fibres showing as yellow or green, a possible consequence of the mechanics of sectioning. This interpretation is supported by the appearance of similar quantities of yellow or green fibres in the *tunica adventitia* of the adjacent vessels, where degradation is unlikely. There was also a higher incidence of yellow/green interference colours in tissue obviously distorted during sectioning. The indication that, in the two regions studied, the frequency of smaller diameter fibres was very similar suggests that the basis for lower retardation readings in the aneurysm collagen is also

not a consequence of there being less collagen.

Since degradation of mature collagen cannot satisfactorily account for the experimental evidence, the presence of immature collagen must be considered Theoretically, tissue from the area of the bifurcation is insufficient to account for more than limited aneurysm enlargement (Canham and Ferguson 1985). Therefore, new collagen appears to be required to form the aneurysm As collagen matures, the number of intermolecular cross-links increases (Light and Bailey 1980) and its molecular organisation becomes more ordered (Sinex 1968). As a result of these molecular alterations, the maturing collagen increases in tensile strength (Gillman 1968) and its optical properties change. An increase in the retardation of linearly polarised light by maturing collagen has been observed in a study of regenerating rat Achilles tendon (Mello et al. 1975), and in a study of dermal scar maturation in guinea pigs (Wolman and Gillman 1972). The increase in molecular organisation during maturation also produces an increase in the collagen molecules' ability to bind dyes in an oriented manner, causing an increase in the retardation (Joiner et al. 1968). I observed that aneurysm collagen, both in the imbibition analysis and in the study of stained tissue, consistently exhibited significantly lower retardation than the adventitial collagen. Slight differences in staining procedures may account for some of the sample-to-sample variations in retardation, however, this does not affect the comparison because for each section the collagen in the aneurysm and adventitia was stained simultaneously and hence under identical conditions. All of the aneurysm showed regional variations in retardation. This variation is accounted for because aneurysm enlargement, and hence the production of new collagen, is probably an intermittent process. One sample which contained a rupture site gave the lowest retardation readings close to this site. As the site of rupture would probably be the area of least strength, it follows that rupture would occur where the collagen was most immature. This is consistent with the lowest retardation readings coming from points closest to the rupture site.

One of the problems encountered when studying aneurysms is that it is impossible to know when the aneurysm first started to develop. The only time when immature collagen is definitely present in the aneurysm occurs when the aneurysm bleeds, then repairs, and the patient survives In response to the bleed, collagen will be laid down to heal the wound. Drawing on the results of many case studies, Jane et al (1977) reported several observations that would fit with my hypothesis They found that 75% of patients who suffered a subarachnoid haemorrhage and who also had a diastolic pressure of 109 mmHg or above had a rebleed, while only 25% of those with a diastolic pressure of 90 mmHg or below had a rebleed. Immature collagen is less able to withstand high pressures than mature collagen. Hence hypertension is a probable contributor to rupture, at least until the collagen has matured to the point at which its strength is the same as that of the collagen in the adventitia. The same authors also found that the incidence of rebleed was highest on the same day as the initial event and then gradually decreased, eventually becoming very low after about six weeks The tensile strength of newly formed collagen increases during this time (Gillman 1968), and the period during which tensile strength increases the most (two weeks after the wounding event) is the same period during which the incidence of rebleed decreases most rapidly.

In summary, I have found a consistent difference in the optical properties of aneurysm collagen compared to the adventitial collagen in adjacent arteries. The paradoxes of stiffness and strength can then be explained because the collagen in the aneurysm wall is different from that of the *tunica adventitia*. The lower retardation values found in the aneurysm indicate that the aneurysm collagen is less organised at the molecular level, probably because of the presence of immature collagen fibres. Therefore, the aneurysm would be less able mechanically to withstand the forces to which it would be subjected.

CHAPTER 8 COLLAGEN FIBRE ORGANISATION IN SACCULAR ANEURYSMS

8.1. Introduction

Collagen fibre organisation will be a determinant of the mechanical properties of saccular aneurysms. Thus, the paradoxes of stiffness and strength described in Chapter 7 might be explained in terms of the three-dimensional organisation of collagen fibres in the aneurysm wall. A model of saccular aneurysms can be used to predict the ideal fibre organisation. Figure 35, a diagram of a spherical aneurysm cut in mid-section, shows the forces acting on the aneurysm. If the aneurysm is in equilibrium, then the force, F_P, of the blood pressure will be balanced by the force F_T in the aneurysm wall. The force, F_P, due to the blood pressure is equal to the luminal area a ($a = \pi r^2$, where r is the radius of the aneurysm) multiplied by the blood pressure P, $F_P = \pi r^2 P$. This force is resisted by an area of the wall $A = 2\pi rt$ (t is the wall thickness). Therefore, the stress in the wall $\sigma = F_P/A = rP/2t$. This stress is uniform in all directions (Wainwright et al. 1976, p.293). The multidirectional stresses predicted by the model indicate that to deal with the stresses in the aneurysm wall, the collagen fibres might also be expected to have a multidirectional organisation. From the equation for wall stress it can be seen that, the thinner the wall, the greater the stress in the wall. The organisation of collagen in the aneurysm wall might also be expected to be influenced by wall thickness.

The analysis of the aneurysm model provides an indication of the expected optimum fibre organisation in aneurysms. To determine if the actual organisation followed the prediction from the model, the orientation of collagen fibres in the aneurysm wall was measured using both the three- and the two-dimensional polarised light techniques.

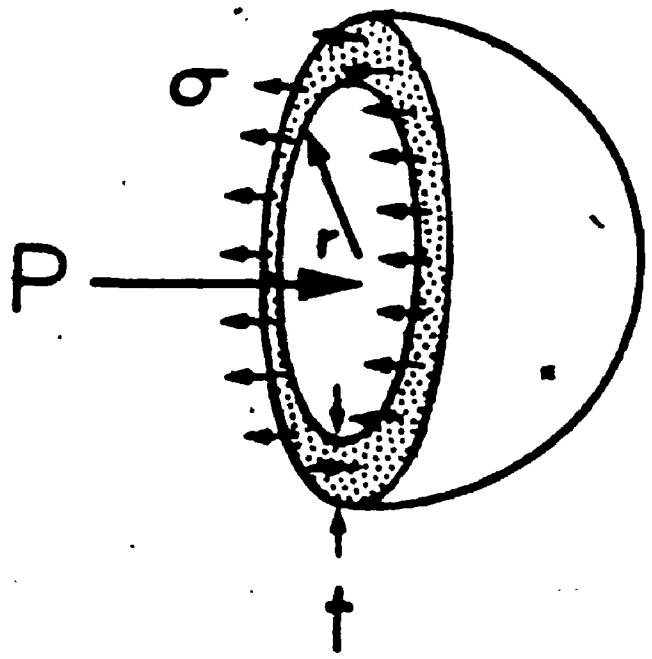

Figure 35: Diagram showing the forces acting on a pressure distended thin-walled aneurysm cut in mid-section. P is the force exerted by the blood pressure. This force is balanced by the wall stress σ.

8.2. Methods

8.2.1. Tissue preparation: Five aneurysms from five patients were studied. Three of the aneurysms were intact and were obtained at autopsy (all males, ages 59, 76, and 82 years). These specimens were perfusion fixed in 10% neutral buffered formalin at a transmural pressure of 120 mmHg. The remaining two samples (1 male 39 and 1 female 62 years old), obtained at surgery following rupture of the aneurysm, were provided by Dr. G.G. Ferguson (Department of Clinical Neurological Sciences, U.W.O.). The surgical specimens were taken from the fundus of the aneurysm. The shape and dimensions of the aneurysms were known from angiograms and from observations at the time of surgery. Based on this information a plasticene mold of the aneurysm was made and the tissue stretched over the mold to simulate a pressure distended geometry. The tissue was then held in position by pins and fixed in formalin. All of the aneurysms were embedded in paraffin wax and 7 μm mid-plane sections taken. The sections were stained with either picrosirius red or haematoxylin and eosin.

8.2.2. Two-dimensional orientation: I used the two-dimensional orientation method to study the relationship between wall thickness and orientation. I measured the two-dimensional orientation of the collagen fibres at several locations around the wall of each aneurysm. In total, orientation measurements were taken at 15 different sites in the five aneurysms. The measurements were made proceeding radially across the wall from the lumen to the outer surface. The locations of the sets of measurements were chosen so that the orientations were measured for a range of different wall thicknesses.

8.2.3. Three-dimensional orientation: I measured the three-dimensional orientation of collagen fibres in picrosirius red stained sections from each aneurysm. Between 20 and 50 orientation measurements were taken on each section. The measurements were taken throughout the wall and plotted on Lambert equal area projections. The fibre orientations

were measured relative to the circumferential direction in the section. Thus a fibre aligned circumferentially in the aneurysm section was represented by a point at the centre of the Lambert projection.

8.3. Results

8.3.1. Two-dimensional orientation: When the aneurysm sections were observed with polarised light and rotated on the planar microscope stage the aneurysm wall appeared laminated (Plate 4), with the layers having different orientations. As the microscope stage was rotated, different layers were at extinction at different angles, indicating that the layers had different collagen fibre orientations. The laminated appearance could not be seen with ordinary light microscopy. The quantitative two-dimensional fibre orientation of each of the layers is shown in Figure 36. Four representative examples are shown. These examples illustrate the relationship between aneurysm wall thickness, the number of different layers and the collagen fibre orientations Generally, the thicker the wall, the more layers there were. The "zig-zag" nature of the orientation plots show the presence of different collagen fibre orientations in the aneurysm wall. Although there were often many different layers, inspection of the plots suggested that the orientation of the collagen fibres in the layers fell into two groups. The average difference between the orientations of the two groups was calculated for each sample and plotted as a function of the wall thickness at the point where the orientation readings were taken (Figure 37).

8.3.2. Three-dimensional orientation: The three-dimensional orientation of the collagen fibres in the aneurysm is shown in the scatter diagrams (Figure 38). The general organisation is circumferential with large helical and spiral components. The scatter in the helical direction is similar to that seen in the *tunica adventitia* of brain arteries but the spiral component is greater. A scatter diagram from a brain artery fixed at a

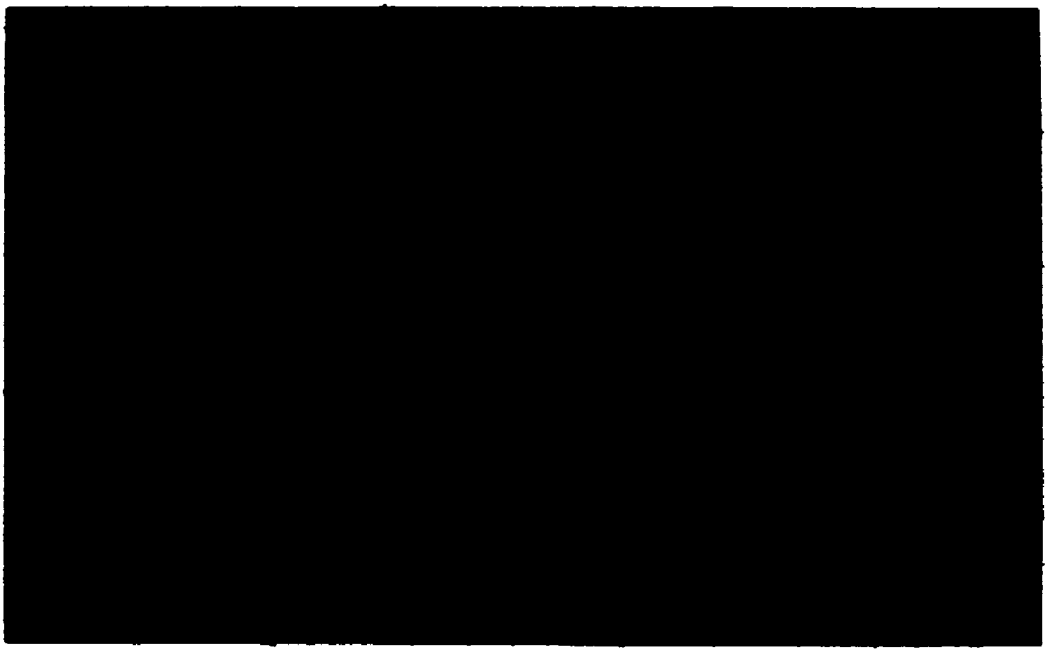

Plate 4: Eosin stained section showing part of an aneurysm wall. The section was photographed using polarised light plus a combination of a full wave plate and a sensitive tint retarder. The result of this combination is that different orientations are represented by different colours. This technique reveals the laminated nature of the aneurysm wall, shown by alternating bands of blue and yellow. (Magnification 85x)

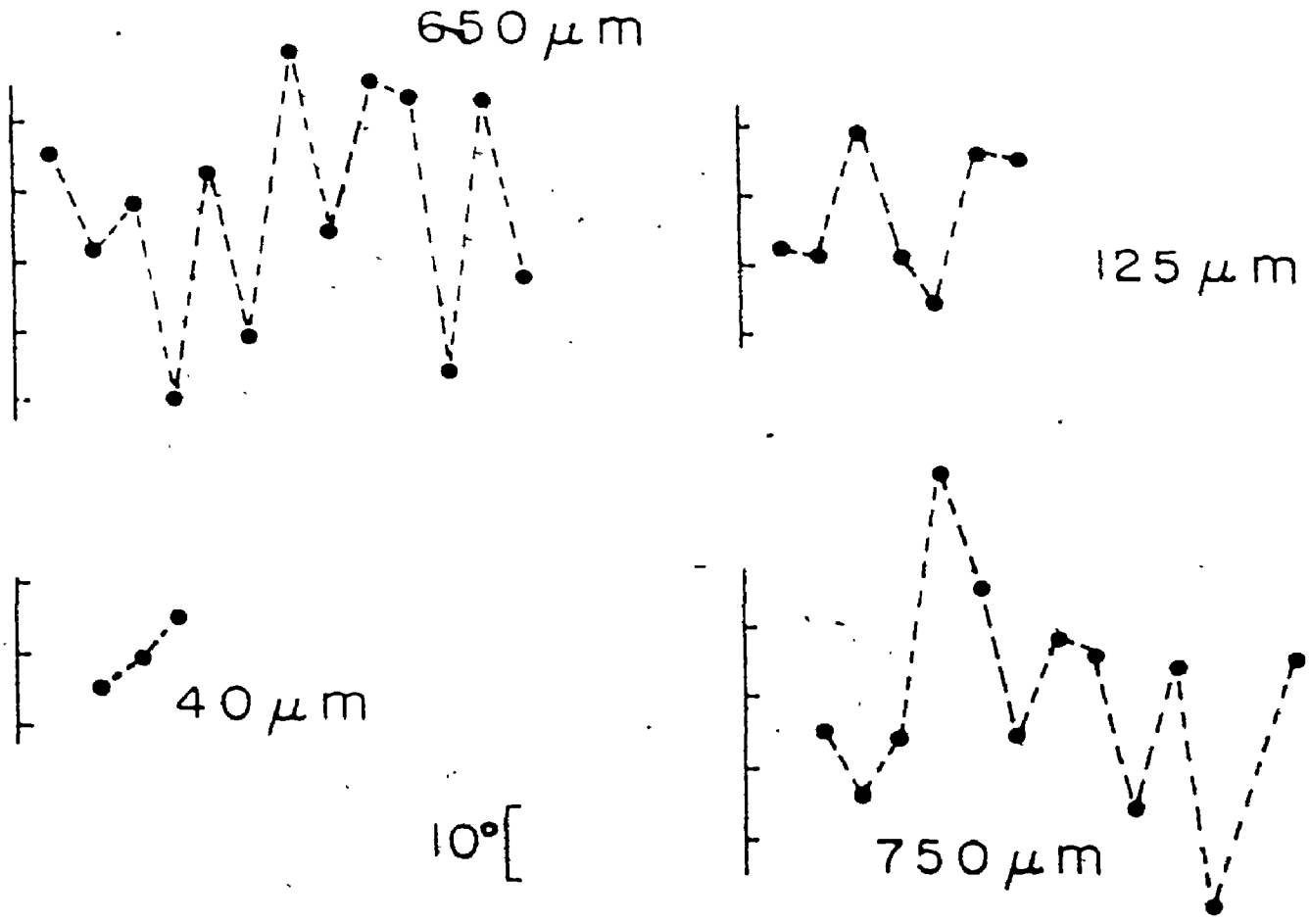

Figure 36. Shows the laminated structure of the aneurysms. Each plot shows the orientation of different layers measured radially across the wall (lumen → outside is left to right on the plots). Four plots from four different aneurysms with different wall thicknesses are shown. The vertical scale shows the orientation in degrees. The horizontal scale indicates distinct layers.

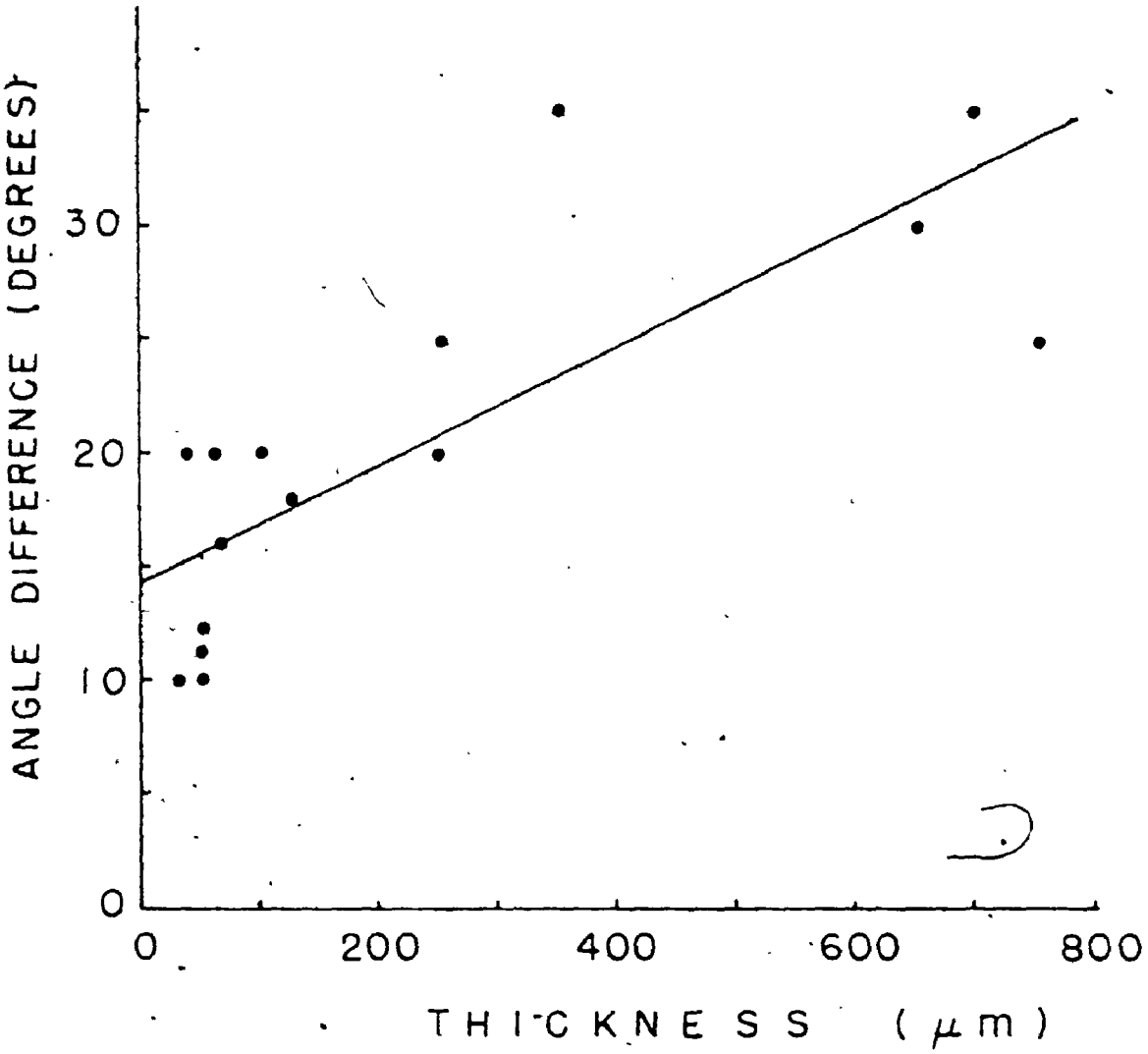

Figure 37. The average difference in orientation between different collagen layers in the aneurysm wall is shown as a function of wall thickness (r=0.78). The graph indicates that the thinner the wall the more aligned the collagen fibres are.

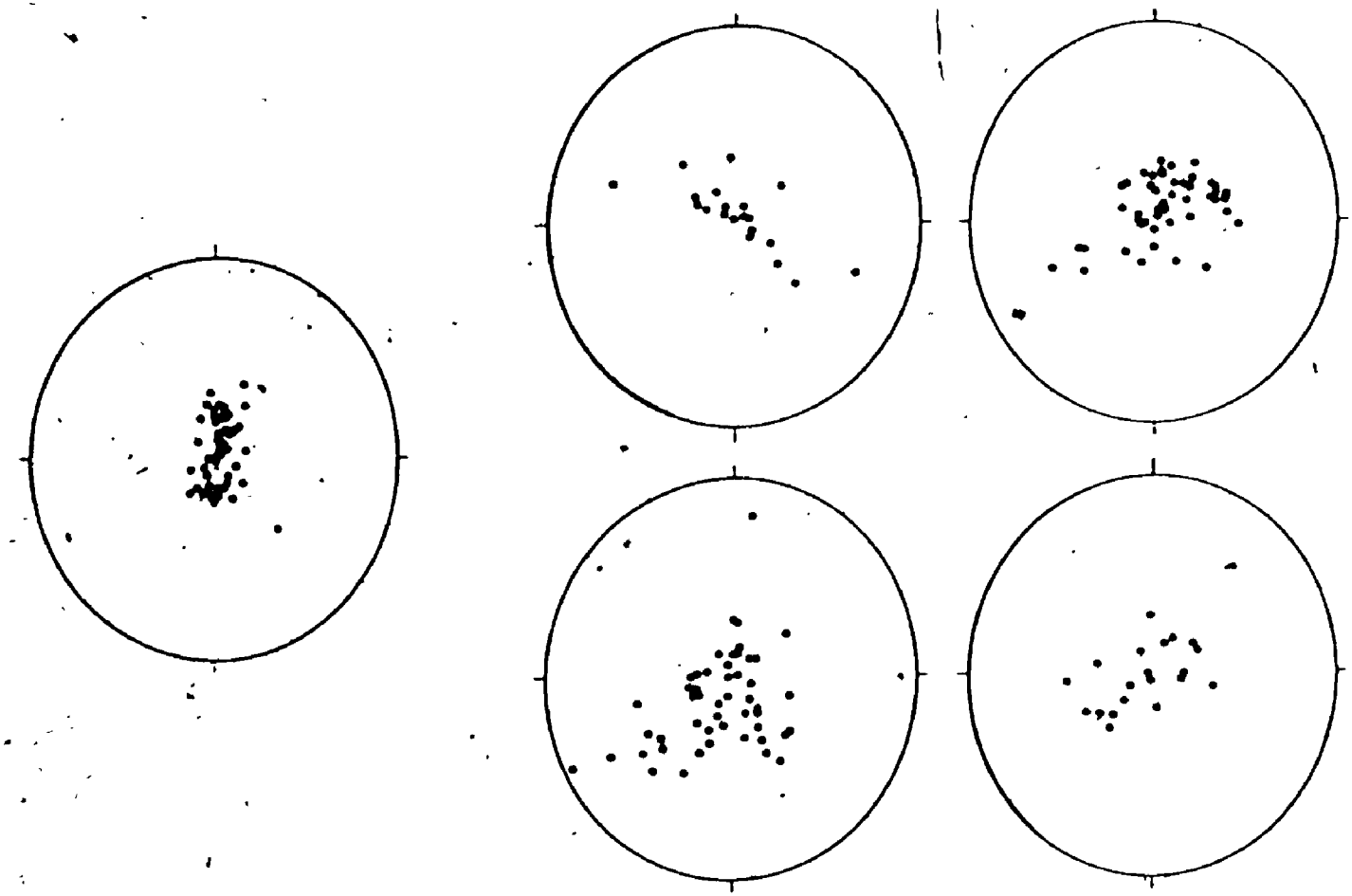

Figure 38: Scatter diagrams from four different aneurysms. For comparison a scatter diagram from collagen in the *tunica adventitia* perfusion fixed at 120 mmHg is shown (a fibre aligned circumferentially would be represented by a point at the centre of the projection).

transmural pressure of 120 mmHg is shown in the figure for comparison.

8.4. Discussion

A complex three-dimensional network of collagen fibres would be the best way to deal with the multidirectional stresses in the aneurysm wall. I indeed found that there is a complex three-dimensional organisation of collagen in the aneurysm wall, but it is difficult to explain the organisation completely in terms of the spherical aneurysm model. The organisation of collagen in the aneurysms lacked the strong circumferential tendency seen in the *tunica adventitia*, hence the collagen has a greater longitudinal or helical component. In the spherical aneurysm model the wall stress would be uniform in all directions. Therefore, one would expect more fibres to have large helical components at the expense of a reduced population of circumferential fibres, which is what I found. However, I did not find many fibres with a predominantly longitudinal orientation. This could have been a result of the difficulty in obtaining such measurements, because of the limitations of the Universal stage. The most striking difference between collagen fibre organisation in the aneurysms and in the adventitia is the large spiral component of orientation found in the aneurysms. In the model there is no need for a spiral component. Although it is not evident from the Lambert projections, because they provide no positional information, the spiral component derives from the laminated nature of the aneurysm walls. The finding of layers of collagen fibres with different orientations was a striking feature of all of the aneurysms when viewed with polarised light. How the different layers are produced is unknown. In the study described in the previous chapter I found that the retardation values differed across the wall, perhaps indicating collagen at different stages of maturity. It is possible then that the different layers are produced at different times, perhaps in response to aneurysm enlargement. The different mechanical constraints in effect at different stages in the growth of the aneurysm might

then cause newly produced collagen to be laid down with different orientations. The relationship between the orientation of the different layers and their retardation values is a promising area for future study. Whatever the reason for its presence, the laminated structure of the aneurysm could be expected to strengthen the wall by producing a plywood effect. The relationship between the fibre angle difference and wall thickness (Figure 37) is not surprising because as wall stress increases (wall stress $\propto 1/t$) the collagen should become more aligned.

In conclusion, collagen fibre organisation in the wall of saccular aneurysms appears appropriate for coping with the multidirectional stresses. This finding lends support to the hypothesis presented in the previous chapter, that aneurysm development and rupture results from immature collagen in the wall, which is unable to resist the stresses, rather than a problem with fibre organisation.

CHAPTER 9 MOLECULAR ORGANISATION OF COLLAGEN IN FLOPPY VALVE DISEASE

9.1. Introduction

This chapter illustrates the use of the imbibition analysis technique to examine the nature of the pathological changes in the disorder called floppy valve or mitral valve prolapse. The mitral valve is a collagenous structure situated within the heart between the left atrium and the left ventricle. When the valve is open, in diastole, it allows blood flow from the left atrium to the left ventricle and when closed, in systole, it prevents reverse flow. The valve consists of two leaflets, anterior and posterior, which are tethered to the ventricular wall by tendons (chordae tendineae) (Figure 39). When atrial pressure rises above that in the left ventricle, the leaflets open into the ventricular cavity and blood can flow from the atrium into the ventricle. When the pressure below the leaflets rises during ventricular systole, they are lifted up and closed (Davies 1980). The leaflets are prevented from sagging into the left atrium during ventricular systole by the chordae tendineae attached to the undersurface of the valve. These tendons are composed mainly of collagen with the fibres aligned parallel to each other and parallel to the direction of tension. In floppy valve disease, the cusps increase in size and the chordae elongate. These changes usually result in one or both of the leaflets sagging into the atrium during systole. Although the degree of valve involvement is variable, floppy valves are a relatively common abnormality, affecting about 5% of the population. There are usually no serious consequences; however, problems may arise if the valve leaks significantly. Such severe leakage most commonly results from rupture of one or more of the chordae, which can cause complete functional failure of the valve.

The widespread occurrence of floppy mitral valves has provoked much interest, both in its clinical aspects and in the pathological process(es) that cause it. But no

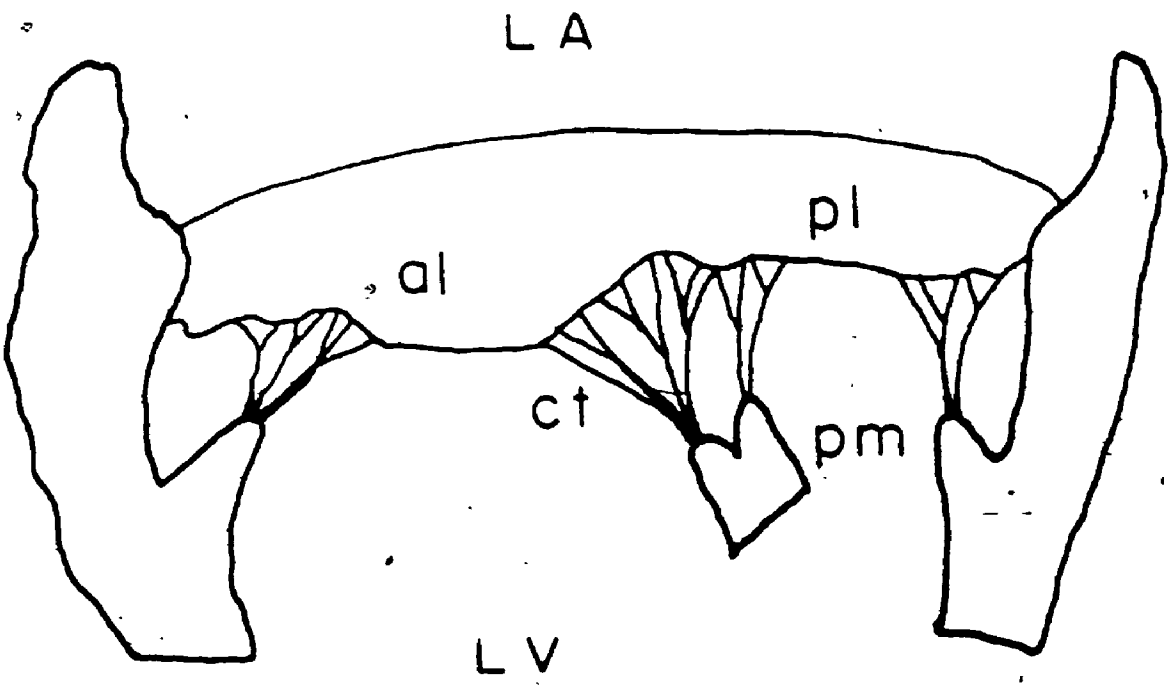

Figure 39: The mitral valve. LA - left atrium, LV - left ventricle, al - anterior leaflet, pl - posterior leaflet, ct - chordae tendineae, pm - papillary muscle. (redrawn from Lim, 1976).

single defect has been identified as the main factor causing floppy valves. Since Read et al. (1965) first observed mitral prolapse and introduced the term floppy valve, there have been many suggestions regarding the nature of the abnormality. One histological feature that is frequently associated with floppy valves is the presence of large aggregated amounts of proteoglycans (often called myxomatous infiltration). The accumulation of proteoglycans was thought to be the primary lesion in floppy valves. Myxomatous change is, however, not seen in every floppy valve, and may also be observed in valves without clinical manifestations of the condition (e.g., King et al. 1982). Based on their morphological and histological study of mitral valves, King et al. (1982) proposed that collagen dissolution in the valves and chordae tendineae was the basic pathological process. They did not, however, identify the exact nature of the collagen dissolution. Genetic collagen abnormalities such as Marfan's syndrome (Simpson et al. 1969) and the various types of Ehler's-Danlos syndrome (Leier et al. 1980) have also been associated with floppy valves, but the exact nature of this relationship remains unclear. Hammer et al. (1979) suggested that the collagen in the valve apparatus was abnormal due to an absence of Type III and Type V collagen, but this conclusion was based on the study of a single mitral valve with ruptured chordae. A later study by Lee et al. (1983), with a larger sample size, showed no difference in the collagen type composition of normal and floppy valves. Henney et al. (1982) found that there was an increased synthesis of collagen in the valve complex. Others, however, have shown evidence for a breakdown in the normal collagenous structure of the chordae (Caulfield et al. 1971, Scott-Jupp et al. 1981). Both these groups used electron microscopy to demonstrate extensive degradation of collagen in ruptured chordae, which they suggested could be due to enzyme activity. Guthrie and Edwards (1976) proposed that chordal elongation observed in mitral valve prolapse was the result of abnormal chordal tension caused by the prolapsing leaflet. This would seem to be unlikely unless the collagen in the chordae was also abnormal, since it has been shown using mechanical testing that normal chordae are very stiff at strain

values above 15% (Lim and Boughner 1975).

The one factor common to all these proposals is that collagen structure is a key element in floppy valves. Since the above studies did not reveal a consistent abnormality of collagen fibre structure the problem could be at the molecular level. In that case imbibition analysis might reveal changes that would not be apparent from either electron or ordinary light microscopy. I therefore examined the collagen in the chordae tendineae of normal and floppy valves.

9.2. Methods

A randomly selected chorda was removed from each of 23 mitral valves. Of these specimens, 14 (8 males, 6 females) were obtained from autopsies of patients who had died from non-cardiac causes (age range 26-92) and 9 (5 males, 4 females) were from patients undergoing valve replacement for mitral valve disease (age range 58-81). In the latter group the clinical diagnosis was mitral valve prolapse (or floppy valve) in 6 patients and rheumatic mitral valve disease in the remaining three. Sections were prepared as described in the Methods chapter. Where possible, the chordae were fixed under tension This reduced or eliminated waviness of the collagen and produced larger coherent zones, which make measurement easier. The chordae were then sectioned longitudinally, such that the collagen fibres lay in the section plane.

Imbibition analysis was then done on sections from each sample. Ten retardation measurements on collagen from each tendon were taken in each of the imbibing media. The form birefringence curves were then plotted. From the minimum of each curve the intrinsic birefringence of each sample was calculated. The results were compared using t-tests.

Sections from each chorda were stained with picrosirius red and examined for degradation, indicated by the presence of yellow or green fibres. Sections were also

stained with haematoxylin and eosin (H&E) and with Movat's pentachrome stain, which contains Alcian Blue, a stain used to demonstrate the presence of proteoglycans. Each of the H&E and Movat's pentachrome stained sections were examined, without knowledge of their source, by Dr. D.G. Perkins, (Department of Pathology, U.W.O.) for evidence of proteoglycan infiltration. Each tendon was then classified by Dr. Perkins as being either normal or abnormal on the basis of the presence of proteoglycan infiltration.

9.3. Results

The results from the imbibition analysis were divided into two groups based on Dr. Perkins' histological classification of "normal" or "abnormal". The average form birefringence curve for each group was then calculated (Figure 40). The retardation values for the histologically normal group were significantly higher than for those tendons with abnormal proteoglycan infiltration ($p<0.05$). For both normal and abnormal tissue the curves showed that the minimum retardation occurred in the 100% glycerol solution. I used the minimum retardation to calculated the intrinsic birefringence of the collagen in each of the tendons (Figure 41). The average intrinsic birefringence of the abnormal chordae was significantly lower ($p<0.001$) than that of the normal chordae. Two chordae showed regions of collagen degradation when stained with picrosirius red. These regions had been avoided in the imbibition analysis measurements. Both of these chordae also had proteoglycan infiltration.

The correlation of the histological findings with the autopsy and surgical reports is shown in Table 6. Of the sixteen chordae identified as being normal with no evidence of proteoglycan infiltration, five were from valves obtained at time of surgery for valve replacement, and the remaining eleven were from autopsy samples. The surgical reports and the gross pathological descriptions of the surgical specimens from this group indicated that three were from stenotic mitral valves and two were from floppy valves.

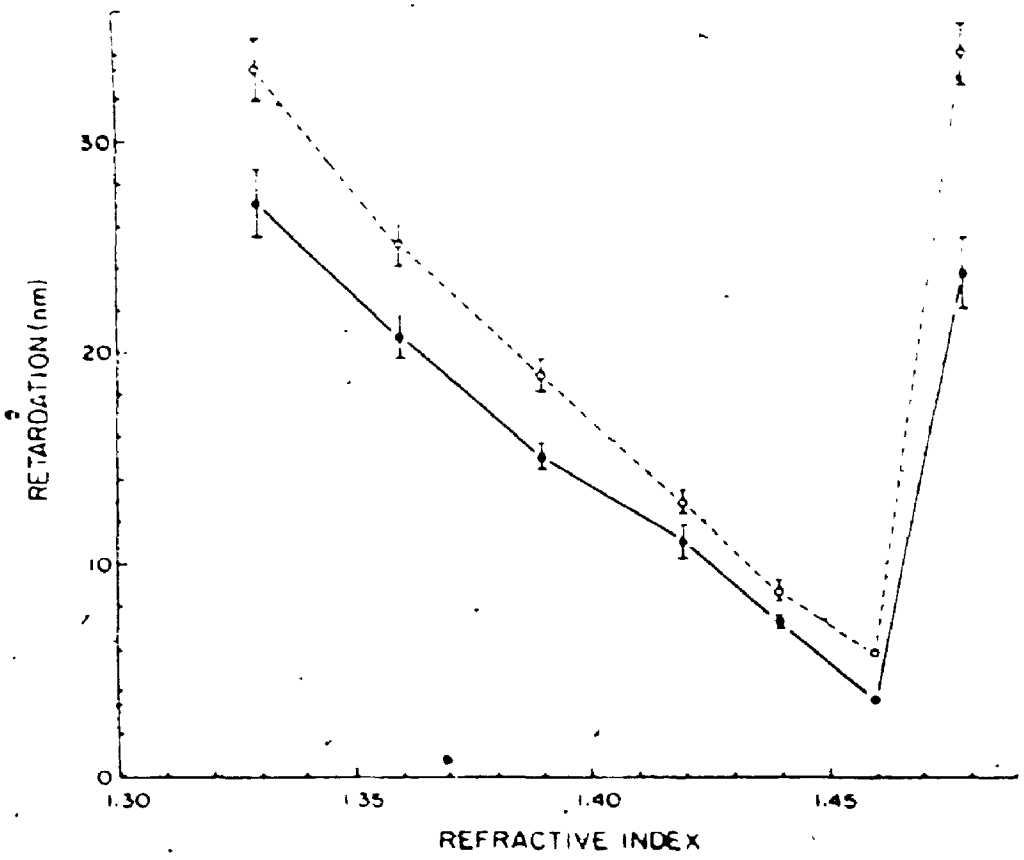

Figure 40: Combined form birefringence curves for collagen sections from normal chordae tendineae (open circles) and those with proteoglycan infiltration (closed circles). Where large enough the standard error of the mean is shown.

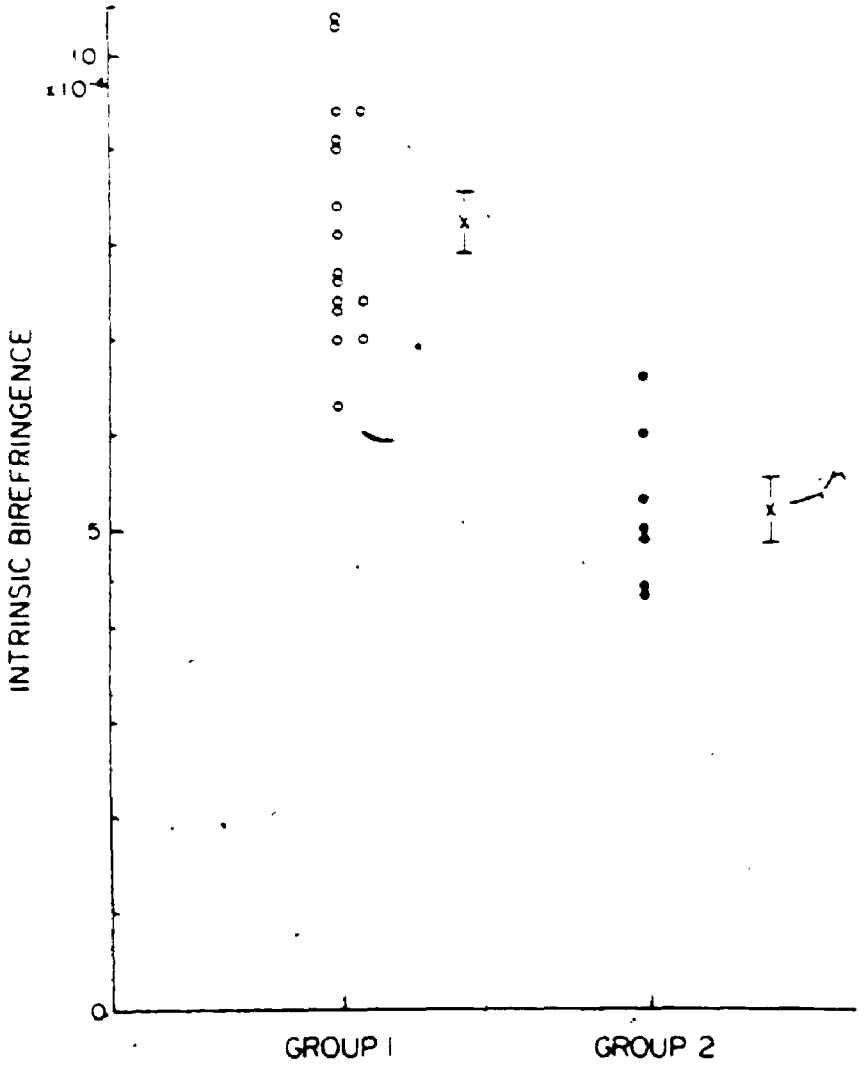

Figure 41: The intrinsic birefringence of the collagen from the normal tendons (group 1) and those with proteoglycan infiltration (group 2). The mean and standard error of the mean is shown for both groups. The intrinsic birefringence was significantly higher ($p<0.001$) in the normal tendons.

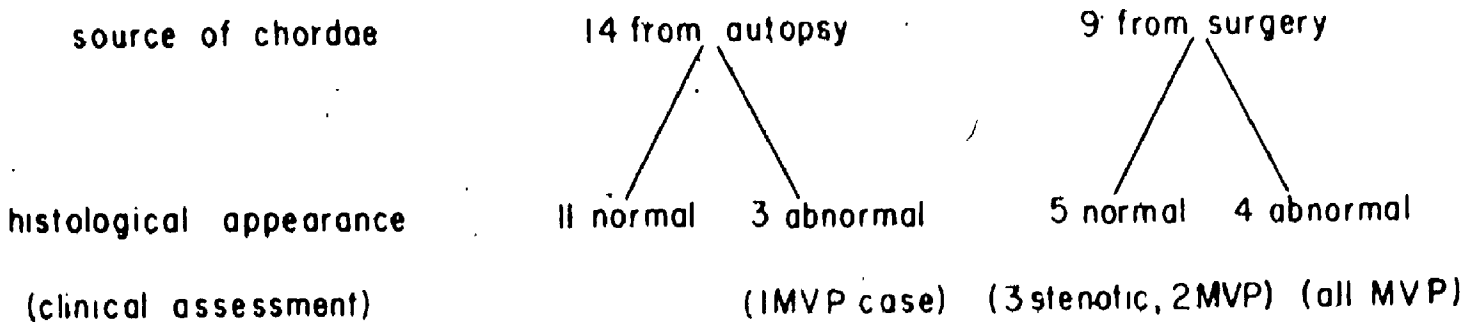

Table 6 Correlation of the histological findings on the chordae tendineae with the autopsy and surgical reports. The cases of mitral valve prolapse (MVP) were produced by floppy valves.

Of the seven chordae identified as histologically abnormal due to proteoglycan infiltration, four were from surgical specimens all of which were floppy valves, while the other three were autopsy specimens, of which one was also identified as a floppy valve The other two autopsy specimens appeared normal on gross inspection.

In summary, I found that collagen in all of the sections with proteoglycan infiltration had a reduced value of intrinsic birefringence compared to sections with no proteoglycan infiltration. This indicates that collagen in such sections is less organised than normal at the molecular level.

9.4. Discussion

I chose chordae tendineae rather than the mitral valve leaflets themselves for this study because collagen fibres in the chordae are highly aligned. In valve leaflets, collagen fibre organisation is multidirectional. Since retardation is dependent on orientation it is difficult to ensure that the true retardation is measured when the fibres do not lie in the section plane.

Involvement of mitral chordae by the myxomatous process is known to be variable, and the finding of some normal chordae in patients with clinical prolapse is to be expected, especially since I was only able to obtain a single tendon from each valve. Also, localised myxomatous change has been found in otherwise unremarkable valves (King et al. 1982, Malcolm 1985).

The molecular organisation of the collagen in the chordae tendineae will influence their mechanical properties. The imbibition analysis technique was used to examine that molecular organisation. It is a well established technique in ultrastructure research (Frey-Wyssling 1974), and in particular has been used to study the changes occurring in the molecular organisation of collagen in the healing and ageing of rat Achilles tendon (Mello et al. 1975, 1979).

The significantly lower intrinsic birefringence values of collagen in the chordae with proteoglycan infiltration indicated a decrease in molecular organisation in these chordae There are several possible explanations for this First, the collagen in the abnormal chordae could be immature. This seems unlikely because the results would suggest that all the collagen is immature (recall that from the study of the scar collagen, retardation measurements were only able to detect changes in the molecular organisation of the collagen up to about two months). The finding of increased production of collagen and glycosaminoglycans plus cell proliferation in the valve (Cole et al. 1984) does, however, suggests that a repair process is occurring. The repair process might indicate the presence of immature collagen and so could be partially responsible for the lower intrinsic birefringences observed. Immature collagen is extensible and relatively weak when compared to mature collagen (Gillman 1968), therefore, its presence might enable the valve leaflets to prolapse into the atrium.

The second possible explanation is that the altered intrinsic birefringence was due to collagen degradation. This would also lead to increased extensibility and a decrease in the tensile strength. In vivo, such a change could result in increased chordal extension at any given stress, causing the valve cusps to prolapse into the atrium. With extensive collagen degradation, chordal rupture could occur. Obvious collagen degradation was seen in only two of the abnormal samples when stained with picrosirius red, but since this method is dependent on collagen fibre diameter (Junqueira et al. 1982) it may not detect the early stages of degradation.

The third possible explanation, and the one that I think is most likely, is that the initial degradation does not involve the collagen per se, but rather represents the removal of ground substance bound to the collagen fibre. It has been shown that proteoglycans are bound by collagen fibres in an organised manner, contributing to the birefringence (Vidal 1965 and 1980). Therefore, if the ground substance is removed from the collagen, the intrinsic birefringence would decrease. The proteoglycan "pools"

characteristic of myxomatous infiltration could be the area where the removed proteoglycans accumulate. Removal of ground substance bound to the collagen could also explain the difference in the shape of the form birefringence curves. Although further experiments would be required to determine the significance of these changes, the shape of the form birefringence curves that I obtained are similar to those of Vidal (1980), in which enzymes were used to remove bound ground substance from normal rat Achilles tendons. Ground substance is known to play an important role in the mechanical properties of tendons (Viidik et al. 1982). Treatment of human Achilles tendon with α-amylase, which removes structural glycoproteins from collagen, caused a substantial reduction (up to 38%) in breaking strength and an increase in distensibility (Minns et al 1973). In chordae tendineae, this effect would allow the chordae to extend and the valve cusps to prolapse. Indeed, the possibility of proteoglycan degradation has been demonstrated in vitro. Porcine mitral valve cultures have been found to secrete a factor (catabolin) that stimulates the degradation of the collagen matrix, especially the proteoglycans (Decker and Dingle 1982, Decker et al. 1984).

In summary, my results indicate that, although proteoglycan infiltration may not be a specific marker for floppy valve syndrome, its presence is associated with evidence for degradation of the collagenous matrix. The findings agree with the opinion of King et al. (1982) and suggest that the extent of valvular involvement in this process is most likely a major factor in determining the functional effect. It is yet to be determined whether it is the collagen itself that is degraded, or if it is the ground substance that is removed from the collagen. The possibility exists that a catabolic factor may induce a degradation and repair process that results in the lower intrinsic birefringences found in the floppy valves. The polarised light technique of imbibition analysis thus provided data not obtainable by the scanning electron microscopy studies that have been used previously to investigate the ultrastructure of floppy mitral valves.

CHAPTER 10 DISCUSSION

I have demonstrated, by studies on muscle and collagen in cardiovascular tissue, that the techniques of polarised light microscopy can provide a unique approach to the examination of tissue structure. The physical principles underlying this research deal with the interaction of linearly polarised light with biological material. Not only can the polarised light methods provide data on the orientation of muscle and collagen fibres within a tissue, but they can also provide insight into the molecular organisation. My results can be summarised as follows;

(1) The two-dimensional orientation method that I developed provided a means of quantifying cardiac muscle organisation in hypertrophic cardiomyopathy (HCM). The orientation distributions from HCM cases had larger angular deviations than normal but were never random. I also found that regions of muscle that appeared qualitatively normal in HCM cases had abnormal orientation distributions.

(2) I measured the orientation of collagen fibres throughout the wall of human brain arteries as a function of perfusion pressure using the Universal stage. I found that Type III collagen in the tunica media was coherently aligned circumferentially even at low pressures and its orientation did not change much with increased pressure. The Type I collagen in the tunica adventitia was also generally circumferentially aligned, but, in addition possessed a large helical component. At high pressure (190 mmHg) the fibre orientations resolved into three distinct groups. One was circumferentially aligned and the other two helically aligned with a pitch angle of approximately 30° with respect to the circumferential direction.

(3) Molecular organisation methods were used to document the change in optical

properties of maturing scar collagen in a dog model of myocardial infarction. I was able to detect differences in retardation for at least six weeks post infarction. In addition I demonstrated that treatment with methylprednisolone, which causes profound scar thinning, did not affect the optical properties of the collagen.

(4) The orientation methods plus transmission electron microscopy were used to investigate collagen structure at the apex of human cerebral artery bifurcations, a common site of aneurysm formation. I found that collagen is very highly aligned in the apex, indicating that no structural defect in collagen fibre organisation is present and perhaps even that the apex is a region of strength.

(5) I examined the molecular organisation of the collagen in saccular aneurysms comparing it with collagen from adjacent vessels. The retardation of collagen in the aneurysms was lower than in the control samples. As there was no evidence of degradation, using picrosirius red staining, in the sections the lower retardation values imply that the aneurysm collagen is immature.

(6) The orientation of collagen fibres in the aneurysms was found to be a complex three-dimensional weave with fibres that possessed substantial helical and spiral components. I also found that the wall had a laminated appearance. These findings imply that the general organisation of collagen fibres in the aneurysm is adequate to deal with the multidirectional stresses to which the aneurysms would be subjected.

(7) I used imbibition analysis to examine the collagen in mitral valve tendons from both normal and floppy valves. I found that collagen in tendons with proteoglycan infiltration had a lower intrinsic birefringence than those without infiltration. This finding is compatible with degradation of the collagen matrix.

The versatility of the polarised light methods was demonstrated by the diversity of problems addressed in this research. The projects undertaken in the thesis have been selected primarily for their clinical applicability, and in this way provide the best demonstration of the value of polarised light microscopy.

10.1. Polarised Light Microscopy As A Tool In Structural Studies

For a material to be studied using the polarised light methods described in this thesis, it must be birefringent i.e., it has two refractive indices because of the anisotropic molecular organisation of the material. This permits a vast array of tissues to be studied, including collagen; cardiac, skeletal and smooth muscle; and elastin. Since these "building blocks" of body tissue are birefringent, many different organs and structures, such as arteries, bone, skin, cartilage, ligaments, lung and heart can be examined. Also the birefringence of membranes, enhanced by staining, allows blood cells and polymorphonuclear leucocytes to be studied.

The polarised light methods can readily be used to relate tissue structure to function or dysfunction because of the magnification range employed. Regular histological sections are studied, which allows regional fibre orientation or molecular organisation to be related directly to the overall section structure. In electron microscopy only small tissue samples are analysed and it is sometimes difficult to determine the spatial relationship between the samples and the organ or tissue from which they came. While polarised light microscopy uses the same magnifications as ordinary light microscopy, polarised light exploits effects produced at the molecular level and therefore effectively extends the resolution of ordinary light microscopy.

In biochemical studies, tissue architecture is generally destroyed entirely, because of the homogenisation that is used to prepare the tissue for analysis. The preservation of tissue architecture in sections studied with polarised light is important because it allows

observation of localised tissue changes. For example, the molecular organisation methods described in this thesis can be used to examine individual fibres. Biochemical tests may fail to detect localised changes because they would be masked by a larger amount of normal tissue. This consideration is important because the function of a tissue can be severely compromised if even a small component has been damaged and does not function normally. For example, saccular aneurysms are only as strong as their weakest part: for rupture to occur, only one weak region is required.

Tissue function is governed by tissue structure at both the fibre and the molecular levels. It is therefore important that fibre orientation and molecular organisation should be considered together and not in isolation. For the myxomatous mitral valve tendons, the orientation of the collagen fibres parallel to the direction of stress was appropriate for the function that they perform, but the molecular organisation of the collagenous matrix appeared inadequate to prevent the valve prolapsing into the atrium. Likewise with the aneurysm, the three-dimensional organisation of the collagen fibres appears to be ideal for coping with multidirectional stresses in the aneurysm wall, but, because the molecular organisation was different from normal, the aneurysms appear to be (at least in the short term) vulnerable to expansion and rupture. It is therefore of special significance in my structural studies that both fibre and molecular organisation could be studied on the same section. As demonstrated in the aneurysm study, this permits direct comparison of fibre orientation and molecular organisation. With rare or small tissue samples this option may be preferable to the exclusive choice between biochemical or electron microscopical analysis.

10.2. Fibre Orientation

I used two- and three-dimensional methods to analyse fibre orientation. Although both methods are based on the same physical principles they serve different functions

and are not directly comparable.

Two-dimensional orientation: Qualitative observation of sections using linearly polarised light provides a quick method of obtaining information about fibre orientation For example, Plate 1. shows that cardiac muscle fibre disorganisation in hypertrophic cardiomyopathy is more readily seen using polarised light than with ordinary light. Plate 4. reveals the laminated nature of the cerebral aneurysm wall, a feature that was not apparent using ordinary light microscopy.

The two-dimensional organisation revealed in these micrographs can be quantified by making use of the fact that, at two specific orientations relative to the polarising filters, a fibre will be at extinction, or appear dark in the field of view. I found that the colour of the fibre following insertion of a full wave plate into the light path and rotating the fibre through +45° could be used to ensure that the correct angle had been chosen (Chapter 2). The interpretation of the quantitative orientation data provided by this technique does, however, require special methods. To analyse the orientation data I have applied statistical analysis and graphical presentation methods developed for the study of such things as homing ability in birds and insects (Batschelet 1981).

I applied the two-dimensional orientation method to quantify the orientation of cardiac muscle fibres in hypertrophic cardiomyopathy, a disease characterised histologically by muscle fibre disorganisation in the ventricular septum of the heart. A quantitative study of muscle orientation has direct pathological relevance because diagnosis of the condition is currently made only by subjective assessment of the tissue Application of the method revealed that the distributions of fibre orientation obtained from areas of muscle that subjectively appeared normal from patients with hypertrophic cardiomyopathy were in fact different from the distributions obtained from hearts without the disease. Previously it was thought that the muscle disorganisation in hypertrophic cardiomyopathy was patchy, interspaced with regions of normally organised muscle. In contrast, I found using polarised light that none of the muscle in the central layer of

the ventricular septum had a normal organisation in these patients

For the two-dimensional method to be effective, the fibres analysed should lie predominantly in the section plane This may often be achieved by the appropriate choice of sectioning angle. For example, when the ventricular septum is sectioned transversely, the muscle fibres in the central layer of the septum lie in the section plane.

In conclusion, the two-dimensional method of analysis provides an effective, quick and accurate means of measuring fibre orientation As many laboratories either possess polarising microscopes or have microscopes that may be easily adapted, the two dimensional method has the potential for widespread clinical and scientific application.

Three-dimensional orientation: It has been stated that the Universal stage cannot be used for the study of biological materials (Bennett 1950, p.629). Although it is true that the measurement of biological material is difficult, when compared to the measurement of crystal orientation in geology, the pioneer work of Smith (1980) demonstrated that it is indeed feasible

My work in this area has been an extension of Smith's initial studies on the orientation of collagen in the tunica adventitia of cerebral arteries. I have obtained measurements of collagen orientation throughout the thickness of the arterial wall. My data revealed a coherent pattern in the organisation of the collagen, which is generally aligned circumferentially around the artery, but also possesses a significant longitudinal component.

Smith studied the orientation of arterial collagen fixed by perfusion at 120 mm Hg, the normal systolic physiological pressure. I extended this study to determine changes in orientation as a function of perfusion pressure. I was also able to determine how the orientation of medial Type III collagen changed as a function of perfusion pressure through the use of picrosirius red staining (which can be used to differentiate Type I

from Type III collagen but does not enhance the birefringence of smooth muscle) This is important because medial collagen has been presumed to play an important role in artery mechanics (Dobrin and Canfield 1984)

From my results it has been possible to relate collagen fibre orientation to the mechanical function of the arteries The medial Type III collagen was highly aligned, even at low pressures. This finding, coupled with the evidence that Type III collagen is not as stiff as Type I collagen, implies that the rapid increase in circumferential stiffness observed in the pressure-volume curves of brain arteries is not due to the medial collagen, but to the increasingly coherent alignment of Type I adventitial collagen

Once the normal fibre organisation in arteries is fully defined, it will be possible to study pathological arteries and determine the role played by fibre architecture in that pathology. For example, Cox (1982) found that, in an experimental model of hypertension, thoracic, carotid and tail arteries from rats were stiffer than normal. However, the collagen and total connective tissue content of the hypertensive arteries decreased, which would be expected to result in greater extensibility of the arteries One possibility is that the organisation of the components of the artery is different, with the collagen perhaps having a greater longitudinal component. This is just one example of an area where the Universal stage could be usefully employed. Since it has been shown that the Universal stage is able to measure collagen orientation in brain arteries, which is a complex three-dimensional organisation, the analysis of more simply organised tissue such as tendons should be straightforward.

When using the Universal stage, one of the requirements is that the zones of birefringent tissue with the same orientation must be sufficiently large (2 μm x 2 μm) to allow a reading to be taken. If the zones are too small, then, as the stage is tilted, light from neighbouring zones with different orientations may interfere with that from the zone of interest. The interference makes extinction difficult if not impossible to attain. This was sometimes a problem with the collagen fibres in 7 μm sections of the

tunica adventitia of brain arteries. Therefore, fibre orientation in thicker sections may only be analysed using the universal stage if the tissue is very highly organised e.g., a tendon fixed under tension. Related to the problem of zone size is the inherent tendency of the observer to select the more strongly birefringent (and hence most easily seen) zones. This can be minimised by using a random sampling procedure. There are certain angles at which orientation measurements from the universal stage are unreliable. Fibres with an inclination angle of around 45° with respect to the section plane are difficult to measure as the stage must be tilted to high angles and thereby introduces the interference problems mentioned earlier. This was not a factor in the studies of collagen orientation in the brain arteries and the aneurysms since very few of the fibres had such orientations. If a tissue is analysed where such fibre orientations are common the problem can be overcome by changing the angle of sectioning.

It should be emphasised that in either two or three dimensions, orientation measurements will only be physiologically meaningful if the in vivo tissue architecture has been preserved i.e., if blood vessels are to be analysed they should be fixed at an appropriate pressure or if a tendon is to be analysed it should be fixed under tension.

While the three-dimensional method has been adapted from its use in geology, the two-dimensional method has not, to my knowledge, been previously described. This is probably because such a need did not exist in geology where three-dimensional crystal orientations could be easily measured.

In conclusion, the universal stage provides an effective means of accurately measuring the three-dimensional orientation of birefringent fibres. Data obtained from such analysis will be especially useful for the study of tissues that have a specialised mechanical function, since mechanical function is greatly influenced by structure.

10.3. Molecular Organisation

The second aspect of the thesis was the study of molecular organisation. I used

two different methods: the measurement of retardation in imbibition analysis and the measurement of retardation in stained tissue. Although the methods derive from the same physical principles (i.e., the concepts of birefringence and the resultant retardation of linearly polarised light) they are not directly comparable because they provide different information.

Imbibition analysis involves measuring the retardation of linearly polarised light by a material immersed in a series of fluids with different refractive indices. From the minimum of the form birefringence curve, the intrinsic birefringence of the material, a direct function of its molecular organisation, can be calculated. In this way imbibition analysis is useful for comparing relative molecular organisation among different tissue samples. For collagen, analysis of the actual form birefringence curve is restricted to qualitative interpretation because of the complex nature of the collagen matrix. The analysis can only be done on two component systems; while collagen, the ground substance and the imbibing fluid comprise a three component system. Quantitative analysis of muscle using imbibition analysis is possible (Maeda 1978) and imbibition analysis has proved to be valuable in the past in the ultrastructural study of bone, myelin and erythrocytes (reviewed by Frey-Wyssling 1974).

The information provided by analysis of the *retardation in stained tissue* is slightly different from that provided by imbibition analysis. The stained tissue method assesses molecular organisation indirectly by measuring the amount of dye that the molecule is able to bind with a preferred orientation. The dye binding abilities will depend on the molecular organisation of the material, and on the presence and number of different chemical groups.

These methods were first applied to scar collagen during the healing phase of myocardial infarction to assess the temporal changes in optical properties of collagen as it matured. This study provided (1) an indication of the ability of the polarised light techniques to resolve known temporal changes in collagen organisation during maturation,

and (2) a method to assess the effect of various pharmacologic interventions on scar healing. For example, I found that treatment with methylprednisolone, a drug which has been found to reduce infarct size but which also results in profound scar thinning (Hammerman et al. 1983), did not alter the optical properties of the scar collagen. This finding indicates that the scar thinning associated with methylprednisolone treatment is not the result of delayed maturation of the collagen.

After defining the resolution of these methods in the healing model, I then applied them to the study of collagen in two situations where the nature of the collagen was unknown.

Aneurysms. It appeared from earlier studies that saccular aneurysms are relatively stiff and that the stresses in the aneurysm wall are well below that which would cause normal collagen fibres to break (Ferguson 1972). However, aneurysms are known to increase in size and rupture. The paradox could be resolved if the aneurysm collagen was shown to be different from that normally present in brain arteries. I found, using both of the retardation methods, that the collagen in the aneurysms was different: collagen in the aneurysms appears to be more immature than the collagen in the *tunica adventitia* of adjacent arteries.

Chordae tendineae: Several studies have indicated that the reason for the inability of floppy mitral valves to function properly is a defect in the collagen of the valve apparatus. I used imbibition analysis to study mitral valve tendons from both floppy and normal valves. I found that in tendons which had proteoglycan infiltration, a common feature in floppy valves, there was a reduction of intrinsic birefringence of the collagen. This finding is compatible with degradation of the collagen matrix and is in good agreement with the recent suggestion that a catabolic factor may be produced in floppy valves (Decker and Dingle 1982). Such a catabolic factor would be expected to produce regional changes in the collagen. Therefore, further application of polarised light methods would be ideal for testing this hypothesis.

10.4. Relationship between optical properties and mechanical properties

Fundamental to the value of the research in this thesis are the established links between the optical and the mechanical properties of the tissues studied. The two are related at both the fibre and the molecular levels. I have drawn on the work from other laboratories to make inferences regarding the mechanical consequences of the results of the optical studies

The connection between the organisation of the birefringent collagen fibres in a tissue and the mechanical properties is well documented. For example, tendons are stiffer than brain arteries when subjected to uniaxial stress because of the unidirectional orientation of tendon collagen compared to the complex three dimensional weave of collagen in tunica adventitia of brain arteries.

A strong connection between the optical properties of collagen at the molecular level and the mechanical properties is expected when one considers the factors that determine the retardation of linearly polarised light. It has been shown that the molecular organisation and the number of intermolecular cross-links in collagen are related to the retardation (Mello et al. 1975, 1979). The removal of proteoglycans and glycoproteins bound to collagen fibres causes a reduction in retardation (Vidal 1980). Both of these facets of molecular organisation have been found to affect both the tensile strength and the extensibility of the collagen (e.g., Gillman 1955, Minns et al 1973).

10.5. Summary

The orientation methods are especially useful in quantifying the structure of tissues and relating it to their mechanical function, while the measurement of retardation is useful in comparing normal and pathological tissue. These polarised light techniques should not be considered an alternative or replacement for biochemical or electron

microscopy studies, but rather as a complementary method.

In conclusion, for determining tissue structure, polarised light microscopy provides a biophysical bridge between biochemical and morphological methods

REFERENCES

Allcock, J.M. and P.B. Canham (1976). Angiographic study of the growth of intracranial aneurysms. J. Neurosurg 45: 617-621.

Batschelet, E. Circular Statistics in Biology Academic Press, London (1981).

Becker, A.E. and G Caruso (1982). Myocardial disarray. A critical review. Br. Heart J. 47: 527-538

Bendet, I.J. and I Bearden (1972). Birefringence of spermatozoa. J. Cell. Biol 55 501-510.

Bennett, H.S. The microscopical investigation of biological materials with polarized light. In R. McClung-Jones(Ed) McClung's Handbook of Microscopical Technique. New York, P.B. Hoeber, 1950.

Booy, F.P. and A.G. Fowler (1985). Cryo-electron misroscopy reveals macromolecular organization within biological liquid crystals seen in the polarizing microscope. Int J Bio. Macromolec. 7. 327-335.

Bulkley, B.H., M.L. Weisfeldt and G.M. Hutchins (1977). Isometric cardiac contraction. a possible cause of the disorganised myocardial pattern of idiopathic hypertrophic subaortic stenosis. N. Engl. J. Med. 296: 135-139.

Bulkley, B.H., M.L. Weisfeldt and G.M. Hutchins (1977). Asymmetric septal hypertrophy and myocardial fiber disarray: Features of normal, developing and malformed hearts. Circulation 56: 292-298.

Burton, A.C. Physical principles of circulatory phenomena: the physical equilibria of the heart and blood vessels. In Handbook of Physiology. Section 2. Circulation Vol.1. American Physiological Society, Washington, D.C., 1962, pp. 85-106.

Cajander, S. and O. Hassler (1976). Enzymatic destruction of the elastic lamella at the mouth of cerebral berry aneurysms? Acta Neurol. Scand. 53: 171-181.

Canham, P.B. and G.G. Ferguson (1985). A mathematical model for the mechanics of saccular aneurysms. Neurosurg. 48: 505-514.

Canham, P.B., H.M. Finlay, P. Whittaker and J. Starkey (1986). The tunica muscularis of human brain arteries: three dimensional measurements of alignment of the smooth muscle mechanical axis, by polarized light and the universal stage. Neurol. Res. 8: 66-74.

Carrasco, F.H., G.S. Montes, R.M. Krisztan, K.M. Shigihara; J. Carniero and L.C.U Junqueira (1981). Morphological and histochemical studies on the collagen of vertebrate arteries. Blood Vessels 18: 296-302.

Caulfield, J.B., D.L. Page, J.A. Kastor and C.A. Sanders (1971). Connective tissue abnormalities in spontaneous rupture of chordae tendineae. Arch. Pathol. 91: 537-541.

Clark, R.B. and J.B. Cowey (1958). Factors controlling the change of shape of certain

nemertean and turbellarian worms. J. Exp. Biol. 35: 731-743.

Cole, W.G., D. Chan, A.J. Hickey and D.E.L. Wilcken (1984). Collagen composition of normal and myxomatous human mitral heart valves. Biochem J 219: 451-460.

Constantine, V.S. and R.W. Mowry (1968). The selective staining of human dermal collagen. II The use of picrosirius red F3BA with polarization microscopy. J. Invest. Derm. 50: 419-423.

Collett, E. (1968). The description of polarization in classical physics. Am. J Phys. 36 713-725.

Cox, R.H. (1982). Time course of arterial wall changes with DOCA plus salt hypertension in the rat. Hypertension 4: 27-38.

Crompton, M.R (1966). Mechanisms of growth and rupture in cerebral berry aneurysms Br. Med. J. 1: 1138-1142

Davies, M.J. Pathology of Cardiac Valves. London, Butterworths, 1980.

Davies, M.J. (1984). The current status of myocardial disarray in hypertrophic cardiomyopathy. Br. Heart J. 51: 361-363.

Decker, R.S. and J.T. Dingle (1982). Cardiac catabolic factors: The degradation of heart valve intercellular matrix. Science 215: 987-989.

Decker, R.S., A. Henney and J.T. Dingle (1984). Characterization of a cardiac catabolic factor isolated from porcine heart valves. Circulation 70 (suppl.II): 80.

Dobrin, P.B. and T.R. Canfield (1984). Elastase, collagenase and the biaxial properties of dog carotid artery. Am. J. Physiol. 247: H124-131.

Drury, R.A.B. and E.A. Wallington, Carleton's Histological Technique 4th Edition, London, Oxford University Press, 1967.

Emmon, R.C. (1943). The Universal Stage. Geol. Soc. Am. Mem. 8: 1-24.

Epstein, E.H. Jr. (1974). $[\alpha 1(III)]_3$ Human skin collagen. J. Biol. Chem. 249: 3225-3231.

Fatou, J.G. Optical microscopy of fibres. In F.Happey (Ed.) Applied fibre science. New York, Academic Press, 1978, 69-180.

Fawcett, D.W. Histology. 11th ed. Philadelphia, W.B. Saunders Co., 1986.

Ferguson, G.G. (1972). Physical factors in the initiation, growth and rupture of intracranial saccular aneurysms. J. Neurosurg. 37: 666-677.

Ferrans, V.J., A.G. Morrow and W.C. Roberts (1972). Myocardial ultrastructure in idiopathic hypertrophic subaortic stenosis. A study of operatively excised left ventricular outflow tract muscle in 14 patients. Circulation 45: 769-2.

Fischer, E. (1944). The birefringence of striated and smooth mammalian muscles. J. Cell. Comp. Physiol. 23: 113-130.

Fisher, R.A. (1953). Dispersion on a sphere. Proc Roy Soc. Lond. A217: 295-305.

Flint, F.O. and K. Pickering (1984). Demonstration of collagen in meat products by an improved picro-sirius red polarisation method. Analyst 109: 1505-1506.

Forbus, W.D. (1930). On the origin of miliary aneurysms of the superficial cerebral arteries. Bull. Johns Hopkins Hosp. 47: 239-284.

Frey-Wyssling, A. (1974). Ultrastructure research in biology before the electron microscope. J. Microsc. 100: 21-34.

Fujiwara, H., T. Hoshino, T. Fujiwara, C. Kawai and Y. Hamashima (1982). Classification and distribution of myocardial fascicle and fibre disarray in 14 hearts with hypertrophic cardiomyopathy in 25 μ thick sections. Jpn. Circulation J. 46: 225-234.

Gelsinger B.E. (1970). Lodestone and sunstone in medieval Iceland. Mariner's Mirror 56: 219-226.

Gelsinger B.E. (1970). Book review. Scandinavian Studies 42:362-363.

Gillman, T. On some aspects of collagen formation in localized repair and in diffuse fibrotic reactions to injury. in Treatise on Collagen, Vol.2, part B, B.S. Gould (Ed), Academic Press, New York, 1968, pp. 331-407.

Glynn, L.E. (1940). Medial defects in the circle of Willis and their relation to aneurysm formation. J. Pathol. Bacteriol. 51: 213-222.

Greenbaum, R.A., S.Y. Ho, D.G. Gibson, A.E. Becker and R.H. Anderson (1981). Left ventricular fibre architecture in man. Br. Heart J. 45: 248-263.

Guthrie, R.B. and J.E. Edwards (1976). Pathology of the myxomatous mitral valve. Minn. Med. 59: 637-647.

Hammer, D., C.V. Leier, N. Baba, C.F. Vasko, C.F. Wooley and S.R. Pinnell (1979). Altered collagen composition in a prolapsing mitral valve with ruptured chordae tendineae. Am. J. Med. 67: 863-866.

Hammerman, H., R.A. Kloner, S. Hale, F.J. Schoen and E. Braunwald (1983). Dose dependent effects of short term methlyprednisolone on myocardial infarct extent, scar formation and ventricular function. Circulation 68: 446-452.

Hansen, J.E. and A. Arking (1971). Clouds of Venus: evidence for their nature. Science 171: 669-672.

Harkness, M.L.R. and R.D. Harkness. Changes with age in some mechanical properties of the skin in the rat. In Connective Tissue and Aging, H.G. Vogel (Ed.), Excerpta Medica, Amsterdam, 1973, pp. 219-221.

Harkness, R.D. (1961). Biological functions of collagen. Biol.Rev. 36: 399-463.

Hartshorne, N.H. and A. Stuart. Crystals and the Polarising Microscope. 4th ed., London, Edward Arnold, 1970.

Hassler, O. (1961). Morphological studies on the large cerebral arteries, with reference to

the aetiology of subarachnoid haemorrhage. Acta Psychiat. Neurol. Scand. Suppl. 154: 1-145..

Hecht, E. and A. Zajac. Optics. Addison-Wesley, Reading, Massachusetts, 1974.

Henney, A.M., D.J. Parker and M.J. Davies (1982). Collagen biosynthesis in normal and abnormal human heart valves Cardiovasc. Res. 16: 624-630.

Hutschenreiter, V.J. and G. Scheuner (1970). Untersuchungen zur Eigendoppelbrechung des Kollagens. Acta Histochem. 35: 337-342.

Jane, J.J., H.R. Winn and A.E. Richardson (1977). The natural history of intracranial aneurysms: rebleeding rates during the acute and long term period and the implication for surgical management. Clin. Neurosurg. 24: 176-184.

Joiner, D.W., H. Puchtler and F. Sweat (1968). Staining of immature collagen by resorcin-fuchsin in infant kidneys. J. Royal Microscopical Soc. 88: 461-471.

Jones, R.C. (1941). A new calculus for the treatment of optical systems. J. Optical Soc. Am. 31: 488-493.

Junqueira, L.C.U., W. Cossermelli and R. Bretani (1978). Differential staining of collagens Type I, II and III by sirius red and polarization microscopy. Arch. Histol. Jap. 41: 267-274.

Junqueira, L.C.U., G. Bignolas and R. Bretani (1979). Picrosirius staining plus polarizing microscopy, a specific method for collagen detection in tissue sections. Histochem. J 11: 447-455.

Junqueira, L.C.U., M. Zugaib, G.S. Montes, O.M.S. Toledo, R.M. Krisztan and R.M. Shigihara (1980). Morphology and histochemical evidence for the occurence of collagenolysis and for the role of neutrophilic polymorphonuclear leukocytes during cervical dilation. Am. J. Obstet. Gynecol. 138: 273-281.

Junqueira, L.C.U., G.S. Montes and E.M. Sanchez (1982). The influence of tissue section thickness on the study of collagen by the picrosirius-polarisation method. Histochemistry. 74: 153-156.

Kenedi, R.M., T. Gibson, C.H. Daly and M. Abrahams (1966). Biomechanical characteristics of human skin and costal cartilage. Fed. Proc. 25: 1084-1087.

King, B.D., M.A. Clark, N. Baba, J.W. Kilman and C.F. Wooley (1982). "Myxomatous" mitral valves: collagen dissolution as the primary defect. Circulation 66: 288-296.

Lazarus, G.S., J.R. Daniels, J. Lian and M.C. Burleigh (1972). Role of granulocyte collagenase in collagen degradation. Am. J. Pathol. 68: 565-578.

Lee, Y.S., F.Y. Lee, A.H. Lu, C.H. Chang, H.C. Chen, K.F. Liang and C.S. Chang (1983). Biochemical analysis and electron microscopy of human mitral valve collagen in patients with various etiologies of mitral valve diseases. Jpn. Heart J. 24: 529-538.

Leeson, T.S. and C.R. Leeson, Histology. 4th ed. Philadelphia, W.B. Saunders Co. 1981.

Leier, C.V., T.D. Call, P.K. Fulkerson and C.F. Wooley (1980). The spectrum of cardiac

defects in the Ehlers-Danlos syndrome, Types I and III. Ann. Int. Med. 92: 171-178.

Light, N.D. and A.J. Bailey. Molecular structure and the stabilization of the collagen fibre. In A. Viidik and J. Vuust (Eds.), Biology of collagen, London, Academic Press, 1980, 15-38.

Lillie, R.D. (Ed) H.J. Conn's Biological Stains (9th Edition), Williams and Wilkins, Baltimore, 1977.

Lim, K.O. (1976). Mechanical properties of chordae tendineae and anterior leaflets from human mitral valves and of aortic valve cusps. Ph.D. Thesis. The University of Western Ontario, London, Canada.

Lim, K.O. and D.R. Boughner (1975). Mechanical properties of human mitral valve chordae tendineae: variation with size and strain rate. Can. J. Physiol. Pharmacol. 53: 330-339.

Ling, S.C. and C.H. Chow (1977). The mechanics of corrugated collagen in arteries. J. Biomech. 10: 71-77.

Macfarlane, T.W.R., M.R. Roach and K.Chan (1980). The geometry of human cerebral bifurcations: effect of static distending pressure. J. Biochem. 13: 265-277.

Maclean, D., M.C. Fishbein, E. Braunwald and P.R. Maroko (1978). Long-term preservation of ischemic myocardium after experimental coronary occlusion. J. Clin. Invest. 61: 541-551.

Maeda, Y. (1978). Birefringence of oriented thin filaments in the I-bands of crab striated muscle and comparison with the flow birefringence of reconstituted thin filaments. Eur. J. Biochem. 90: 113-121.

Malcolm, A.D. (1985). Mitral valve prolapse associated with other disorders. Casual coincidence, common link, or fundamental genetic disturbance? Br. Heart J. 53: 353-362.

Maron, B.J. and W.C. Roberts (1979). Quantitative analysis of cardiac muscle cell disorganisation in the ventricular septum of patients with hypertrophic cardiomyopathy. Circulation 59: 689-706.

Maron, B.J. and W.C. Roberts (1981). Hypertrophic cardiomyopathy and cardiac muscle cell disorganisation revisited: relation between the two and significance. Am. Heart J. 102: 95-110.

Mello, M.L.S., C. Godo, B.C. Vidal and J.M. Abujadi (1975). Changes in the macromolecular orientation of collagen fibres during the process of tendon repair in the rat. Ann. Histochem. 20: 145-152.

Mello, M.L.S., B.C. Vidal, A.C. de Carvalho and A.C. Caseiro-Filho (1979). Change with age of anisotropic properties of collagen bundles. Gerontology 25: 2-8.

Minns, R.J., P.D. Soden and D.S. Jackson (1973). The role of fibrous components and ground substance in the mechanical properties of biological tissue: preliminary investigation. J. Biomech. 6: 153-165.

Montes, G.S., R.M. Krisztán and L.C.U. Junqueira (1985). Preservation of elastic system

fibres and of collagen molecular arrangement and stainability in an Egyptian mummy. Histochemistry 83: 117-119.

Nimni, M.E. (1980). The molecular organisation of collagen and its role in determining the biophysical properties of the connective tissues. Biorheology, 17: 51-82.

Olsen, E.G.J. (1985). An endocrine experimental model for myofibrillar disarray as found in hypertrophic cardiomyopathy. J. Mol. Cell. Cardiol. 17 (Suppl. 2): 35-40.

Park, J.B., C.H. Daly and A.S. Hoffman (1976). The contribution of collagen to the mechanical response of canine artery at low strains. Front. Matrix Biol. 3: 218-233.

Parry, D.A.D., G.R.G. Barnes and A.S. Craig (1978). A comparison of the size distribution of collagen fibrils in connective tissue as a function of age and a possible relation between fibril size distribution and mechanical properties. Proc. R. Soc. Lond. B 203: 305-321.

Perez-Tamayo, R. and I. Montfort (1980). The susceptability of hepatic collagen to homologous collagenase in human and and experimental cirrhosis of the liver. Am. J. Pathol. 100: 427-440.

Phillips, W.R. Mineral Optics, Principals and Applications. San Francisco, W.H. Freeman, 1971.

Pierard, G. and C.M. Lapière (1976). Microanatomy and mechanical properties of the dermis in bovine foetus and newborn calves. Arch. Int. Physiol. Biochem. 84, suppl., abstr. 91.

Preston, J.M. and P.C. Tsien (1950). The cellulose-dye complex, part V- a comparison of orientation factors derived from dichroism and other parameters. J. Soc. Dyers and Colourists 66: 361-365.

Puchtler, H., F.S. Waldrop and L.S. Valentine (1973). Polarization microscopic studies of connective tissue stained with picro-sirius red FBA. Beitr. Pathol. Bd. 150: 174-187.

Ramskou, T. Solstenen: Primitiv Navigation i Norden for kompasset. Rhodos, Copenhagen, 1969.

Read, R.I., A.P. Thal and V.E. Wendt (1965). Symptomatic valvular myxomatous transformation (the floppy valve syndrome). A possible forme fruste of the Marfan syndrome. Circulation 32: 897-910.

Rigby, B.J. N. Hirai, J.D. Spikes and H. Eyring (1959). Mechanical properties of rat tail tendon. J. Gen. Physiol. 43: 265-283.

Roach, M.R. and A.C. Burton (1957). The reason for the shape of the distensibility curves of arteries. Can. J. Biochem. 35: 681-690.

Roberts, E.W. and P.C. Robinson (1985). Light microscopy of ceramics. J. Microsc. 104: 137-158.

Roubault, M. Determination des minereaux des roches au microscope polarisant. Lamarre-Poinat, Paris, 1963.

Scott, S., G.G. Ferguson and M.R. Roach (1972). Comparison of the elastic properties of human intracranial arteries and aneurysms. Can. J. Physiol. Pharmacol. 50: 328-332.

Scott-Jupp, W., N.L. Barnett, P.J. Gallagher, J.L. Munro and J.L. Ross (1981). Ultrastructural changes in spontaneous rupture of mitral chordae tendineae. J. Pathol 133: 185-201.

Sekhar, L.N. and R.C. Heros (1981). Origin, growth, and rupture of saccular aneurysms: A review. Neurosurg. 8: 248-260.

Shurcliff, W.A. Polarized Light. Harvard University Press, Cambridge Mass., 1962.

Simpson, J.W., J.J. Nora and D.G. McNamara (1969). Marfan's syndrome and mitral valve disease: acute surgical emergencies. Am. Heart J. 77: 96-99.

Sinex, F.M., The role of collagen in aging. In B.S. Gould (Ed.) Treatise on Collagen Vol.2 Biology of Collagen, part B., New York, Academic Press, 1968, 409-448.

Smith, J.F.H. (1980). The orientation of collagen in the tunica adventitia of human cerebral arteries measured with a polarizing microscope and a universal stage. M.Sc. Thesis. The University of Western Ontario, London, Canada.

Smith, J.F.H., P.B. Canham and J.Starkey (1981). Orientation of collagen in the tunica adventitia of the human cerebral artery measured with polarised light and the universal stage. J. Ultrastruc. Res. 77: 133-145.

Stehbens, W.E. (1959). Medial defects of the cerebral arteries of man. J. Pathol. Bacteriol. 78: 179-185.

Stehbens, W.E. (1975). Ultrastructure of aneurysms. Arch. Neurol. 32: 798-807.

Stehbens, W.E. Arterial structure at branches and bifurcations with reference to physiological and pathological processes, including aneurysm formation. In Structure and Function of the Circulation, Vol. 2. C.J. Schwartz, N.T. Werthessen and S. Wolf (Eds.), Plenum Press, New York, 1981, pp. 667-693.

Stehbens, W.E. and R.M. Ludatscher (1973). Ultrastructure of the renal arterial bifurcation of rabbits. Exp. Mol. Pathol. 18: 50-67.

Streeter, D.D.Jr, Gross morphology and fibre geometry of the heart. In: Berne R.M. and N. Sperelakis (Eds.) Handbook of Physiology. Section 2, Vol 1. The Heart. (American Physiological Society) Williams and Wilkins, Baltimore. 1979.

Suzuki, J. and H. Ohara (1978). Clinicopathological study of cerebral aneurysms. J. Neurosurg. 48: 505-514.

Tarling, D.H. Principles and Applications of Paleomagnetism. Chapman and Hall, London, (1971).

Teare, D. (1958). Asymmetrical hypertrophy of the heart in young adults. Br. Heart J. 20: 1-8.

Torp, S., R.G.C. Arridge, C.D. Armeniades and E. Baer, Structure-property relationships in tendon as a function of age. In E.D.T. Aitkens and A. Keller (Eds.) Structure of

Fibrous Biopolymers, London, Butterworths, 1975, 197-221

Van der Bel-Kahn, J. (1977) Muscle fibre disarray in common heart diseases Am J. Card 40: 355-364.

Vidal, B.C. (1965). The part played by the mucopolysaccharides in the form birefringence of collagen. Protoplasma. 59: 472-479

Vidal, B.C. (1970). The part played by proteoglycans and structural glycoproteins in the macromolecular orientation of collagen bundles Cell. Mol. Biol. 26: 415-421.

Vidal, B.C., M.L.S. Mello and E.R. Pimentel (1982). Polarization microscopy and microspectrophotometry of sirius red, picrosirius and chlorantine fast red aggregates and their complexes with collagen. Histochem J. 14: 857-878.

Viidik, A., C.C. Danielson and H. Oxlund (1982) On fundamental and phenomenological models, structure and mechanical propeties of collagen, elastin and glycosaminoglycan complexes Biorheology. 19: 437-451.

Wainwright, S.A., W.O. Biggs, J.D. Currey and J.M. Gosline. Mechanical Design in Organisms. New York, Halsted Press, 1976

Wolinsky, H. and S. Glagov (1964). Structural basis for the static mechanical properties of the aortic media. Circ. Res. 14: 400-413.

Wolman, M. (1975). Polarized light as a tool of diagnostic pathology. J. Histochem. Cytochem 23: 21-50.

Wolman, M. and T. Gillman (1972) A polarised light study of collagen in dermal wound healing. Br. J. Exp. Pathol. 53. 85-89.

Zar, J.H. Biostatistical Analysis. 2nd ed. Englewood Cliffs N.J., Prentice-Hall Inc., 1984.

VITA

NAME	Peter Whittaker
PLACE OF BIRTH	Nottingham, England
POST-SECONDARY EDUCATION AND DEGREES	Nottingham University, England 1978-1981 B.Sc. (Hons.) Physics University of Western Ontario, London, Ontario, Canada 1981-1986 Ph.D. Biophysics

PUBLICATIONS

1. Whittaker, P. and P.B. Canham (1983) Cylindrical symmetry and aligned smooth muscle provide an internal reference for three dimensional reconstruction. Acta Stereol. 2 (Suppl. 1): 155-158.

2. Canham, P.B., H.M. Finlay, P.Whittaker and J. Starkey (1983) Three dimensional orientation of optically anisotropic muscle in brain arteries using the Universal Stage. Acta Stereol. 2 (Suppl. 1) 265-268.

3. Canham, P.B., H.M. Finlay, P. Whittaker and J. Starkey (1986) Quantitative evidence from polarised light microscopy of the uniform alignment of the tunica muscularis of the brain artery. Neurol. Res. 8: 66-74.

4. Whittaker, P., M.E. Schwab and P.B. Canham (1985). Collagen's molecular organisation in saccular aneurysms compared to the tunica adventitia, using polarised light. (Submitted, Conn. Tis. Res.)

5. Whittaker, P., D.R. Boughner, D.G. Perkins and P.B. Canham (1985) Quantitative structural analysis of collagen in chordae tendineae and its relation to mitral valve prolapse and proteoglycan infiltration. (Submitted, Br. Heart J.).

ABSTRACTS

1. Whittaker, P., P.B. Canham and J. Starkey (1982). Three dimensional orientation of collagen in human brain artery by polarisation microscopy and a Universal Stage. 25th Annual Meeting of the Canadian Federation of Biological Societies.

2. Whittaker, P. and P.B.Canham (1983). Cylindrical symmetry and aligned

smooth muscle provide an internal reference for three dimensional reconstruction. 6th International Congress for Stereology

3 Canham, P.B., H.M. Finlay, P. Whittaker and J. Starkey (1983). Three dimensional orientation of optically anisotropic muscle in brain arteries using the Universal Stage. 6th International Congress for Stereology

4 Whittaker, P. P.B Canham and M.E Schwab (1984). Retardation of polarised light by collagen in cerebral aneurysms 68th Annual Meeting of the Federation of American Societies for Experimental Biology.

5 Whittaker, P., D.G. Perkins, P.B Canham and D.R Boughner (1985) Quantitative structural analysis of collagen in mitral valve prolapse 12th Interamerican Congress of Cardiology.

6 Whittaker, P., T.M. Romano, M.D. Silver and D.R. Boughner (1985) A new approach to muscle disorganisation in hypertrophic cardiomyopathy. Circ. Vol. 72 Suppl.III, p.348. 58th meeting of the American Heart Association.

7 Whittaker, P. and P.B. Canham (1986). Two dimensional organisation of tissue determined by polarised light microscopy. 29th Annual Meeting of the Canadian Federation of Biological Societies.

8 Whittaker, P., K. Przyklenk, D.R. Boughner, P.B. Canham, H. Hammerman and R.A. Kloner (1986). Maturation of myocardial scar collagen assessed by polarized light microscopy. Mid-East Meeting of the American Federation for Clinical Research (in press Clin. Res)

END

06·08·87

FIN